

The Biology of Glass Sponges

S. P. Leys,^{*} G. O. Mackie[†] and H. M. Reiswig^{†,‡}

^{}Department of Biological Sciences, University of Alberta,
Edmonton, Alberta T6G 2E9, Canada*

*[†]Department of Biology, University of Victoria,
Victoria V8W 3N5, Canada*

*[‡]Natural History Section, Royal British Columbia Museum,
Victoria V8W 9W2, Canada*

1. Introduction	3
2. General Organisation	5
2.1. Gross morphology.....	5
2.2. Structure of the body wall.....	5
3. Cells and Syncytia	9
3.1. Definitions.....	9
3.2. Plugged junctions	10
3.3. Hexactinellid plugs compared with other junctions	13
3.4. Trabecular syncytium.....	15
3.5. Sclerocytes and sclerosyncytium.....	17
3.6. Archaeocytes.....	18
3.7. Cells with inclusions.....	18
3.8. Choanocytes	20
3.9. Mesohyl.....	24
4. Tissue Dynamics	24
4.1. Reaggregation of dissociated sponge tissue.....	24
4.2. Fusion.....	27
4.3. Cytoskeleton	29
4.4. Organelle transport.....	33
4.5. Comparison with cellular sponges.....	37
4.6. Immune response.....	38
5. Physiology.....	39
5.1. Hexactinellids as experimental animals.....	39

5.2. Food and wastes	40
5.3. Production and control of feeding currents	50
6. The Siliceous Skeleton	59
6.1. Discrete spicules	59
6.2. Megascleres and microscleres	60
6.3. Spicule locations	66
6.4. Fused silica networks	68
6.5. Silication	76
7. Ecology	85
7.1. Habitats: distribution and abundance	85
7.2. Succession: glass sponge skeletons as substrates	87
7.3. Reefs or bioherms	90
7.4. Growth rates and seasonal regression	94
7.5. Predation, mortality and regeneration	96
7.6. Recruitment	99
7.7. Symbioses: animal-plant associations	101
8. Reproduction	104
8.1. Sexual reproduction	104
8.2. Asexual reproduction	116
9. Classification and Phylogeny	116
9.1. Classification of recent Hexactinellida	116
9.2. Classification of fossil Hexactinellida	119
9.3. Phylogeny of Hexactinellida within Porifera	125
9.4. Phylogeny within Hexactinellida	128
10. Conclusions	131
Acknowledgements	132
References	132

As the most ancient extant metazoans, glass sponges (Hexactinellida) have attracted recent attention in the areas of molecular evolution and the evolution of conduction systems but they are also interesting because of their unique histology: the greater part of their soft tissue consists of a single, multinucleate syncytium that ramifies throughout the sponge. This trabecular syncytium serves both for transport and as a pathway for propagation of action potentials that trigger flagellar arrests in the flagellated chambers. The present chapter is the first comprehensive modern account of this group and covers work going back to the earliest work dealing with taxonomy, gross morphology and histology as well as dealing with more recent studies. The structure of cellular and syncytial tissues and the formation of specialised intercellular junctions are described. Experimental work on reaggregation of dissociated tissues is also covered, a process during which histocompatibility, fusion and syncytialisation have been investigated, and where the role of the cytoskeleton in tissue architecture and transport processes has been studied in depth. The siliceous skeleton is given special attention, with an account of discrete spicules and fused silica networks, their diversity and distribution, their importance as taxonomic features and the process of silication. Studies on particle capture, transport of internalised food

objects and disposal of indigestible wastes are reviewed, along with production and control of the feeding current. The electrophysiology of the conduction system coordinating flagellar arrests is described. The review covers salient features of hexactinellid ecology, including an account of habitats, distribution, abundance, growth, seasonal regression, predation, mortality, regeneration, recruitment and symbiotic associations with other organisms. Work on the recently discovered hexactinellid reefs of Canada's western continental shelf, analogues of long-extinct Jurassic sponge reefs, is given special attention. Reproductive biology is another area that has benefited from recent investigations. Seasonality, gametogenesis, embryogenesis, differentiation and larval biology are now understood in broad outline, at least for some species. The process whereby the cellular early larva becomes syncytial is described. A final section deals with the classification of recent and fossil glass sponges, phylogenetic relationships within the Hexactinellida and the phylogenetic position of the group within the Porifera. Palaeontological aspects are covered in so far as they are relevant to these topics.

1. INTRODUCTION

Glass sponges, Hexactinellida, are emerging as an important group of animals which, because of their ancient heritage, can shed light on fundamental questions such as the origin of multicellular animals, molecular evolution, and the evolution of conduction systems. Glass sponges are unusual animals with a skeleton of silicon dioxide whose triaxonal (cubic), six-rayed symmetry and square axial proteinaceous filament distinguishes them from other siliceous sponges. The fossil record suggests glass sponges were established by the Late Proterozoic, thrived during the middle Cambrian, diversified during the Jurassic when they formed vast reefs in the Tethys Sea and reached their maximum radiation and diversity during the Late Cretaceous. Estimated rates of molecular evolution place their origin even earlier at 800 million years ago (Ma).

However, it is their soft tissues that are really remarkable. They are interestingly different from all other animals (including other sponges) in having syncytial tissues that arise by fusion of early embryonic cells. The larva and adult have an elegant combination of multinucleate and cellular cytoplasmic regions unknown in any other animal. The continuity of this tissue not only allows food to be transported around the animal symplastically as in plants, it allows electrical signals to travel throughout the animal—in essence it functions analogously to the nervous system of other animals. These unusual features show how Nature has a few tricks up her sleeve none of us could have imagined 30 years ago.

What we know of these unusual animals has been constrained by limited access to their deep-water habitat. There are approximately 500 species world wide; the greatest diversity inhabit 300- to 600-m depths and only a few populations inhabit shallow (>15 m) water. Glass sponges were first sampled in the late nineteenth century during the Challenger Expedition, and though we owe much of our understanding of the taxonomy to that early descriptive work, use of modern techniques such as SCUBA, submersibles and remote operated vehicles (ROVs) have vastly extended our knowledge of the cytology and physiology of the group. Recently, use of submersibles and ROVs coupled with modern multibeam surveys have revealed modern reefs in the Northeast (NE) Pacific, and have now made it possible to study the ecology and even physiology of feeding *in situ*.

These are exciting times, but much remains to be done in several key areas. Reproductive individuals are hard to encounter, and our only detailed information comes from a tiny cave-dwelling species that is both accessible by SCUBA and is reproductive year round. How other species reproduce, whether their larvae are similar, and how they colonise new habitats and maintain the massive reef structures over time are areas we know nothing about. Syncytial tissues are remarkable structures that we little understand. How do nuclei arise in the multinucleated regions; how are the microtubule transport pathways nucleated—are there ‘roaming’ microtubule-organizing centres as there are in some protists? How does the tissue differentiate zones for fusing and how does fusion of the membrane occur? What is the protein and molecular make up of the unusual plugged junctions that separate functional regions of cytoplasm into ‘cells’ and to what extent do they function to regulate transjunctional traffic? The syncytial tissues can propagate action potentials, but intracellular recordings have yet to be achieved, and the basis of the impulse as a calcium spike requires verification by analysis at the membrane level. Glass sponges inhabit many sediment-rich regions, yet particulates in the incurrent water are one of the principal irritants that trigger feeding current arrests. What limits glass sponges to their present habitats and how robust are modern-day shallow populations in the face of growing human impact on this habitat?

This is the first review of glass sponge biology, and thus will likely be an important resource for those who continue to advance our knowledge of the group. Here we have tried to cover as much of the biology of the group as possible, but only lightly touched on palaeontology as it pertains to systematics and skeletal structure. The reader may find more information in other excellent papers (Steiner *et al.*, 1993; Reitner and Mehl, 1995; Mehl, 1996, Brasier *et al.*, 1997; Mehl-Janussen, 2000). Our ultimate goal is to stimulate interest and continued research into a fascinating and ancient group of animals.

2. GENERAL ORGANISATION

2.1. Gross morphology

Glass sponges are vase, plate or tube-shaped animals (never encrusting) that range in size from 0.5-cm diameter in *Oopsacas minuta* up to 2-m diameter in *Aphrocallistes vastus* or *Scolymastra joubeni* (Figure 1). The sponge body may arise directly from the substratum and be organised around a single atrial feeding cavity, or the sponge can be suspended on a tall stalk of glass spicules, in which case the atrial cavity is all but absent and numerous excurrent canals simply merge on an oscular ‘field’ at one side of the animal (e.g. *Hyalonema*). Budding is common in many non-stalked species.

Most hexactinellids require a hard substratum for settlement (either rocks or shell debris), but two groups, all Amphidiscophora (including *Hyalonema* and *Monorhaphis*) and Euplectellinae (including *Euplectella*) anchor in soft sediments with special basal spicules. Deviations from the vase-form in a few genera are thought to represent adaptations to the deep sea environment. In four species (in the genera *Polioplogon*, *Sericolophus*, *Platylistrum* and *Tretopleura*) the sponge body is bilaterally symmetrical, an adaptation which is thought to expose the dermal surface to currents and place the atrial chamber in the lee of currents. In some specimens of *Farrea occa* and another species (possibly *Chonelasma*), tubes and oscula alternate along a central axis in an apparent form of metamerism (Tabachnick, 1991).

Glass sponges fall into two gross morphological categories based on the type of skeleton the animal produces (Figure 2): those with a loose spicule skeleton—lyssacine—that is held together by strands of the trabecular tissue, and those with a fused spicule skeleton—dictyonine—that forms a rigid three-dimensional scaffold. Sponges with a dictyonal framework form part of the Subclass Hexasterophora (Figure 55).

2.2. Structure of the body wall

The whole sponge is formed by a single continuous syncytial tissue, the trabecular reticulum (Section 3.4), which stretches from the outside or dermal membrane to the inside, or atrial membrane, and encloses cellular components of the sponge. The dermal and atrial tissues are called membranes by convention because they are two-dimensional syncytial extensions of the trabecular reticulum.

The body wall is divided into three regions (Figures 3 and 4). The major component occupying the centre of the body wall is the choanosome, which contains the flagellated chambers. The choanosome is bordered on either

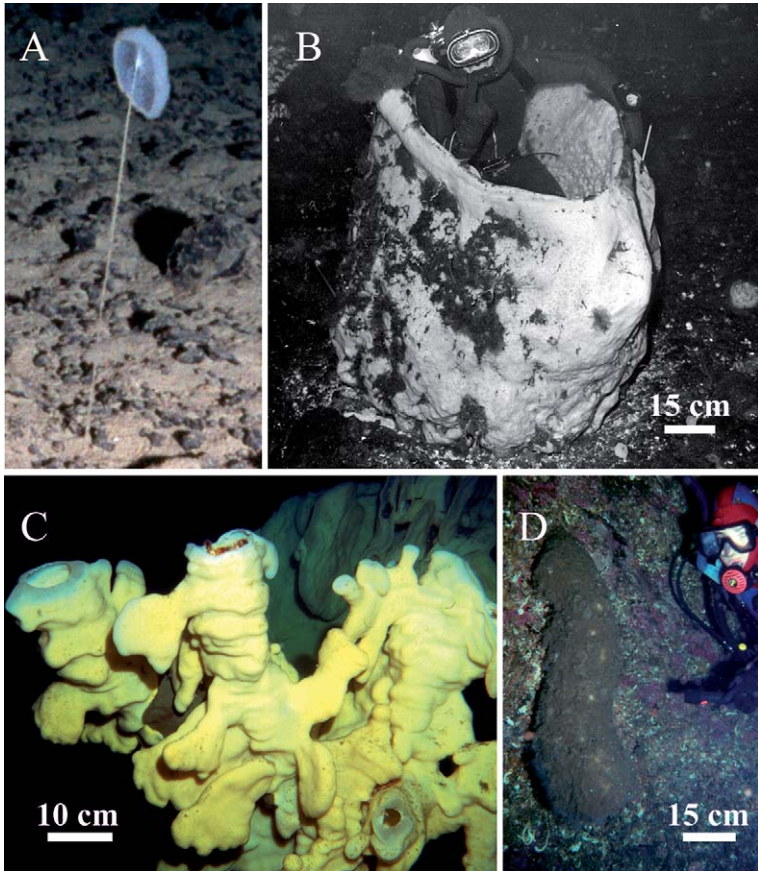


Figure 1 Glass sponge diversity. (A) A stalked glass sponge, possibly *Caulophacus* sp. photographed by submersible at an oligotrophic site in the North Pacific (courtesy of S. Beaulieu). (B) *Scolymastra joubini*, a vase-shaped sponge that grows large enough for a diver to perch inside the osculum during a 1967 dive at 54 m (180 ft) at McMurdo Sound, Antarctica (courtesy of P. K. Dayton). (C) *Aphrocallistes vastus*, a billowy series of cream-yellow tubes, photographed at 35 m depth in Saanich Inlet, British Columbia, Canada. (D) *Rhabdocalyptus dawsoni*, a tube-shaped sponge that hangs with osculum down from the near vertical fjord walls at 30 m in Barkley Sound, Canada (S. Leys, unpublished data).

side by a network of fine strands of the trabecular reticulum called the peripheral trabecular network (Reiswig and Mehl, 1991; Leys, 1999). The inner and outer trabecular networks occupy a similar amount of the body wall (5–12%) in both *F. occa* and *Rhabdocalyptus dawsoni*.

Water enters the sponge through pores in the dermal membrane (Figure 4A) that have a diameter of 5–22 μm (*F. occa*) and 4–30 μm (*Rhabdocalyptus*

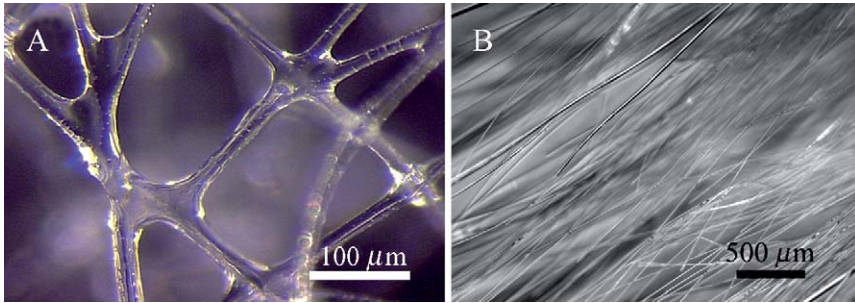


Figure 2 Cleaned spicule skeletons from glass sponges. (A) Dictyonine (fused) from *Aphrocallistes vastus*. (B) Lyssaccine (loose) from *Rhabdocalyptus dawsoni*.

dawsoni) (Mackie and Singla, 1983; Reiswig and Mehl, 1991). The size and shape of incurrent and excurrent canals have been determined both from sections of several species and from plastic casts of the canal systems in *Rhabdocalyptus dawsoni*, *Aphrocallistes vastus* and *Scolymastra joubini* (Leys, 1999; Bavestrello *et al.*, 2003). In *Rhabdocalyptus dawsoni*, the outer peripheral trabecular network lines a loose system of broad, interconnected channels. From this region, distinct incurrent canals (lined by the trabecular reticulum) lead into the body of the sponge and taper from a broad starting diameter of 1.25 mm just below the dermal membrane to approximately 0.5 mm in the centre of the body wall, whereupon they give rise to numerous narrow branches that terminate at individual flagellated chambers. Casts of the incurrent canals show them to be discrete channels throughout their length (Leys, 1999). Canals in *Aphrocallistes vastus* are also discrete channels, but are more uniform in diameter throughout their length. Incurrent and excurrent canals are interlacing pillars 550 and 350 μm in diameter, respectively. Branches off the principal incurrent canals 200 μm in diameter bifurcate once before terminating at flagellated chambers.

In *Rhabdocalyptus*, the fine branches of each incurrent canal terminate in several cup-shaped spaces that surround flagellated chambers. The water enters the chambers through over a hundred pores (prosopyles) formed in the trabecular reticulum, and because there is a second layer of the trabecular reticulum that fits snugly around each collar in the flagellated chamber, the water must be drawn through the collar mesh into the flagellated chamber (Figure 4B). Chambers are large, 55 to 70 μm internal diameter cavities in *Aphrocallistes vastus* and *Rhabdocalyptus dawsoni* and up to 100 μm internal diameter in *Oopsacas minuta*. The water exits the flagellated chambers through large openings (apopyles), 20–35 μm in diameter, directly into small ‘collecting’ excurrent canals 100–150 μm in diameter. These in turn empty into tubular excurrent canals that increase in diameter from 0.3 to 1.5 mm from the centre of the sponge body wall to the peripheral trabecular

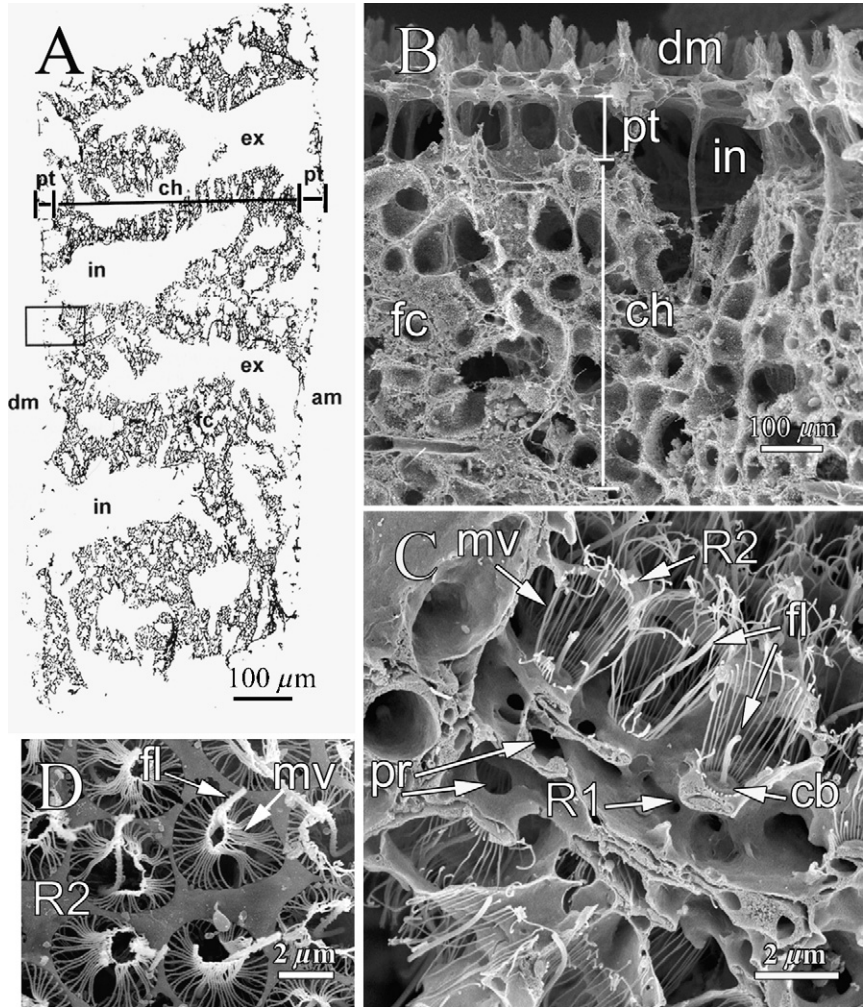


Figure 3 The canal system and tissue structure of the body wall in lysaccine (A, D) and dictyonine (B, C) glass sponges (A, Leys, 1999). (A) Composite of paraffin sections through the body wall of *Rhabdocalyptus dawsoni*. A region equivalent to that in the box is shown in B. (B) Scanning electron micrograph of a fracture through the outer wall of *Aphrocallistes vastus*. Discrete incurrent (in) canals lead via fine branches to flagellated chambers (fc) in the choanosome (ch). The outer zone of both incurrent and excurrent canals (ex) in both sponges consists of a loose network of the trabecular reticulum, the peripheral trabecular network (pt) that supports the dermal (dm) or atrial (am) membranes. (C) A fracture through the wall of two adjacent flagellated chambers in *Aphrocallistes vastus*. Primary (R1) and secondary (R2) reticula, extensions of the trabecular reticulum, incurrent pores, prosopyles (pr), collar bodies (cb) branching from choanocytes, with collar microvilli (mv) and flagellum (f). (D) A view from the inside of the chamber of *Rhabdocalyptus dawsoni* showing the secondary reticulum (R2) surrounding the collar microvilli (mv) and flagellum that arise from each collar body.

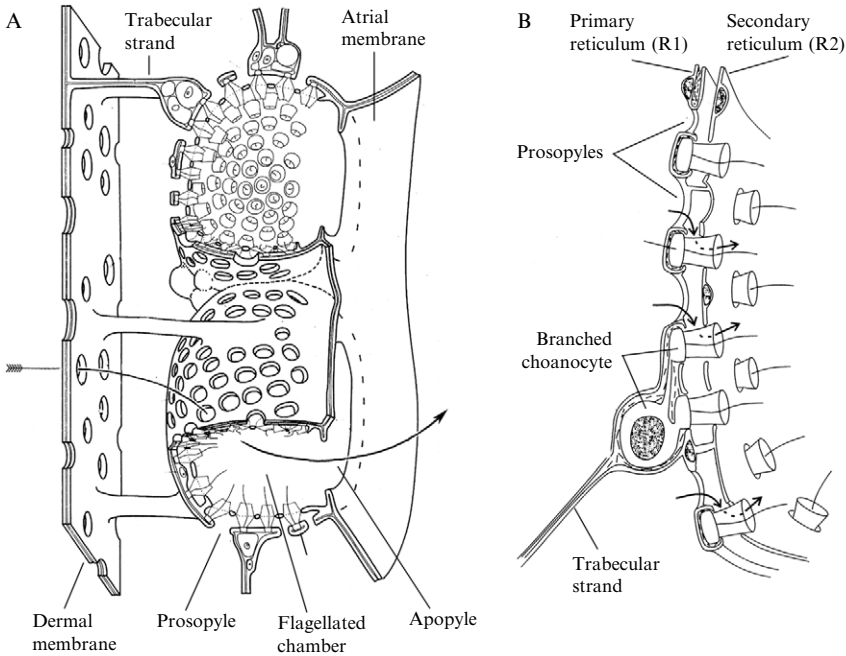


Figure 4 Hexactinellid soft tissue organisation. (A) *Farrea occa*: two flagellated chambers connected to the dermal membrane by trabecular strands. Arrow shows water flow (after [Reiswig and Mehl, 1991](#), with kind permission of Springer Science and Business Media). (B) Section through the wall of a flagellated chamber, based on *Rhabdocalyptus dawsoni*. Water (arrows) is drawn through prosopyles in the primary reticulum and through the choanocyte collars by the beating of the flagella. The secondary reticulum surrounds the collars, forcing water through the collar microvilli (after [Leys, 1999](#)).

network on the atrial side. At the atrial side of the sponge the excurrent canals merge once again to form a loose network of broad interconnected canals. The water passing through these canals vents into the atrium of the sponge through openings 100 to 200 μm diameter.

3. CELLS AND SYNCYTIA

3.1. Definitions

Hexactinellids differ from other sponges in consisting largely of a single syncytial tissue, the trabecular syncytium, but cells are also present and some explanation is necessary as to how these words will be used in this review, as terminology has always been a problem in this group.

Eukaryotic cells may be defined as membrane-enclosed cytoplasmic bodies containing a single nucleus. If a number of such units fuse, or become multinucleate by internal nuclear division, they are referred to as syncytia. The trabecular reticulum of hexactinellids is a syncytium, containing thousands of nuclei within a single, ramifying, cytoplasmic domain that permeates all parts of the sponge. As noted in [Section 2.2](#), it forms the dermal and atrial covering layers and the trabecular strands, and provides the structural support for the flagellated chambers, as well as the secondary reticulum that directs water flow through the choanocyte microvilli ([Figure 4B](#)). We also recognise a second syncytial tissue, here termed sclerosyncytium, that secretes the spicules.

Cells in animals, plants and fungi are frequently joined by specialised junctional structures such as gap junctions, plasmodesmata and perforate septa that permit some degree of direct exchange of materials between cells via aqueous pathways. This does not disqualify the nucleated domains on either side from consideration as cells in the sense of ‘separate working units of protoplasm’ ([Dahlgren and Kepner, 1930](#)). Accordingly, we also recognise cells in hexactinellids, even though they are typically connected to one another or to the trabecular syncytium by cytoplasmic bridges. Despite sharing a common plasmalemma, the cells have their own distinctive cytoplasmic components. The intercellular bridges may be open initially, but in the mature state they become ‘plugged’ with dense material. These plugs evidently provide partial barriers against the free exchange of components between the two sides, judging from the fact that the cytoplasm on either side of plugged junctions is often markedly different ([Figure 5A](#)). We recognise several categories of cells, chief of which are branched choanocytes (formerly termed ‘choanosyncytium’), archaeocytes, cystocytes and gametocytes. [Leys \(2003b\)](#) further discusses the concept of syncytiality in hexactinellids and its phylogenetic significance.

The chief sources drawn in this section are [Reiswig \(1979a\)](#) and [Leys \(1999\)](#) for *Aphrocallistes vastus*; [Mackie and Singla \(1983\)](#) for *Rhabdocalyptus dawsoni*; [Reiswig and Mehl \(1991\)](#) for *Farrea occa*; [Mehl et al. \(1994\)](#) for *Schaudinnia rosea* (reported as *S. rosea*); [Köster \(1997\)](#) for species of *Rossella* and [Boury-Esnault and Vacelet \(1994\)](#), [Perez \(1996\)](#), [Boury-Esnault et al. \(1999\)](#) and [Leys \(2003a\)](#) for *Oopsacas minuta*.

3.2. Plugged junctions

These junctions were first described in *Rhabdocalyptus dawsoni* as ‘perforate septal partitions’ or ‘plugs’ ([Mackie, 1981](#); [Mackie and Singla, 1983](#)). They have since been observed in many other hexactinellids studied by transmission electron microscopy and may be regarded as a defining feature of the group.

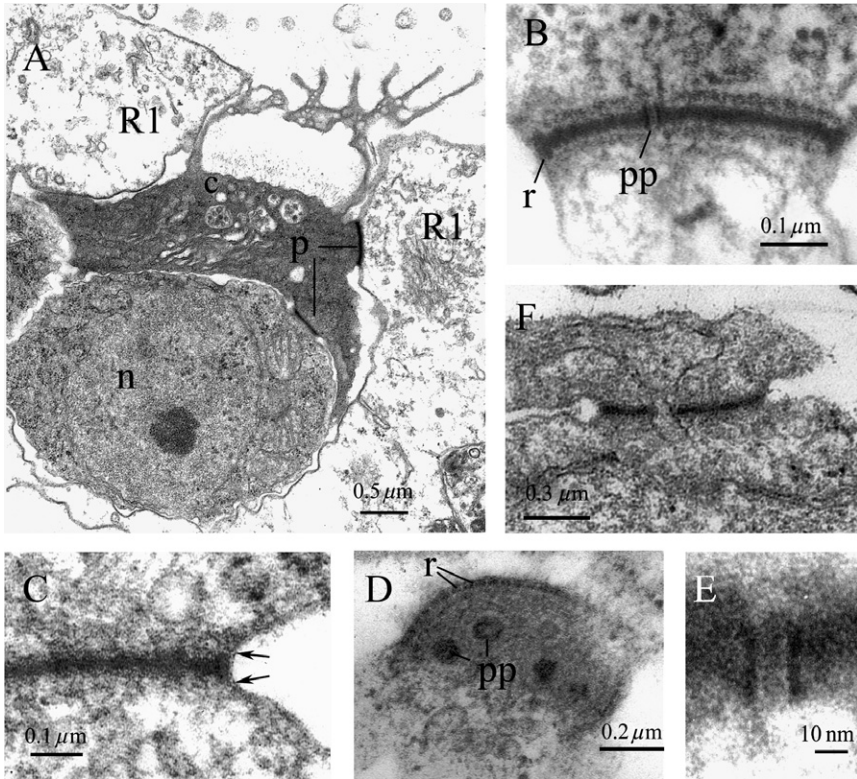


Figure 5 Plugged junctions and plug structure in *Rhabdocalyptus dawsoni* (A–D, F, from Mackie and Singla, 1983) and *Rossella racovitzae* (E, courtesy of J. Köster, 1997). (A) Developing choanocyte with a single collar body (c). The cytoplasm of the collar body is markedly darker than that of the nucleated body (n) and the trabecular syncytium (R1) to both of which it is connected by plugged junctions (p). (B) Section through a plug showing trilaminar structure revealed by chrome-osmium fixation. Rodlets (r) and pore particles (pp) are visible in the plug. (C) Section through a plugged junction showing continuity of the cell membrane (arrows) around the edge of the plug. (D) Horizontal section through a plug showing rodlets (r) and pore particles (pp). (E) Pore particle at high magnification. (F) Membrane-bounded vesicle apparently in transit through a plug.

In *Oopsacas minuta*, the equivalent structures were termed ‘dense osmiophilic junctions’ (Boury-Esnault *et al.*, 1999). In *Rhabdocalyptus dawsoni*, they are seen as flat, trilaminar plaques or discs inserted into bridges between cells (Figure 5B). The plaque is a sandwich whose outer layers consist of loose fibrous or granular material and the inner of finer, electron-dense material. The whole plaque is about 50 nm thick. No lipid bilayer has ever been observed within or enveloping the plug. In fact, the cell membrane can

be seen going around the edges of the plug (arrows in [Figure 5C](#)) joining the cell membranes of the domains on either side. Peripheral rodlets form an orderly array around the perimeter of the plug, lying closely adjacent to the cell membrane ([Figure 5B and D](#)). Structures interpreted as pore particles are also visible within the plug. In *Rhabdocalyptus dawsoni*, these seem to be hollow cylinders about 50 nm in diameter, with a 7 nm central channel ([Figure 5B and D](#)). In *Rossella racovitzae*, the central channel is given as 11 nm ([Figure 5E](#)), and there are other minor differences in the dimensions of the plug components, but the overall picture is very similar. The term pore particle implies that the central channel is a true pore but in some images it contains electron-dense material similar to that of the surrounding plug material. Finally, membrane-bounded saccules or cisternae are frequently observed apparently crossing plugs ([Figure 5F](#)). [Reiswig and Mehl \(1991\)](#) call them ‘transit vesicles’. They are probably not permanent fixtures as many plugs lack them, and it is not clear if the vesicles pass through expanded pore particles or insinuate themselves directly through the plug material.

As noted, the cytoplasm on the two sides of a plug often differs strikingly in terms of electron density and organellar content. Plugs evidently represent a barrier to the free passage of materials, allowing certain components to cross while blocking others, but no experimental work has been done to determine precisely what sort of materials can cross, or how they are selected. It is clear that plugs are not a barrier to the passage of ions, as electrical impulses can spread from the trabecular syncytium into choanocytes, bringing about flagellar arrests ([Section 5.3.3](#)).

Stages in the formation of plugs have been described in *Rhabdocalyptus dawsoni* ([Pavans de Ceccatty and Mackie, 1982](#); [Mackie and Singla, 1983](#); reviewed by [Leys, 2003b](#)). Plugs first appear as plaques of electron-dense material lying close to the nuclear membrane ([Figure 6A and B](#)). In these areas, pores in the nuclear membrane sometimes show material (presumably ribosome precursors) in transit to the cytoplasm. The plaques become associated with small vesicles in the vicinity of the Golgi complex ([Figure 6B and C](#)), but there does not appear to be any regular progression of the plaque material through the classic *cis-trans* Golgi sequence. The fate of the small vesicles is uncertain, but larger vesicles, probably of *trans*-Golgi origin, are later seen around the edges of the plaque ([Figure 6D](#)). These appear to fuse, forming a more or less complete, toroidal cisterna around the plug ([Figure 6E](#)). Pore particles can already be seen in the plaque at this stage. The plaque with its satellite vesicles or cisterna moves into a region where a narrow bridge will form connecting adjacent cytoplasmic domains. The cisternal membrane fuses with the cell membrane, lodging the plaque firmly into the equatorial region of the bridge. At this point the structure becomes a ‘plug’. Plugs are often seen attached to the cell membrane on one side only ([Figure 6F](#)),

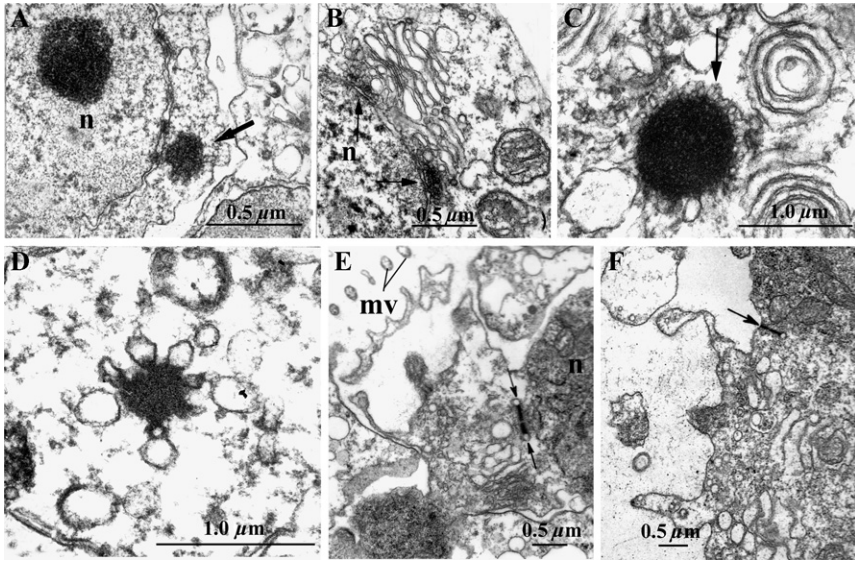


Figure 6 Formation of plugged junctions in *Rhabdocalyptus dawsoni*. A–D after Pavans de Ceccatty and Mackie (1982); E, F after Mackie and Singla (1983). (A) First appearance of plug (arrow) adjacent to pores in the nuclear membrane. (B) Early plugs (arrows) on *cis* side of Golgi complex. (C) Plug surrounded by small vesicles (arrow). (D) Plug surrounded by larger vesicles. (E) Plug still free in the cytoplasm, cut transversely, showing vesicles at the ends (arrows). (F) Plug attached to cell membrane at one end (arrow), the other still free. mv, microvilli; n, nucleus.

presumably a transitional stage preparatory to full insertion. This sequence of events is based entirely on interpretation of static images, and may be defective in some respects. For instance, if plugs eventually detach from the cell membrane and go through a recycling process some similar images might result.

3.3. Hexactinellid plugs compared with other junctions

Hexactinellid plugged junctions (Figure 7A) resemble the pit plugs of red algae and the plasmodesmata of higher plants more than they do the gap junctions of other animals. In the simplest, and presumably most primitive, algal pit plugs, the core of the plug is inserted into a narrow intercellular bridge lined by the plasma membrane (Figure 7C). In other pit plugs, caps are associated with the core on one or both sides, and cap membranes are also present, effectively isolating the core in an extracellular compartment (Pueschel, 1989). Traversing endoplasmic reticulum (ER) cisternae may be

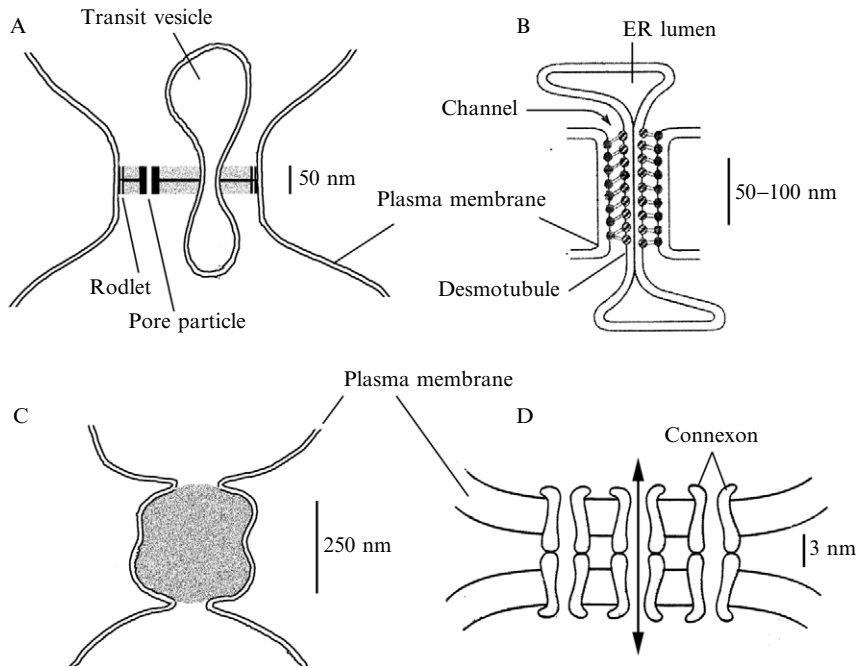


Figure 7 Intercellular junctions in animals and plants. (A) Hexactinellid plugged junction (based on *Rhabdocalyptus dawsoni*, from Mackie and Singla, 1983). (B) Plasmodesma in a higher plant (after Mezitt and Lucas, 1996, with kind permission of Springer Science and Business Media). (C) Red algal pit plug (after Pueschel, 1989). (D) Mammalian gap junction (after Goodall, 1985).

present during core deposition, but they disappear after the plug is complete. There are no reports of pores within the mature plug core and no definite information on what materials can cross, but it seems likely that the plugs allow transit of certain materials on a selective basis.

In typical plasmodesmata (Figure 7B), an ER cisterna (desmotubule) extends through a plasmalemma-lined pore. While the inner faces of the desmotubule are closely appressed, globular proteins on its outer face are loosely linked to proteins on the inner face of the adjacent plasmalemma, creating 8–10 tortuous intercellular paths (microchannels) each 2–3 nm in diameter. Thus, plasmodesmata establish both a cytoplasmic and an ER continuum that extends from the shoot apical meristem all the way down the plant axis (Mezitt and Lucas, 1996). Small metabolites, ions and signalling molecules up to about 1000 MW can pass through plasmodesmata. Viruses spread between cells by secreting movement proteins which act as carriers

for the virus's nucleic acids, which in turn produce viral replicas on reaching the other side. Interestingly, the plasmodesmal microchannels undergo dilation during viral transport, showing that plasmodesmata, like gap junctions, are labile structures.

Gap junctions (Figure 7D) are formed by transmembrane proteins that form cylindrical structures (connexons) that, when aligned in apposing plasma membranes, form a continuous aqueous channel 1.5 nm in diameter connecting the two cell interiors. Numerous such channels assemble to form a single gap junction. Gap junctions differ in permeability according to the character of the component proteins (connexins, innexins) and they can close completely. In the open state, they are freely permeable to ions, allowing electrical and dye coupling. Molecules up to about 1000 MW can also cross mammalian gap junctions.

Despite profound structural differences, it is clear that gap junctions and plasmodesmata function in remarkably similar ways, and we predict that hexactinellid-plugged junctions will prove to function similarly in regulating intercellular traffic.

3.4. Trabecular syncytium

Modern understanding of the trabecular syncytium dates from Ijima (1901) who found that the entire trabecular system in *Euplectella marshalli* consisted of a network of syncytial protoplasm, containing 'free' nuclei. This ran counter to an earlier view (Schulze, 1899) that the trabeculae and other internal surfaces were covered by a flat epithelium. Ijima thought that the 'trabecular cobweb' was probably unstable during life owing to 'protoplasmic contractility'. He regarded the trabecular system as distinct from the tissue forming the walls of the flagellated chambers, and also cellular elements (archaeocytes and thesocytes). Later work by this author (Ijima, 1904, 1927) suggested that the trabecular syncytium was a feature common to all hexactinellids. Owing to difficulties in obtaining well-fixed material, little new histological work was done on the group until Reiswig (1979a) took advantage of the availability of hexactinellids within SCUBA range around Vancouver Island, British Columbia to obtain well-fixed material of *Aphrocallistes vastus* and *Chonelasma* (now *Heterochone*) *calyx*. His optical and electron microscopic study confirmed the syncytial nature of the trabecular reticulum.

The trabecular syncytium constitutes much the greater part (ca. 75%) of the soft tissues of the sponge including the dermal and atrial membranes and it provides the interface separating the living tissues from water flowing through the sponge, except for the collars of the choanocytes which project

into the flagellated chambers. Hexactinellids lack pinacocytes, but the term ‘pinacoderm’ has been used in *Oopsacas minuta* to describe the surface layers mentioned above (Boury-Esnault and Vacelet, 1994; Perez, 1996). The trabecular tissue can take the form of flat, perforated sheets like the dermal membrane or thin trabecular strands, often $<1.0 \mu\text{m}$ in diameter. The trabecular syncytium extends into the lining of the flagellated chambers (Figure 4B) providing a supporting framework (primary reticulum, R1) for the collar bodies of the branched choanocytes (Mackie and Singla, 1983). With the possible exception of *Caulophacus cyanae* (Boury-Esnault and de Vos, 1988) and *Dactylocalx pumiceus* (Reiswig, 1991) trabecular processes also extend into the lumen of the flagellated chambers forming the secondary reticulum (R2) at the mid-collar level, while in *F. occa*, centripetal projections from R2 form yet another reticular layer, the inner membrane, at the level of the flagellar tips (Reiswig and Mehl, 1991). Reiswig’s comment (1979a) that the trabecular syncytium ‘may constitute a single, continuous cytoplasmic network throughout an entire specimen’ has been echoed by later workers and is a central concept in all discussions relating to nutrient transport and electrophysiological conduction pathways.

The trabecular syncytium contains countless small nuclei (ca. $2\text{--}3 \mu\text{m}$), several of which may be visible in transmission electron micrographs (TEM) within the same mass of cytoplasm (Figure 8A). The cytoplasm contains mitochondria, rough ER, Golgi elements, cytoskeletal components (actin filaments and microtubules) and a wide variety of vesicular inclusions including phagosomes and residual bodies from phagocytic processing. The composition of the cytoplasm varies locally, depending on activities such as wound repair, growth, regeneration and nutrient uptake.

Ijima’s suggestion (1901) that the trabecular syncytium is a labile, ‘contractile’ structure has been borne out by observation of thin pieces of living, intact sponge tissues (‘spicule preparations’) grown between glass slides and coverslips (‘sandwich cultures’, Leys, 1995; Wyeth *et al.*, 1996; Leys, 1998; Wyeth, 1999). Cytoplasmic streaming has been observed throughout the trabecular reticulum. It seems likely that the thicker tracts seen in fixed tissues, measuring up to $20 \mu\text{m}$ in diameter and termed ‘cord syncytia’ (Reiswig, 1979a), represent ‘rivers’ of actively streaming cytoplasm stabilised *in situ* by fixation. The velocity of particle transport in these bulk streams is ca. $0.33 \mu\text{m s}^{-1}$ (Leys, 2003b), some eight times faster than in thin areas of the syncytium, but within the range of values observed in plated aggregates (Leys, 1995). It now seems clear that the activities observed in the *in vitro* preparations fairly represent processes carried on *in vivo* within the trabecular syncytium and that the syncytium provides the main pathway for all forms of translocation within the sponge as well as for spread of electrical events. Transport in plated aggregates and electrical conduction are dealt with in later sections.

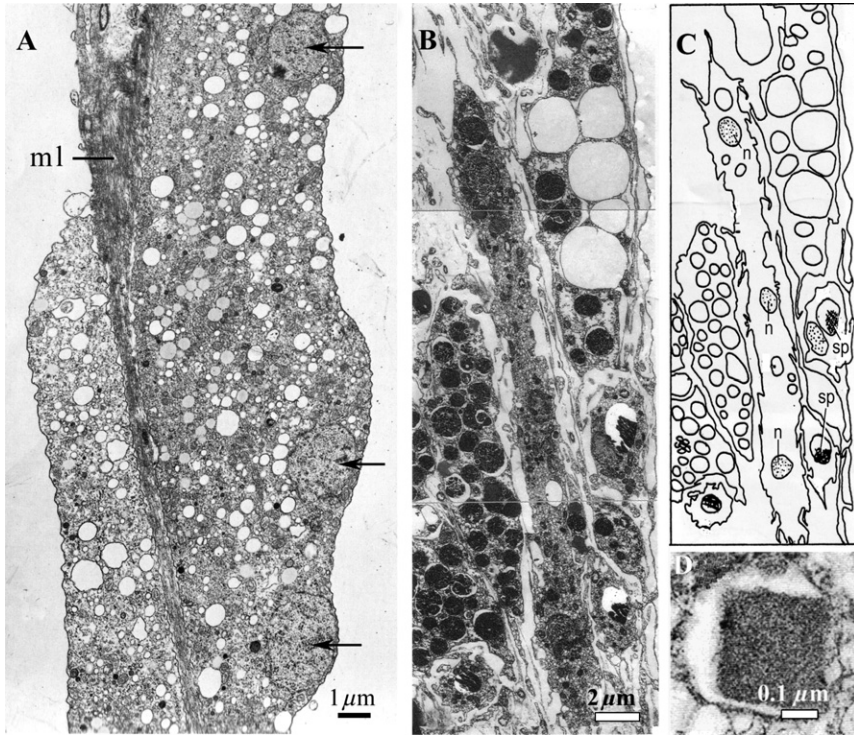


Figure 8 (A) Trabecular syncytium in *Rhabdocalyptus dawsoni* with three nuclei (arrows) in a continuous mass of cytoplasm; ml, mesolamella (from Mackie and Singla, 1983). (B, C) Sclerosyncytium in *Oopsacas minuta*. The section photographed in B passes longitudinally through a sclerosyncytium containing three nuclei in a continuous mass of cytoplasm, as drawn in C. On the right, several sclerocytes are cut transversely, showing nuclei (n) and fragments of spicules (sp) within vacuoles lined with silicolemma (after Boury-Esnault *et al.*, 1999). (D) Axial filament in a sclerocyte of *Oopsacas minuta* (from Leys, 2003a).

3.5. Sclerocytes and sclerosyncytium

In the development of *Farrea sollaris*, spicule production is described as occurring within sclerocytes, originally mononucleate but becoming multinucleate (Okada, 1928). Subsequent work on other species has confirmed that spicule production is intracellular within a syncytial structure, here termed sclerosyncytium (Figure 8B and C). Young sclerocytes in *Oopsacas minuta* embryos bear numerous, long pseudopodial extensions (Leys, 2003a). It was originally thought (Mackie and Singla, 1983) that the sclerosyncytium was completely isolated from surrounding trabecular elements, but in *Oopsacas minuta* embryos sclerocytes are connected by plugged

bridges to surrounding tissues (Leys, 2003a). Spicules develop within a silica deposition space (Section 6.5.1) bounded by a membrane (silicalemma) and containing an axial filament. Silica is probably initially deposited around the axial filament. The filament is quadrangular in cross section (Figure 8D), which determines the similar form of the completed spicule (Reiswig, 1971a). After desilication, sections of hexactinellid tissues show holes where spicules were formerly located. These sometimes contain traces of organic material, but the nature of the axial filament and other organic matter present is unknown. Spicule morphology and silication is covered in Section 6.

3.6. Archaeocytes

Typically clustered in groups, or congeries (Ijima, 1901), archaeocytes are spherical or sub-spherical cells, ca. 3–5 μm in diameter in *Aphrocallistes vastus*, *Oopsacas minuta* and *Rhabdocalyptus dawsoni* but up to 8.8 μm in *F. occa*, with densely granular cytoplasm and numerous mitochondria (Figure 9A). The Golgi component and ER are not prominent and phagosomes are rare. Archaeocytes in congeries are frequently attached to one another and to the trabecular syncytium by plugged junctions. Their rounded form and lack of pseudopodia suggest that they are not mobile like archaeocytes in sponges of other classes. It is extremely likely that archaeocytes in hexactinellids as in other sponges are pluripotent cells giving rise to various other cell types. Spermatogonia and oogonia arise within archaeocyte congeries (Section 8.1.2). The nucleated domains of the branched choanocytes closely resemble archaeocytes and are presumably derived from them, as are cystocytes according to Ijima (1901).

3.7. Cells with inclusions

Sponges have various types of cells with inclusions, some with large inclusions and some with small (Simpson, 1984; Harrison and de Vos, 1991). They go under a wide variety of names and their functions are poorly understood.

In hexactinellids, round or ovoid cells with large, empty-looking vacuoles were described in *Rhabdocalyptus dawsoni* as spherulous cells. They appear similar to the vacuolar cells (the preferred term) observed in other species. Thinly dispersed flocculent matter can be seen in the vacuole but the content is probably largely aqueous. In *Oopsacas minuta* and *Rossella nuda*, some vacuolar cells have several vacuoles rather than just one. This was also noted in *Rhabdocalyptus dawsoni* (Leys, 1996). Köster (1997) recognises two types of vacuolar cells in *Rossella nuda*, Type 1, large cells (<20 μm) with rounded

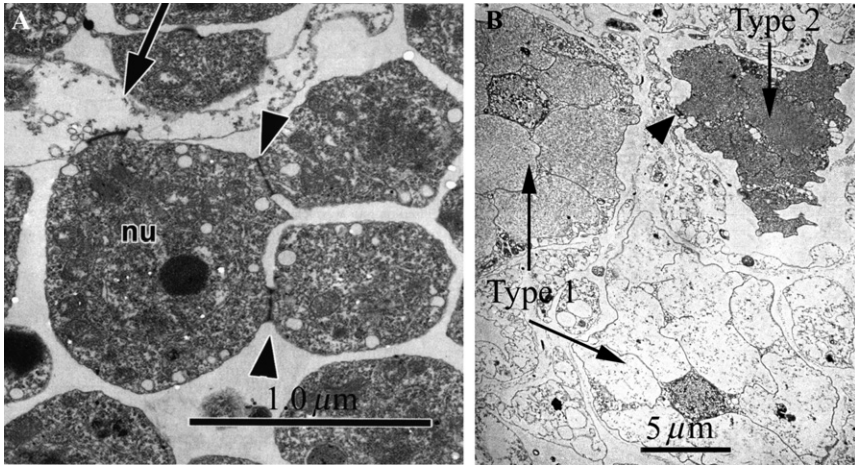


Figure 9 (A) An archaeocyte (n, nucleus) in *Rhabdocalyptus dawsoni* is attached to two other archaeocytes by plugged junctions (arrowheads) and similarly to the trabecular syncytium (arrow) (from Leys, 2003b). (B) Two types of vacuolar cell in *Rossella nuda*. Arrowhead shows a plugged junction (courtesy of E. Köster).

contours and lying within pockets in the trabecular syncytium, but not joined to them by plugged junctions, and Type 2, smaller with irregular borders and denser contents, connected to the trabecular reticulum with plugged junctions (Figure 9B). Köster's specimens were collected in late summer and vacuolar cells were very prominent in them, suggesting that they may contain nutrients stored for the Antarctic winter.

Reiswig (1979a) described thesocytes as oval or globular cells, $5 \times 7 \mu\text{m}$ to $7 \times 12 \mu\text{m}$ in dimensions, with an interior almost filled by a single homogeneous inclusion that leaves the nucleus flattened to one side in a thin peripheral layer of cytoplasm. Similar but larger ($<17 \mu\text{m}$) cells occur in *Rhabdocalyptus dawsoni*, sometimes clustered in groups. In some cases, the inclusion body contains crystals, an indication that the inclusion is proteinaceous. The cells are completely enveloped by the trabecular syncytium. Similar cells have since been described as cystocytes (the preferred term) in both *F. occa* and *Oopsacas minuta*. In *F. occa* (Figure 10A), the electron-dense inclusion contains patches of lower density crystalloid material with a regular layer spacing of 3.7 nm.

Granular cells, first observed by Schulze (1899, 1900) measure $<8 \mu\text{m}$ in *Rhabdocalyptus dawsoni* and *F. occa*, and contain numerous small ($1\text{--}2 \mu\text{m}$) electron-dense granules. Unlike cystocytes they do not lie completely within pockets of the trabecular syncytium, but are typically attached to the mesohyl and project through openings in the trabecular syncytium into the external medium (Figure 10B). In some cases, plugged junctions are seen

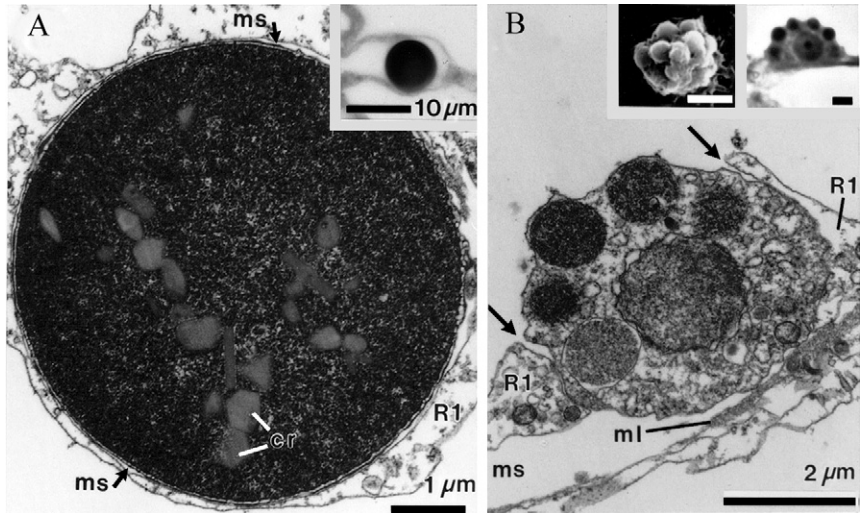


Figure 10 Cells in *Farrea occa* (from [Reiswig and Mehl, 1991](#), with kind permission of Springer Science and Business Media). (A) Cystocyte-containing crystals (cr) lying within a thin mesohyl space (ms) bounded by primary trabecular reticulum (R1). Inset shows a cystocyte seen by light microscopy. (B) Granular cell projecting from the mesohyl space (ms) through a gap (arrows) in the primary reticulum (R1). Insets (scale bars, 2 μm) show granular cells seen by scanning electron microscopy and light microscopy.

at the trabecular interface. Granular cells are also prominent in *Rossella vanhoeffeni* (reported as *Aulorossella vanhoeffeni*, [Salomon and Barthel, 1990](#)) and in *Schaudinnia rosea* (reported as *S. arctica*, [Mehl et al., 1994](#)) where they measure 10–25 μm in diameter and are densely packed along the walls of the aqueous canals. The cells show marked fluorescence with aureomycin indicating high levels of Ca²⁺ in the granules, and weaker fluorescence with calcein dyes. [Mehl et al. \(1994\)](#) suggest that the cells store lectins. These workers also note the presence of what appear to be stages in the transformation of archaeocytes into granular cells.

If vacuolar and granular cells are indeed storage sites as suggested, it would be interesting to study their abundance and distribution at different times of the year.

3.8. Choanocytes

Hexactinellids lack choanocytes of the type found in other sponges, which are compact, well-defined cells bearing a flagellum surrounded by a collar of microvilli. Instead, we find branching structures consisting of a basal nucleated

domain that sends out processes bearing separate collar bodies ('choanomeres') each resembling the apical portion of a conventional choanocyte (Figure 11A).

The terminology here has been especially problematic. The term choanoscyncytium was used by Reiswig (1979a) to describe *all* the tissues lining the flagellated chambers. Electron microscopy (Mackie and Singla, 1983) subsequently showed that the chamber wall is a composite of trabecular

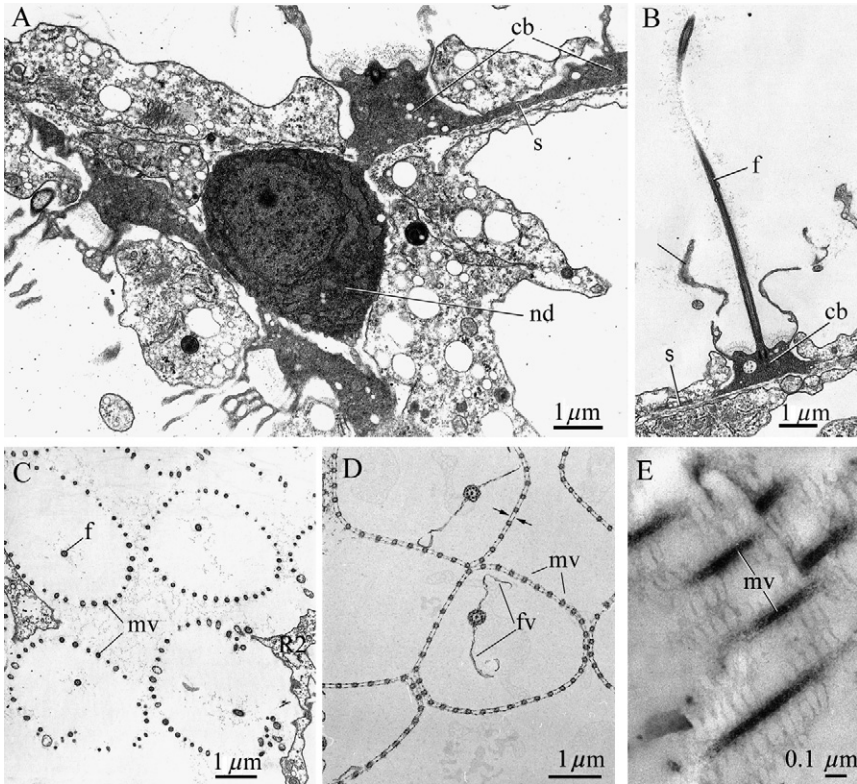


Figure 11 Structure of branched choanocytes in *Rhabdoclyptus dawsoni* (A–C, from Mackie and Singla, 1983), *Aphrocallistes vastus* (D, from Mehl and Reiswig, 1991, with kind permission of Springer Science and Business Media) and *Rossella racovitzae* (E, courtesy of E. Köster). In A, several collar bodies (cb) are shown attached by stolons (s) to a single nucleated domain (nd). This cell supplies collar bodies to two flagellated chambers. (B) Shows a collar body (cb) in a section passing vertically through the flagellum (f). Part of a stolon (s) is also visible. (C) A transverse section at the collar level shows flagellum (f) and collar microvilli (mv). (D) A similar section in *Aphrocallistes vastus* shows flagellar vanes (fv) and the mucous sheets (arrows) spanning the gaps between the microvilli (mv). (E) Mucous sheet spanning gaps between microvilli (mv) shown in a near-longitudinal section through the collar.

reticular elements and the nucleated domains ('choanoblasts') and their processes that give rise to collar bodies. The word choanosyncytium has continued in general use to refer to the nucleated cell body plus its attached collar bodies. The latter are located at the ends of cytoplasmic processes that sometimes stretch for considerable distances in the form of narrow stolons. The collar bodies may be connected to the nucleated zone by open cytoplasmic bridges, but more frequently by plugged junctions. So far as is known, only one nucleus is present in the fully formed structure although there may be three or more stolons (Figure 11A and B), each with two or three collar bodies. The exact numbers are hard to estimate, as serial reconstructions have not been carried out.

It is difficult to know what to call a complex of this sort. The term choanosyncytium is misleading, as it implies a multinucleate structure, and there is no evidence that more than one nucleus is present at any stage in the development of the complex. On the other hand, if we are dealing with a single, elaborately branched cell, it is one which has several distinct cytoplasmic domains, of which the collar bodies are segregated from the rest of the cell by plugged junctions (Figure 5A). We have earlier seen that plugs occur at intercellular junctions, but here they are clearly intracellular. Perhaps because of these anomalies, workers have continued to use the older terminology but it seems more appropriate and accurate to speak of these complex cells as *branched choanocytes*, and we will describe them as such in this account, abandoning the earlier terms choanosyncytium and choanoblast. The picture is essentially similar in *Rhabdocalyptus dawsoni*, *F. occa* and *Oopsacas minuta*, but in *Dactylocalyx pumiceus* the collar bodies appear to be completely separate structures, isolated from any nucleated structure (Reiswig, 1991).

In *Rhabdocalyptus dawsoni*, the nucleated portion of the branched choanocyte resembles a large archaeocyte having a compact, rounded form and electron-dense cytoplasm. It has a richly developed rough ER and processes run out from it leading to the collar bodies. Like archaeocytes the nucleated bodies often appear grouped in clusters, as well seen in *Aphrocallistes vastus* (Leys, 1999). The cytoplasmic strands running to the collar bodies may be short, wide, open bridges (possibly an early stage) or they may have longer process with a narrow neck containing a plugged junction. What appear to be stages in the formation of these junctions have been described, but such reconstructions are necessarily speculative (Mackie and Singla, 1983). The collar body bears a single long flagellum up to 20 μm long (Figure 11B) containing the usual 9 + 2 array of microtubules. In most hexactinellids, the flagellum has a simple form (Figure 11C) but in *Aphrocallistes vastus*, it bears wing-shaped projections (Figure 11D, 'flagellar vanes') resembling those seen in some genera of cellular sponges (Mehl and Reiswig, 1991).

In *Schaudinnia rosea* (reported as *S. arctica*), the flagella also have vanes, 1.5 μm long, and thread-like cross section (Mehl *et al.*, 1994).

A collar of 30–50 microvilli projects from the outer surface of the collar body. In *Schaudinnia rosea* (reported as *S. arctica*), the cell membrane lying between the microvilli and the flagellum bears a 300 nm thick layer of fibrous material ('glycocalyx') that is organised into distinct proximal and distal layers. Throughout the Hexactinellida, the distal parts of the collars are inserted through pores formed within the secondary reticulum and probably fit tightly enough in life to ensure that the water entering the flagellated chambers must pass between the microvilli rather than around the outside of the collar (Figure 4B). Investing the individual microvilli and spanning the gaps between them are meshes of presumed glycoprotein. In *Rhabdocalyptus dawsoni*, the material was interpreted as a 'filter' with mesh size 50 \times 200 nm (Mackie and Singla, 1983), while in *Aphrocallistes vastus*, the holes in the mesh measured ca. 22 \times 70 nm (Reiswig, unpublished data). In *Rossella racovitzae*, the filter is shown as a perforated sheet (Figure 11E), the ovoid pores measuring 45 \times 125 nm (Köster, 1997). Cross sections through the collar sometimes show the filter as a double structure, one sheet spanning the inner sides of the microvilli and the other the outer (Figure 11D, arrows; Figure 12). A double filter has also been seen in *Aphrocallistes vastus* (Mehl and Reiswig, 1991), *Schaudinnia rosea* (reported as *S. arctica*, Mehl *et al.*, 1994) and *F. occa* (Reiswig and Mehl, 1991) and may be a characteristic of all such filter structures in hexactinellids.

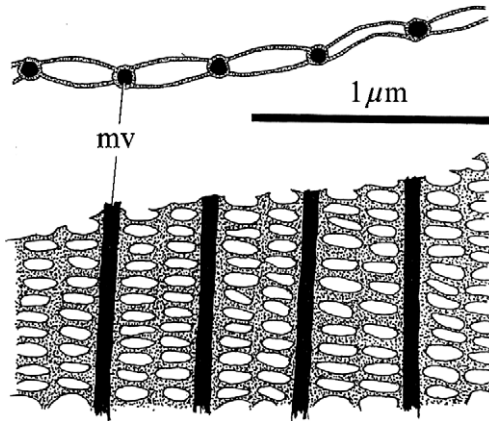


Figure 12 Mucous sheets in the collar of *Rossella racovitzae* shown diagrammatically in transverse and longitudinal section (courtesy of E. Köster).

It is clear that there is little fundamental difference between the apical structures of hexactinellid collar bodies and of choanocytes in other sponges. It is the presence of multiple collar bodies on the branches of a ramifying cell whose nucleus lies far away that makes hexactinellid choanocytes so unique.

3.9. Mesohyl

Ijima (1901) could find no evidence in *Euplectella marshalli* for anything corresponding to the mesohyl of other sponges, but a thin extracellular fibrous layer 0.05 to 0.10 μm thick was observed by Reiswig (1979a) within the trabeculae and was readily demonstrable by its acidophilic staining reaction. The fibrils composing this material showed a 45 to 50 nm periodicity. Mackie and Singla (1983) proposed that this presumably collagenous 'mesolamella' provided internal support for the trabeculae and was probably secreted by the trabecular syncytium itself, as no other cellular elements were present in many regions where it occurred. Reiswig and Mehl (1991) reach similar conclusions for *F. occa*. Dissociated cellular material from *Rhabdocalyptus dawsoni* has been found to adhere well and to spread out on surfaces coated with aqueous extracts from conspecifics (Leys and Mackie, 1994; Section 4.1). It is likely that the extracts contain extracellular matrix components deriving from the mesohyl, and that these mediate cell-substrate adhesion in the normal state of the tissue, as with jellyfish mesoglea (Schmid *et al.*, 1991). The mesohyl is found in most parts of the trabecular syncytium (Figure 8A), but it is absent in the secondary reticulum and inner membrane. As well as forming a supportive lamella within trabeculae, the mesohyl invests various discrete cells and bacterial symbionts, but there is no evidence that it provides a substrate for movement of migratory cells as seen in cellular sponges.

4. TISSUE DYNAMICS

4.1. Reaggregation of dissociated sponge tissue

Wilson (1907) first demonstrated that if a sponge is dissociated by squeezing through cheesecloth, the cells will come together and reconstitute a new sponge. The process depends on cell adhesion molecules and is homeotypic and thus of interest in relation to self–nonself recognition. Extensive studies using reaggregation models in sponges have now shown that sponges possess an effective polymorphic immune system (see reviews by Fernandez-Busquets and Burger, 1999; Müller *et al.*, 1999). Reaggregation experiments

have mostly used demosponges, although calcareous sponges and hexactinellids also reaggregate (McClay, 1972; Pavans de Ceccatty, 1982; reviewed in Simpson, 1984). Typical aggregates in demosponges form an opaque sphere of cells; in only a few cases, however, can the cells reorganise themselves into a functional aquiferous system, and only one paper documents choanocyte chambers forming in such a sponge (Van de Vyver and Buscema, 1981).

In hexactinellid sponges, dissociated tissue also forms opaque spheres (Pavans de Ceccatty, 1982). Although much of the experimental work on hexactinellid tissue has been carried out with *Rhabdocalyptus dawsoni* because of the relative ease of collecting this species, reaggregation of dissociated tissue has also been shown in *Aphrocallistes vastus* (Leys, 1998) and *Heterochone calyx* (Leys, unpublished data). The general characteristics of aggregation are similar in all three species. If a 2 cm² section is cut off the sponge and squeezed through Nitex mesh into a Petri dish, the tissue dissociates into numerous spherical pieces 5–30 μm in diameter (Figure 13). The pieces may be without a nucleus or have one or several nuclei, and some may consist of several ‘cells’ joined by cytoplasmic bridges and plugged junctions. If left in a dish of sea water at 10°C for several hours, the pieces come together to form a large opaque sphere, up to 1 mm in diameter. Transmission electron microscopy of sections of aggregates at various times after plating has shown that the tissue is continually reorganizing the cellular and syncytial components within itself (Pavans de Ceccatty, 1982) (Figure 14). Plugged junctions are commonly encountered in the process of being produced and inserted into cytoplasmic bridges between the syncytial trabecular reticulum and a variety of cellular components (Pavans de Ceccatty and Mackie, 1982).

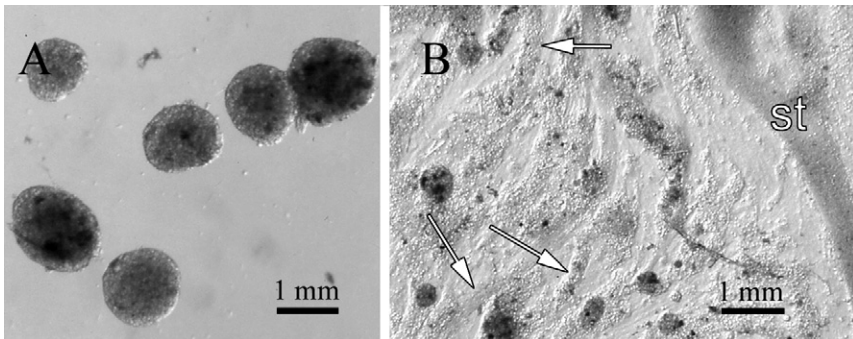


Figure 13 Live aggregates of dissociated tissue from *Rhabdocalyptus dawsoni*. (A) Opaque spherical aggregates and (B) aggregates that have adhered to a substrate coated with acellular tissue extract and in which swaths of cytoplasm (streams, st and arrows) can be seen traversing the coverslip.

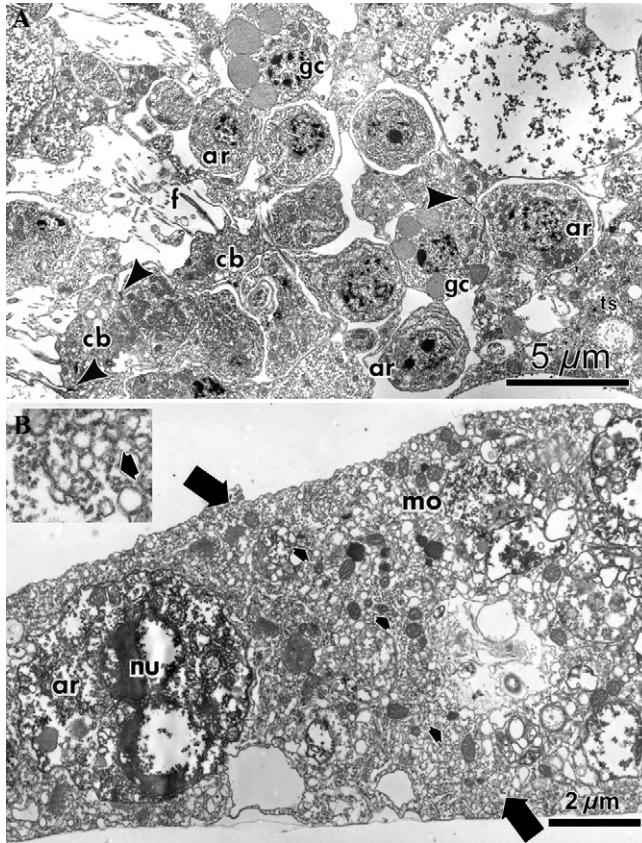


Figure 14 Electron micrographs of thin sections of adherent aggregates (*Rhabdocalyptus dawsoni*). (A) A transverse section through an adherent aggregate showing a region of stationary cytoplasm with archaeocytes (ar), collar bodies (cb) with flagella (f) and microvilli and granular cells (gc). Plugged junctions (arrowheads) connect archaeocytes to the trabecular syncytium (ts) and collar bodies to choanoblasts. (B) A cross section of an adherent aggregate shows microtubule bundles (small black arrows, and inset) form a swath from top to bottom (large black arrows) of the tissue. Microtubule bundles are always associated with numerous mitochondria and membranous organelles (mo). Other vesicles and cells such as archaeocytes (ar) with nuclei (nu) are further away from the microtubule bundles.

Although the contents of spherical aggregates can be studied by thin sectioning, this technique does not allow a view of the relationship between the multinucleate and cellular components, nor does it give a true idea of the extensiveness of the syncytial tissue.

Proof that aggregates truly form a giant cell was found by creating a thin preparation in which the tissue could be examined live by video microscopy,

and which could be fixed and preserved at various stages of fusion to illustrate the extent of the cytoskeleton. The idea for this preparation came from observations made first by Stuart Arkett, a postdoctoral fellow with George Mackie, who spent some time trying to make preparations for electrophysiology. Arkett noticed that in some instances, dissociated tissue did not roll together to form opaque aggregates, but instead, adhered to the substrate and spread out to form a thin sheet. Most remarkably, the cytoplasm in the thin sheet of tissue tracked over the substrate in continually moving streams.

The result was not readily replicable. In order to obtain a consistent preparation of adherent tissue from the glass sponge, Leys (1997) resorted to making an extract of extracellular material from the sponge itself (acellular tissue extract, ATE). The extract was made following the technique of Schmid and Bally (1988) and Schmid *et al.* (1991) for causing adhesion of cells from the hydrozoan medusa *Podocoryne*. Tissue from the sponge was rinsed briefly in calcium- and magnesium-free sea water, and soaked four times for 2 hours each in 20 times the volume of distilled water at 4°C. After the final soaking, the tissue was mechanically dissociated with a glass rod in a new volume of distilled water, causing the release of a cloudy suspension. A drop of the suspension pipetted into normal sea water coagulated into a white buoyant solid. Electron microscopy of osmium- and glutaraldehyde-fixed solid extract showed it to consist of cell debris. A tenfold dilution of the extract dried onto coverslips or petri dishes caused the species-specific adherence of dissociated tissue from sponges (Leys, 1997). In subsequent experiments, not only ATE, but also the lectin, concanavalin A (100 g ml⁻¹) and poly-L-lysine (500 g ml⁻¹) also caused adhesion of the dissociated sponge tissue.

4.2. Fusion

When plated on either the ATE substrate or the commercial lectin or poly-L-lysine, dissociated tissue pieces from both *Rhabdocalyptus dawsoni* and *Aphrocallistes vastus* adhere to the substrate and spread thinly within 5–10 s (Leys, 1995, 1998). Only 20 min after plating, the pieces begin to migrate around the dish using broad lamellipodia and long filopodia. Pieces begin to encounter each other about 1 hour after plating. Lamellipodial membranes of separated pieces first overlap for 10–30 min and then, rather than forming cell–cell junctions, the two membranes fuse; very shortly afterwards, organelles can be seen moving across the bridge. The bridge rapidly expands until the two formerly separate pieces of tissue cannot be distinguished (Figure 15). Numerous pieces of tissue join in this way, and after 12–16 hours a vast amount of cytoplasm is enclosed within a single membrane.

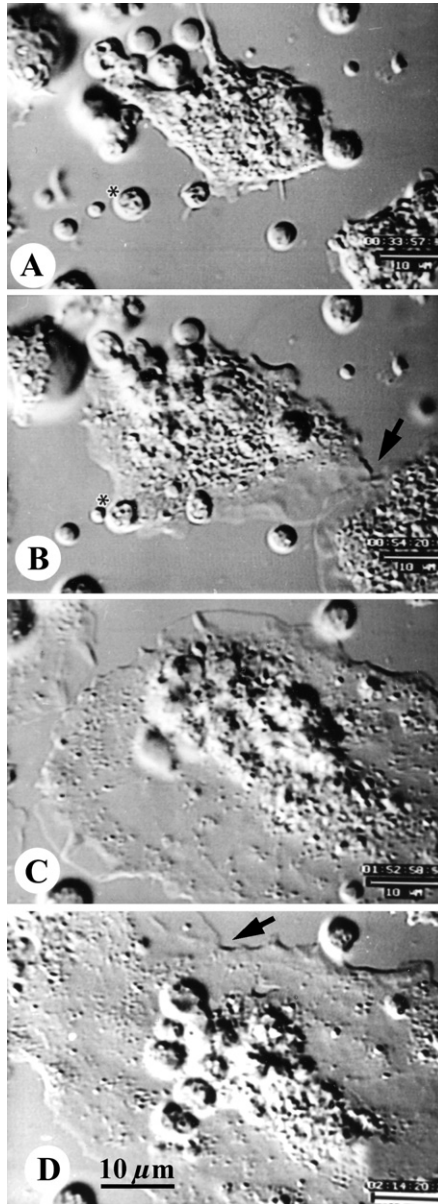


Figure 15 Video images showing fusion of adherent aggregates of *Rhabdocalyptus dawsoni* (from Leys, 1995). (A) Pieces of dissociated tissue adhere and begin to form filopodia. (B) Within 1 hour broad lamellipodia of adjacent pieces contact each other (arrow). Membranes fuse and the two pieces exchange cytoplasm, becoming a single large piece. (C) Fused pieces continue to grow and fuse with others (D, arrow). Time shows minutes after plating dissociated tissue. Asterisks indicate the same location in A and B.

Continuity of cytoplasm within a single membrane (e.g. the processes of neurons) is most frequently demonstrated by injection of cells with a fluorescent dye such as Lucifer Yellow. Unfortunately, injection proved impossible, since a stable penetration of the electrode could not be obtained, or the surface membrane adhered to and blocked the electrode. Nevertheless, by using the fluorescent acetyloxymethyl esters, calcein-AM and calcein blue-AM, which 'self load' through the plasma membrane, separate lots of dissociated tissue from the same sponge were successfully filled with blue and green dyes. When two dye lots were plated together, the tissue pieces formed aggregates that were blue-green, a mixture of the two dyes. Control experiments in which dye was loaded into the cellular sponge *Haliclona* formed aggregates consisting of a mosaic of the two colours; no exchange of dye occurred (Leys, 1995) (Figure 16).

4.3. Cytoskeleton

While video microscopy showing fusion of tissue pieces clearly demonstrates that the tissues really do form a giant cell, images of the cytoskeleton of adherent aggregates illustrate the vast size of this unusual tissue. Preservation of both the actin and microtubule cytoskeleton was not a straightforward task (Leys, 1996). Using typical fixation procedures, the microtubule cytoskeleton disassembled and could not be visualised using antibodies. Lack of antibody cross-reactivity was a problem, and phalloidins did not penetrate the membrane. Techniques developed to circumvent these problems included fixation in the presence of calcium chelators (EGTA) and microfilament stabilisers (e.g. tannic acid), use of Western blots to determine a suitable anti-tubulin antibody, and briefly lysing the adherent aggregate prior to fixation to allow penetration of rhodamine phalloidin (Leys, 1996).

One-hour-old adherent aggregates are 30–100 μm in diameter. The actin cytoskeleton consists of blunt rods (Figure 17A and B) that project out from the centre of the tissue piece (Leys, 1995). In *Aphrocallistes vastus*, the actin rods are several micrometres wide and over 20 μm long (Leys, 1998). As aggregation continues and tissue pieces fuse, aggregates have large microfilament bundles, meeting at focal points around their periphery. In day-old adherent aggregates, rhodamine phalloidin-labelled bundles of microfilaments that traversed the tissue for over 500 μm , and giant 20 μm long filopodia extended from the edges of lamellipodia (Figure 17). Scanning electron micrographs of whole and lysed adherent preparations show that each filopodium contains over a dozen actin rods 60 nm wide and over 20 μm long. The microtubule bundles become equally extensive in older adherent preparations. One hour after plating dissociated tissue from either *Rhabdocalyptus dawsoni* or *Aphrocallistes vastus*, the microtubules form a network of fine

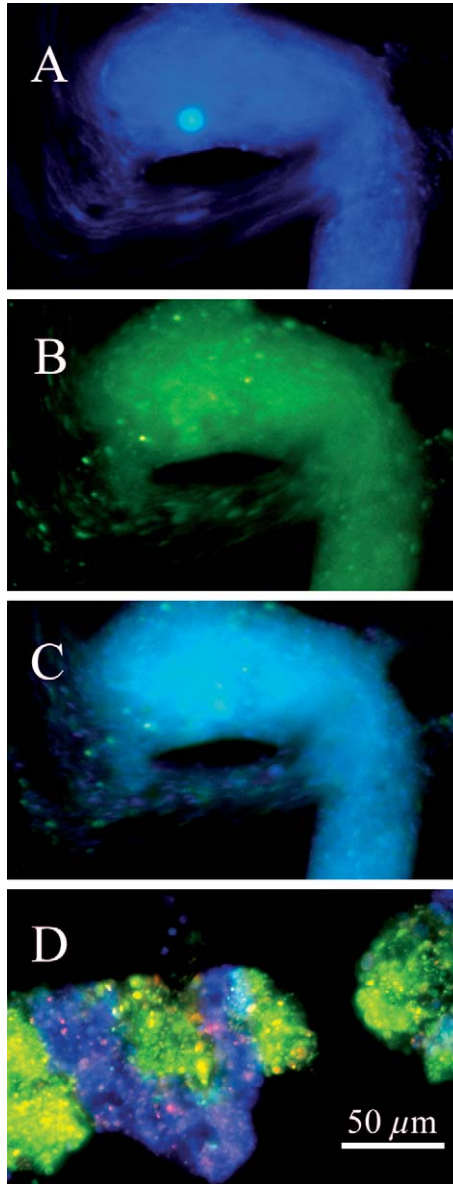


Figure 16 Dye exchange between aggregates of the glass sponge *Rhabdocalyptus dawsoni* (A–C) but not the demosponge *Haliclona permollis* (D) confirms syncytial tissues (Leys, unpublished data). Dissociated tissue from both sponges was divided into two lots, one loaded with Calcein Blue AM ester, the other with Calcein AM ester (green fluorescence). Separate lots of fluorescent tissues were mixed and allowed to continue aggregation. Mixtures of *Rhabdocalyptus* show both blue (A) and green (B)

tracks wandering throughout the 30 to 50 μm diameter aggregate (Leys, 1996). As soon as the aggregates have fused, immunofluorescence shows that multiple parallel tracks of microtubules traverse the entire preparation. Double labelling of microtubules and nuclei shows that the nuclei are randomly distributed among the microtubules; they do not form a cell soma from which the microtubules radiate. Cross sections and tangential sections of streams studied by TEM reveal large bundles of microtubules lying in parallel (Leys, 1995, 1998) (Figure 14B).

The site of nucleation of microtubules in the trabecular syncytium (or adherent syncytial tissue) remains somewhat of a mystery. Microtubule organizing centres (MTOCs, also known as centrosomes and usually distinguished by two centrioles frequently near the cell nucleus) have been found only in archaeocytes and branched choanocytes in adherent aggregates (Leys, 1996) (Figure 18). No centrioles have been found in the syncytial tissue. The

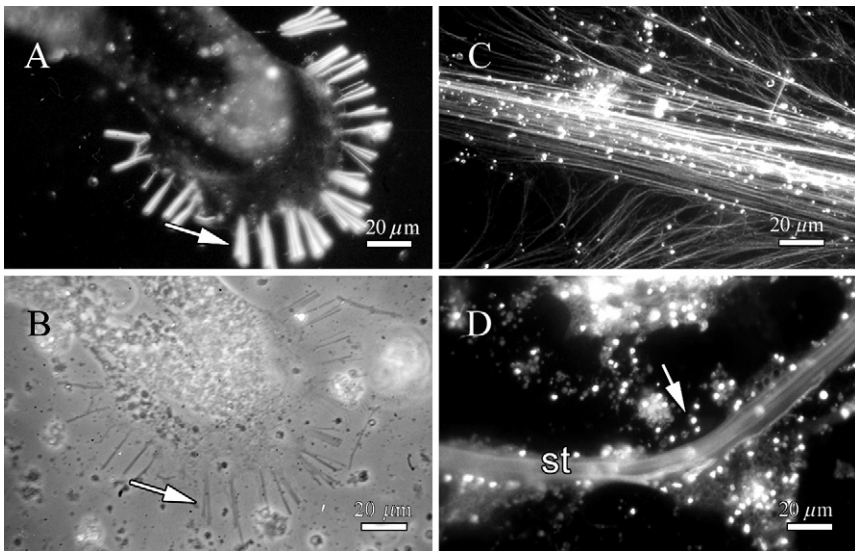


Figure 17 The actin and tubulin cytoskeleton of adherent aggregates of *Rhabdocalyptus dawsoni* (Leys, 1995). (A) Rhodamine phalloidin-labelled actin rods (arrows) at the periphery of adherent aggregates. (B) Light microscopy of the same region. (C) Microtubules labelled with anti-tubulin in an adherent preparation. (D) Nuclei labelled with Hoechst 33242 imaged in a live preparation over 30 s, shows them moving along streams (st) and in the stationary cytoplasm (arrow).

fluorescence throughout, giving the aggregate a blue-green hue (C). Mixtures of dye-loaded cells from the cellular sponge *Haliclona* (D) aggregate but do not exchange the dye, forming chimeras of blue and green aggregates.

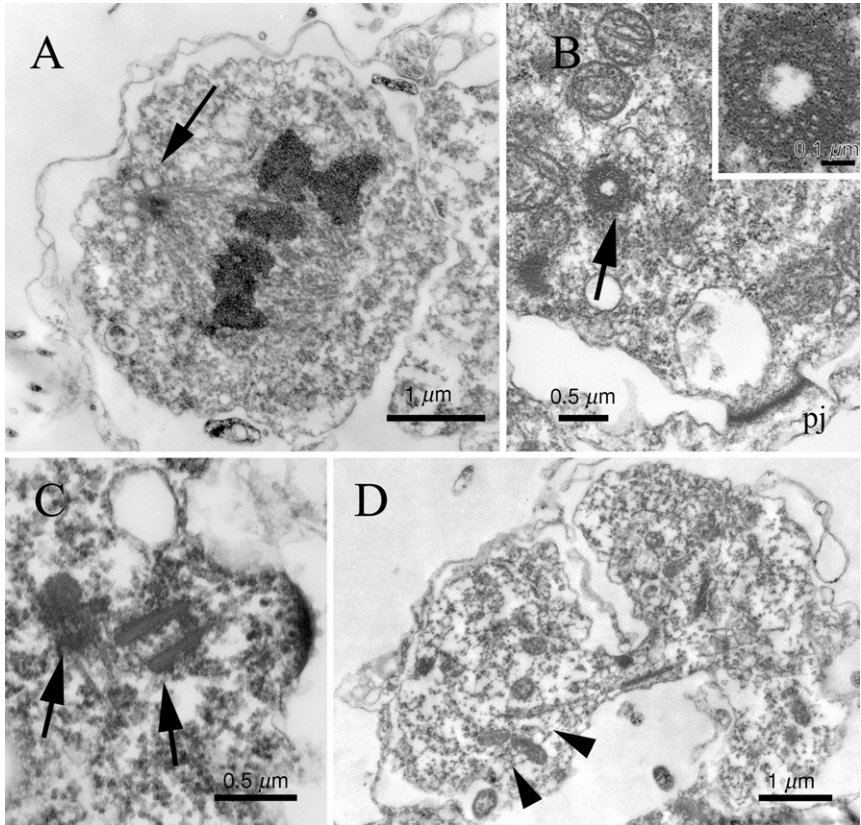


Figure 18 Centrioles and cell division in *Rhabdocalyptus dawsoni* and *Aphrocalistes vastus* (transmission electron microscopy). (A) Chromosomes on the mitotic spindle in a dividing archaeocyte in an aggregate of *Rhabdocalyptus dawsoni*. Note the vesicles clustered around the centriole visible on the left (arrow). (B) Centriole (arrow, enlarged in inset) in an archaeocyte connected to the trabecular syncytium by a plugged junction (pj). (C) Two centrioles (arrows) in an archaeocyte in *Rhabdocalyptus dawsoni*. (D) Archaeocytes dividing in an aggregate from *Rhabdocalyptus dawsoni*. Thread-like fibres (arrowheads) appear to anchor a central shaft of microtubules (arrow) (Leys, unpublished data).

fact that nuclei are transported along microtubules suggests there are no fixed regions of the cytoplasm, and thus no specific locations for nucleating microtubule formation. The freshwater foraminiferan *Reticulomyxa* also lacks centrioles and a readily identifiable MTOC. But the polarity of microtubules (inferred from the direction of microtubule assembly and organelle transport) suggests that microtubule nucleation is controlled by gamma tubulin located in the cell body (Koonce *et al.*, 1986; Kube-Granderath and Schliwa, 1995).

In other cells with extensive tracts of microtubules (e.g. neurons), nucleation occurs in the cell body and microtubules are transported as polymers to neurites (Yu *et al.*, 1993), but polymerisation of microtubules can also occur locally in neurites (Miller and Joshi, 1996).

Centrioles also play a role in organizing spindle poles during cell division. Centrioles and spindle fibres were not uncommon in TEMs of archaeocytes in aggregated tissue from both *Rhabdocalyptus dawsoni* and *Aphrocallistes vastus* (Leys, 1996) (Figure 18). Vesicles were clustered around the centrioles of dividing cells in *Rhabdocalyptus dawsoni*, and similar vesicles were found around centrioles in sections of the adult tissue from *Aphrocallistes vastus*. The cluster of vesicles is most like that found around the newly forming plugged junction (Section 3), and if so, then perhaps membrane is recruited for the daughter cells in this manner. Although one or two archaeocytes in a single aggregate may divide synchronously, by no means do all archaeocytes undergo mitosis synchronously, despite connections by cytoplasmic bridges. Nuclei in the trabecular tissue were not found dividing, and it is possible that these nuclei might be terminal like the nuclei of myoblasts after fusion (Wakelam, 1988; Leys, 1996). This is a question that could readily be followed up by using markers such as Bromodeoxyuridine that incorporate into new nuclei.

4.4. Organelle transport

Almost immediately after fusion of the first membranes of tissue pieces, organelles can be seen moving across the bridge between the pieces (Leys and Mackie, 1994). Within a few hours of plating dissociated tissue, the moving cytoplasm is organised into vast channels up to 20 μm in diameter, which move steadily and unceasingly around the adherent aggregate. In live preparations broken spicule pieces can be identified moving in bulk streams, and preparations labelled with the fluorescent stain Hoechst 33242 and photographed with an extended exposure of 30 s show that the nuclei are transported within cytoplasmic streams (Leys, 1995) (Figure 17D).

The streams of cytoplasm in adherent preparations are constantly changing. They can increase in diameter by merging with other streams, run parallel but in the opposite direction to other streams and cross over other streams without any apparent interruption in volume or velocity of flow (Leys, 1995). The distance any one stream can travel is limited only by the area of the substrate. Using Nomarski optics, individual organelles, as well as bulk cytoplasm can be seen moving along the thinnest areas of the adherent aggregate. The rate of transport is fairly constant for individual organelles and bulk transport in streams: $2.15 \pm 0.33 \mu\text{m s}^{-1}$ in *Rhabdocalyptus dawsoni*

(Leys, 1995) and $1.82 \pm 0.15 \mu\text{m s}^{-1}$ in *Aphrocallistes vastus* (Leys, 1998). Rates were significantly faster at the edge ($2.01 \pm 0.44 \mu\text{m s}^{-1}$) of a bulk stream than at the middle of the stream ($1.71 \pm 0.29 \mu\text{m s}^{-1}$, $n = 31$, $p = 0.008$) (Figure 19) (Leys, 1996). Movement of organelles in lamellipodia differs, however. In these areas, individual organelles depart from the steady tracts and begin a saltatory motion, moving rapidly at times, halting and then continuing at a much slower rate (Figure 20). Rates of transport here are much slower ($0.32 \pm 0.11 \mu\text{m s}^{-1}$). Pharmacological experiments suggest that the movement of bulk cytoplasm occurs along microtubules. Cytoplasmic streaming can be inhibited by nocodazole ($1 \mu\text{g ml}^{-1}$) and colcemid ($10 \mu\text{g ml}^{-1}$), both of which inhibit microtubule polymerisation, but not by cytochalasin B ($10 \mu\text{g ml}^{-1}$), which causes microfilament depolymerisation (Leys, 1995). However, not all organelles moving in a stream are directly attached to microtubules. Electron micrographs of thin sections show numerous membranous vesicles around microtubules and reaching several micrometres out into the cytoplasm (Leys, 1996). Negative stain electron microscopy of adherent pieces captures the interaction between organelles on the microtubules and those pulled along by membranous organelles, much as occurs in characean algae (Kachar and Reese, 1988) (Figure 21).

The mechanism of streaming is of interest given the basal position of the Hexactinellida within the Metazoa. Inhibition by nocodazole and colcemid clearly indicates that bulk streams are transported along microtubule tracks. However, transport within the thin lamellipodia is much slower, and has a saltatory nature, more resembling actin-based transport mechanisms (Bearer *et al.*, 1993). Unfortunately, attempts to determine which motor proteins might be involved in either bulk streaming or saltatory lamellipodial organelle transport have not been very successful so far. Most drugs that inhibit motor activity do not penetrate the plasma membrane. Hence, typical methods for identifying motor proteins involve permeabilizing the plasma membrane with a mixture of gentle detergents in a solution of ATP, and then application of a variety of inhibitors. Attempts were made to lyse and reactivate the preparation using combinations of five different buffers, five different detergents and varying the pH (Leys, 1996). Western blots showed immunoreactivity of cell lysate from *Rhabdocalyptus dawsoni* to two antibodies to cytoplasmic dynein (M74-1 and M74-2), but none to two antibodies to kinesin (SUK4 made against sea urchin kinesin and K1005 made against kinesin in the foraminiferan *Reticulomyxa*) (Leys, 1996).

Movement of individual organelles and of bulk streams of cytoplasm is also evident in pieces of tissue that have been pulled off the intact sponge and allowed to regenerate between a coverslip and slide in 10°C sea water (Leys, 1998). One might think that cytoplasmic streaming is a phenomenon of regeneration, and streaming of cytoplasm is likely the means by which the animal transports materials to repair wounds *in situ*. But transmission

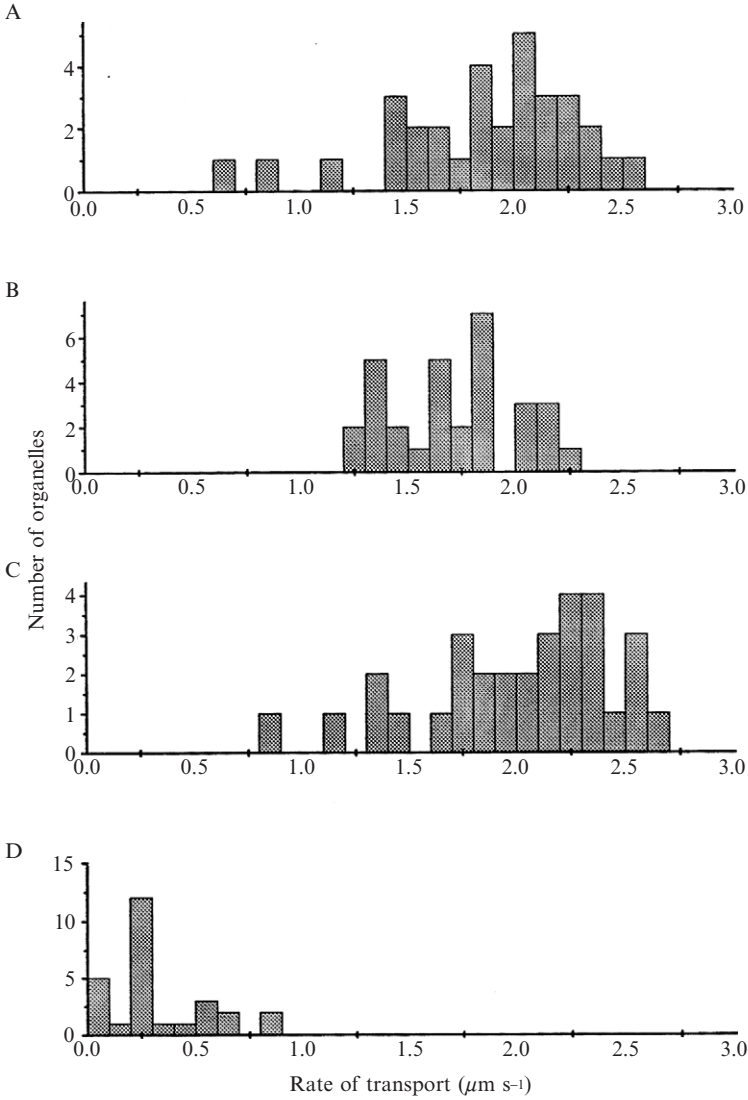


Figure 19 Rates of transport of four classes of organelles in adherent aggregates from *Rhabdocalypus dawsoni* (Leys, 1996). (A) Single organelles moving at a constant velocity. Organelles moving at a constant velocity in the middle (B) and edge (C) of bulk streams. (D) Organelles moving by saltation in lamellipodia (32 measurements were made at each location).

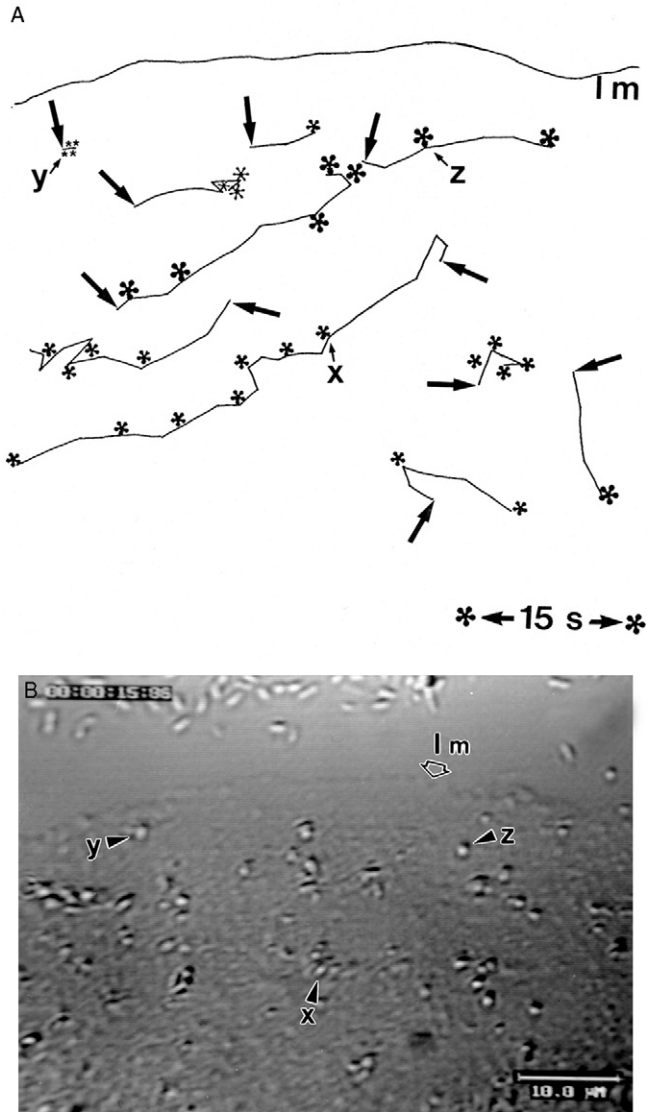


Figure 20 Saltatory movement of organelles in a broad lamellipodium (lm) of an adherent tissue culture, imaged by video microscopy (from Leys, 1996). (A) Arrows indicate the starting point of organelles at $t = 0$ and asterisks show the position of each organelle at 15-second intervals. (B) A single image showing the position of organelles x, y and z at $t = 15$ s.

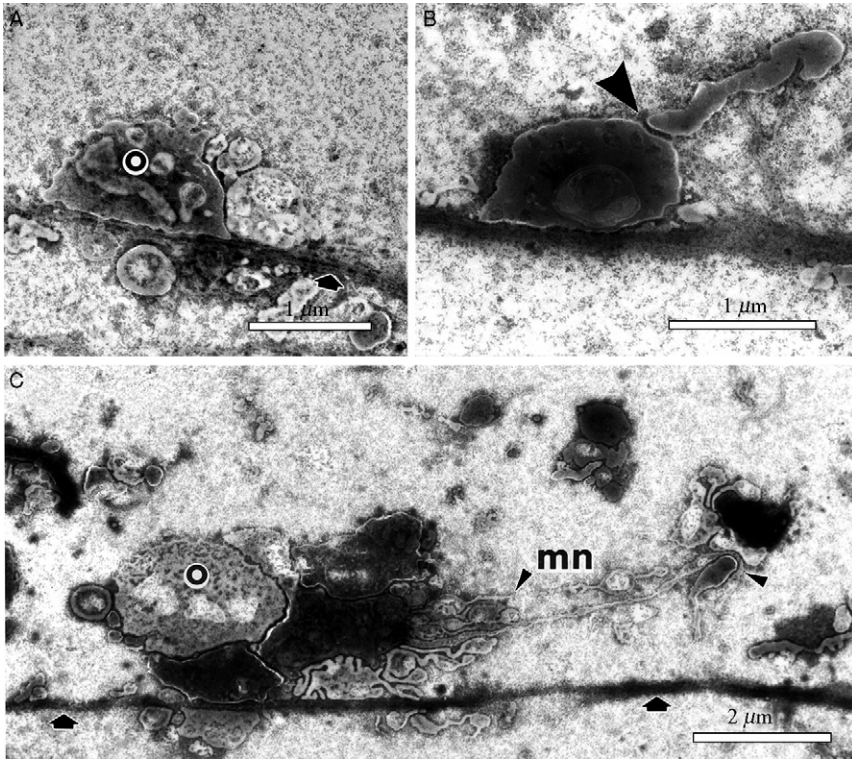


Figure 21 Membranous networks link organelles to fibrous tracks in adherent tissue of *Rhabdocalyptus dawsoni* as revealed by negative stain electron microscopy (from Leys, 1996). (A) Organelles (o) abut fibrous tracts (arrows), and contact other organelles directly (B, arrowhead), or (C) are attached to a membranous network (mn) (arrowheads) that is in contact with the fibrous tracts.

electron microscopy has shown that the content of the cytoplasm in bulk streams in adherent tissue and regenerating preparations is the same as that described as ‘cord syncytia’, regions of the trabecular reticulum of the whole animals (Reiswig, 1979a). Streaming is also visible in sandwich preparations of both *Rhabdocalyptus dawsoni* and *Aphrocallistes vastus* (Wyeth *et al.*, 1996; Leys, 1998; Wyeth, 1999). Thus, ‘streaming’ in itself is probably a normal feature of adult sponge physiology.

4.5. Comparison with cellular sponges

The role of cytoplasmic streaming in nutrient uptake in glass sponges is discussed in Section 5. This is one of the fundamental differences between the

cellular and syncytial organisation. Whereas intrasyncytial transport allows nutrients to be moved over distances of many centimetres within a single cytoplasm, in a cellular system nutrients must be passed to cells that are capable of movement and which migrate through the collagenous mesohyl presumably to distribute the nutrients (Vosmaer and Pekelharing, 1898; Van Tright, 1919; Willenz and Van de Vyver, 1982, 1984; Imsiecke, 1993). Analogues of the cytoplasmic streams—nutrient transport pathways many centimetres in length—exist in cellular sponges as discrete strands of elongate cells that are embedded in collagen (Leys and Reiswig, 1998). Cells in such strands can transport nutrients, but the process occurs by the crawling of individual cells and takes up to 1–2 weeks to traverse a distance of approximately 20 cm. Movement of organelles *within* the cytoplasm (intracellular transport) occurs over much smaller distances (some 10–50 μm) in cellular sponges, but the basic mechanism of transport is much the same as in hexactinellids. In the freshwater sponge, *Spongilla lacustris*, mitochondria are transported from a centrally located nucleus towards the cell periphery and back along microtubules, as in other animal cells (Weissenfels *et al.*, 1990). Also, as in other metazoans, both microtubules and microfilaments have been implicated in the movement of the Golgi apparatus (Wachtmann *et al.*, 1990; Weissenfels *et al.*, 1990; Wachtmann and Stockem, 1992a,b). There is one report of cytoplasmic streaming seen during the reaggregation of cells of *Microciona prolifera* (Reed *et al.*, 1976), but because the aggregates were demonstrated to be cellular using scanning electron microscopy, it has been supposed that Reed *et al.* (1976) were referring to the intracellular movement of organelles within each cell (Leys, 1996).

4.6. Immune response

A calcium-dependent cell adhesion molecule was isolated from *Aphrocallistes vastus* and shown to agglutinate preserved cells and membranes in a non-species-specific manner (Müller *et al.*, 1984). Subsequently, two C-type lectins with molecular weight of around 22 kDa have been purified from the isolate (Gundacker *et al.*, 2001). It is suggested that the lectins bind to the cell membrane by the hydrophobic segment and interact with carbohydrate units on the surface of other cells and syncytia. The finding that the aggregation factor from *Aphrocallistes* works in a non-species-specific manner implies that glass sponges differ from cellular sponges in lacking either individual or species-specific immunoreactivity. Two experiments suggest this is not the case. Dissociated tissue from a selection of cellular sponges does not adhere to the ATE made from *Rhabdocalyptus dawsoni* (Leys, 1997), as would otherwise be expected if species un-specific binding were the case. Evidence

for recognition of individuals of the same species comes from the unusual 'graft' preparation that was developed to allow extracellular recording of electrical events in the sponge (Leys and Mackie, 1997) (Section 5). If aggregates are made from one individual and placed on a slab of the body wall of a different sponge, no fusion between aggregate and host occurs. In fact, the cytoplasm from the host sponge 'thickens' directly under the aggregate as though the animal was transporting to the site of interaction material that causes the rejection of the non-host tissue. The only successful grafts are those that are made between aggregate and host from the same individual. Thus, glass sponges do possess molecules on their membranes that are capable of recognizing and rejecting tissue from other individuals of the same species.

5. PHYSIOLOGY

5.1. Hexactinellids as experimental animals

Most hexactinellids are adapted to life in deep-water habitats (Tabachnik, 1991) or in submarine caves (Vacelet *et al.*, 1994) and subsist on a meagre supply of organic matter originating in surface waters far from their natural habitats, or possibly in a few cases benefiting indirectly from primary production at hydrothermal vents (Boury-Esnault and de Vos, 1988). Most are probably unaffected by diurnal or even seasonal changes and few are built to withstand the mechanical stresses associated with high-energy shallow water environments. Collecting and transporting specimens to the laboratory has to be done with extreme care, avoiding temperature increases, mechanical stresses and introduction of air bubbles into their interiors. Once in the laboratory, they must be kept cool and disturbed as little as possible. The critical role of temperature is illustrated by the findings that in *Rhabdocalyptus dawsoni* pumping is abolished below 7°C and arrests, which are normally exhibited by healthy specimens, are unusual above 12°C (Leys and Meech, 2006).

To date, the only place in the world where specimens have been kept alive in good physiological condition for long periods is the Bamfield Marine Sciences Centre in Barkley Sound, British Columbia, where a continuous supply of high-salinity, cold sea water is pumped into the laboratory from 35 m depth, not far from where *Rhabdocalyptus dawsoni* occurs naturally. As a species adapted to relatively shallow water (>25 m), *Rhabdocalyptus dawsoni* is rugged enough for laboratory research. Specimens have been maintained in the Bamfield sea water system at 10°C with only the food

brought in with the laboratory water supply. Gaseous supersaturation of the water proves fatal, as bubbles rapidly fill up the water passages in the sponge. Movement to aquaria in other laboratories has been attempted with little success. Transported to the University of Washington Laboratories at Friday Harbor, *Rhabdocalyptus dawsoni* rapidly deteriorated and became moribund. The water there, though drawn freshly from the sea, is warmer and generally of lower salinity than that at Bamfield.

Although useful results have been obtained on specimens of *Rhabdocalyptus dawsoni* and *Aphrocallistes vastus* kept in aquaria at the University of Victoria, conditions there are far from ideal. In Wyeth's (1996) sandwich culture work (see below), the preparations deteriorated after 2 weeks. Attempts to improve longevity by providing additional food, artificially circulating the water or cooling it below 10°C were unsuccessful. The flagellated chambers of *Rhabdocalyptus dawsoni* kept in this system all became compartmentalised by inner membranes (Leys, 1999). Viable aggregates could be obtained from dissociated sponge tissue (Leys, 1995), but only very rarely did the aggregates mature into recognisable sponges with oscula. The most obvious sign of physiological deterioration, however, was the loss of the sponges' ability to arrest their feeding currents, which rendered them useless for electrophysiological experiments on the conduction system.

Oopsacas minuta, collected from a submarine cave near La Ciotat and transported under controlled temperature conditions to sea water tanks at the Station Marine d'Endoume, Marseille, were kept at 13°C and proved useful for short-term studies of particle retention (Perez, 1996), but it appears that no solution has yet been found to the problem of long-term maintenance in this species.

Until the water conditions necessary for long-term culture of hexactinellids are better understood, workers on these animals will probably have to go to marine stations located close to the sponges' natural habitat and offering appropriate culture facilities.

5.2. Food and wastes

It has always been assumed that hexactinellids like other sponges are filter feeders, removing particulate matter from the incurrent water stream, but until recently there has been little exact information on what is taken up. In a study comparing the composition of exhalent water from the atrial openings with ambient (inhalent) water, Reiswig (1990) showed that *Aphrocallistes vastus* retained particulate material, including bacteria, as its primary organic carbon source (89% of the total) and made relatively little use of dissolved organic carbon (11%). In a study of *Aphrocallistes vastus* and

Rhabdocalyptus dawsoni in laboratory tanks, [Yahel et al. \(2007b\)](#) found that bacteria and protists accounted for the entire uptake of organic carbon. The sponges showed surprising evidence of size-independent selectivity ([Figure 22](#)). Small, non-photosynthetic bacteria ($<0.4 \mu\text{m}$) and eukaryotic algae ($3\text{--}5 \mu\text{m}$) were removed with almost equal efficiency, but the retention of intermediate-sized bacteria varied seasonally and was sometimes much less

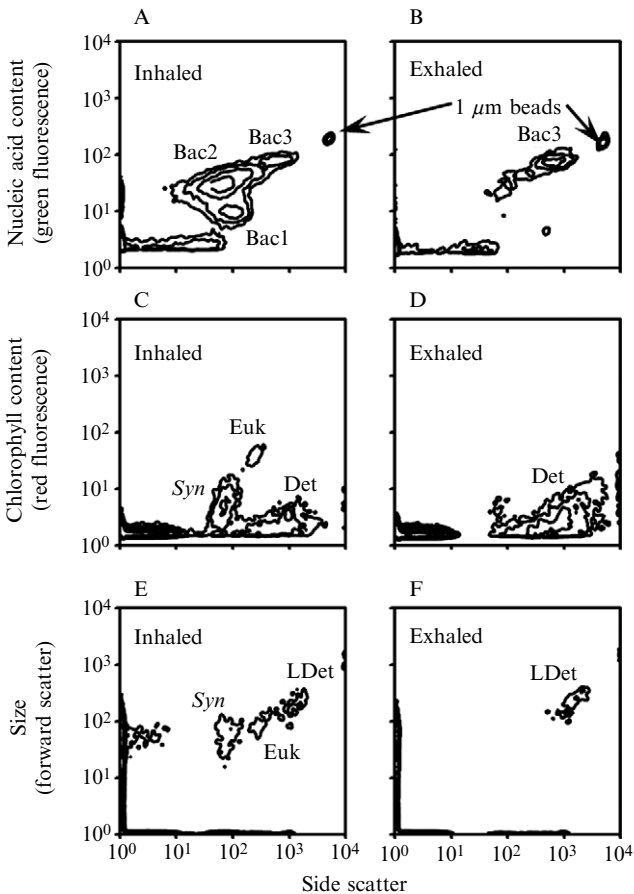


Figure 22 Flow cytometry analysis of inhalant and exhalant water in *Aphrocalistes vastus*. (A, B) Of three populations of bacteria the smaller ones (Bac1, 2) were selectively retained in preference to larger bacteria with higher nucleic acid content (Bac3); $1 \mu\text{m}$ beads are for reference. (C, E) Both eukaryotic algae (Euk) and a cyanobacterium *Synechococcus* (Syn) were present in the inhalant water, along with detritus (LDet), but only detritus was present in the exhalant water (E, F) (courtesy of G. Yahel).

efficient. An intermediate-sized cyanobacteria, *Synechococcus* (1.1–1.5 μm), was also retained less efficiently.

While the sponges in these experiments efficiently removed up to 99% of the smallest and most abundant bacteria and up to 94% of the eukaryotic algae, the amount of detritus present in the exhalent water was not reduced, indeed it was greater than in the ambient water. Clearly, the sponges have some way of getting rid of the detritus as fast as it is brought in with the feeding current. How they do so is unclear, but two possibilities can be considered: (1) indigestible particles are somehow recognised in their passage through the inhalant water passages and allowed to pass directly into the exhalent stream around the edges of the collars or by special 'bypass routes', possibly equivalent to those described on the basis of latex injection preparations (Bavestrello *et al.*, 2003) and (2) indigestible particles are taken up by endocytosis along with digestible, and are then transported through the cytoplasm and egested into the exhalent stream. The first possibility is hard to reconcile with the extraordinarily high retention rate for the smallest category of bacteria. If bypass routes existed, it would be expected that large numbers of bacteria would slip through them along with the detritus. The second proposition is therefore more plausible. It implies that the sponges endocytose all particles indiscriminately but then sort them out intracellularly, targeting the vacuoles containing detritus along exit routes, while breaking down the digestible material in phagosomes. Indigestible residues from intracellular digestion would also be egested, which would explain the fact that the detritus fraction was larger in the exhalent water than in the inhalant. A way of testing these two propositions might be to feed sponges on readily identifiable indigestible particles (e.g. polystyrene beads) and determine how long it takes for the particles to appear in the exhalent water. If they appeared within a few seconds it would support proposition (1) above. If it took a few minutes, (2) would appear more likely.

Microscopic observations on *Rhabdocalyptus dawsoni* (Wyeth *et al.*, 1996) showed that the sponge phagocytised not only *Escherichia coli* and *Isochrysis galbana* but also latex beads. Similarly, *Oopsacas minuta* took up both phototropic sulphur bacteria (1.0–6.0 μm) and latex beads (0.5–1.0 μm), although tentative estimates based on colorimetry suggested that the sponge 'preferred' bacteria to latex beads (Perez, 1996). Beads smaller than 0.1 μm diameter were not retained at all. These observations are consistent with the idea that inorganic particles are phagocytised along with organic and with the evidence for selectivity covered above.

In a study on *Aphrocallistes vastus* and *Rhabdocalyptus dawsoni* carried out with inhalant and exhalent water collected *in situ* from the sponges at 120 to 160 m depth using a remotely operated vehicle, Yahel *et al.* (2007a) were able to assess removal of bacteria and protists along with excretion of

nitrogenous waste in the natural environment. The water at this depth contained a high inorganic sediment load and little phytoplankton compared with the water from nearer the surface used in the tank study. Both sponge species collected bacteria, removing up to 95% of them (median efficiency 79% in both cases). Heterotrophic protists (4–10 μm) were also efficiently removed and contributed ca. 30% of the total organic carbon uptake. Neither in tank experiments nor in the *in situ* study was evidence found for uptake of dissolved organic carbon and the entire organic carbon uptake along with excretion of ammonium could be accounted for on the basis of organic particulates. Surprisingly, given that silica constitutes nearly 80% of the dry weight of a hexactinellid such as *Aphrocallistes vastus*, silica uptake was below detection levels in the study by Yahel *et al.* (2007a), but this can be attributed to the slow growth rate of the sponges (Section 7.4).

Ectosymbiotic diatoms have been suggested as a source of nutrition in the case of *Rhabdocalyptus racovitzae*, where Cattaneo-Vietti *et al.* (1996) propose that long spicules act as optical fibres collecting and delivering light to diatoms in the sponge's interior. Whether they actually function in this capacity (which seems doubtful, Section 7.7), a study of the basalialia of *Euplectella marshalli* shows that they have the structural properties of optical fibres and are capable of acting as light pipes (Sundar *et al.*, 2003; Aizenberg *et al.*, 2005). In *Hyalonema sieboldi*, spectral transmission studies suggest that the stalk spicules filter out wavelengths below 615 nm (Müller *et al.*, 2006). As it is these shorter wave lengths that penetrate deepest in sea water, it seems unlikely that the spicules are adapted for detection of light coming from the surface. Equally, the reduction of transmission below 615 nm argues against spicular transmission of bioluminescent emissions from deep-sea organisms, which typically peak in the range 460–490 nm (Nicol, 1967).

The upper size limit for particles entering the sponge is presumably set by the pores (ostia) in the dermal membrane, the thin, flat sheet covering the outer surface (Figure 23A). In *Rhabdocalyptus dawsoni*, the pores, as seen in living and osmium-fixed preparations, are 4–20 μm in diameter (Mackie and Singla, 1983). Once inside the sponge, there would be nothing to impede passage through the trabecular strands, which are thin and far apart (Figure 23B). Access to the flagellated chambers would require passage through prosopyles (Figure 23C) which have an average diameter of 4.5 μm in *Rhabdocalyptus dawsoni* (Leys, 1999). The dermal pores and prosopyles are not associated with circular bundles of contractile filaments and there is no evidence from observations on living material that hexactinellids can open or close these structures, or not in the short term. Particles too large to enter the flagellated chambers are presumably phagocytised by the trabecular syncytium.

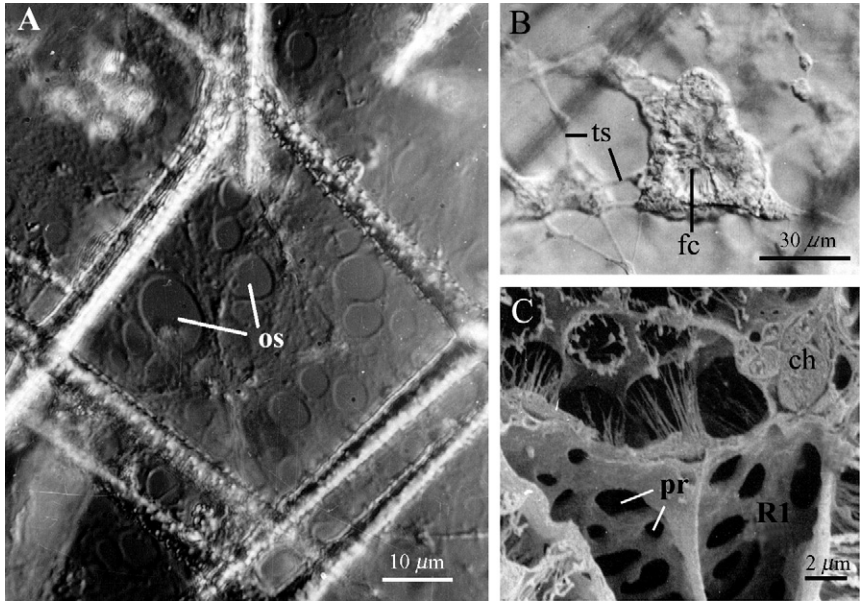


Figure 23 Pores in the inhalant pathway (*Rhabdocalyptus dawsoni*). (A) Ostia (os) in the dermal membrane as seen in a living preparation by Nomarski interference microscopy (from Mackie and Singla, 1983). (B) Wide channels are seen *in vivo* between the trabecular strands (ts) surrounding a flagellate chamber (fc) (from Wyeth *et al.*, 1996). (C) Prosopyles (pr) in the primary reticulum (R1) shown by scanning electron microscopy; ch, choanocyte cell body (from Leys, 1999).

5.2.1. Particle endocytosis

Uptake could in theory occur at any point in the pathway through the sponge, which includes all the water channels bounded by the trabecular syncytium. In *Rhabdocalyptus dawsoni*, phagocytosis of latex beads has been observed in the syncytial strands of plated aggregates, which can be taken as a model of the trabecular syncytium (Leys, 1996). Beads began to change position within 15 min of uptake and after 30 min many were moving in cytoplasmic streams. In sandwich cultures of the same species however, uptake of latex beads, as determined using differential interference contrast and fluorescence microscopy, appeared to be concentrated almost entirely in the vicinity of the flagellated chambers (Wyeth *et al.*, 1996). Only very rarely were beads seen moving in streams far from flagellated chambers. Electron microscopy confirmed the presence of internalised beads in vesicles within the trabecular syncytium close to flagellated chambers.

Uptake in the flagellated chambers has been studied in detail in *Oopsacas minuta* by Perez (1996) (Figure 24) and in *Rhabdocalyptus dawsoni* by

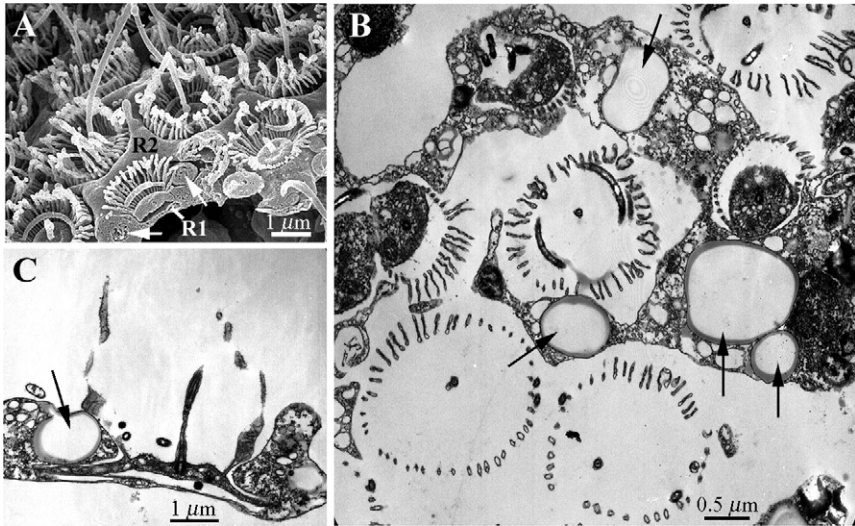


Figure 24 Uptake of red sulphur bacteria (Chromotiaceae) and latex beads in *Oopsacas minuta* (courtesy of T. Perez). (A) Scanning electron micrograph showing bacteria (white arrows) in the primary reticulum, one of which is in an advanced stage of intracellular digestion. A symbiotic bacterium is seen attached to the collar. The picture shows how closely the choanocyte collars fit within holes in the secondary reticulum (R2). (B) Numerous latex beads (black arrows) shown in a tangential section passing through several collars and reticular processes. (C) Vertical section of a collar body showing a latex bead in the adjacent primary reticulum.

Wyeth (1999). Both workers found that particle uptake occurred within components of the trabecular syncytium adjacent to collar bodies rather than within the collar bodies themselves. Both primary and secondary reticula can take up particles. While collar bodies might take up very small particles ($0.05 \mu\text{m}$), their main role appears to be simply one of providing the propulsive force for water movement by means of the beating of their flagella. This contrasts with the situation in demosponges where choanocytes are primary sites of food endocytosis (Simpson, 1984).

In Wyeth's proposed sequence of events (1999) (Figure 25), particles pass through prosopyles and enter the space between the primary and secondary reticula. Reiswig (1979a) suggested that one function of the secondary reticulum was to occlude the space between adjacent collar bodies, forcing water through the microvilli. The collars fit neatly into the pores in the secondary reticulum (Figure 24A) leaving little space around their perimeters for particles to escape into the effluent pathway (Boury-Esnault and Vacelet, 1994; Perez, 1996; Leys, 1999). Particles will tend to lodge against the sides of the collars and will be taken up by the primary or secondary

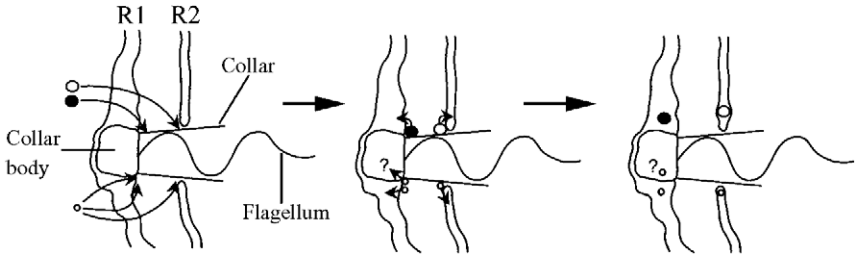


Figure 25 Proposed sequence of events during particle feeding in *Rhabdocalypus dawsoni*, from experiments using 1 μm latex beads (after Wyeth, 1999, with kind permission of Springer Science and Business Media). A single collar body is shown lying in the primary reticulum (R1) and with its microvillar collar fitting tightly within a pore in the secondary reticulum (R2). Water flows through the spaces between the microvilli and enters the flagellated chamber but particles are trapped within a space between primary and secondary reticula, where phagocytic uptake occurs. Filled circles show the main uptake pathway (into the primary reticulum). Open circles denote particles following other routes. Phagocytosis of smaller ($<1 \mu\text{m}$) particles is not excluded and could occur in the reticula or collar bodies.

reticulum. In two species that apparently lack a secondary reticulum, *Caulophacus cyanae* (Boury-Esnault and de Vos, 1988) and *Dactylocalyx pumiceus* (Reiswig, 1991), uptake would presumably be restricted to the primary reticulum. Yahel *et al.* (2007b) calculate that a typical flagellated chamber in *Aphrocallistes vastus* contains 2750 collar bodies and given the known volumes of water filtered and density of particles in typical samples, each collar body may be expected to trap one bacterium and possibly 10 indigestible particles per day.

A meshwork or sheet of glycoprotein-like filaments has been observed in several species spanning the gaps between the microvilli of collar bodies, as described in Section 3.8 and Figures 11 and 12. Water drawn into the collar would have to pass through the pores in this double layer which are variously estimated at 20–50 nm in breadth. The presence of the pores probably causes larger particles to remain outside the collar, circulating within a space largely lined by primary and secondary trabecular reticula, and increasing the probability of capture and uptake. The significance of the double filter is unknown but it seems possible that the filter is a single, continuously secreted sheet that is conveyed up the collar on the inside and down the outside, on the principle of the continuous mucous filter seen in tunicate branchial sacs and elsewhere (Werner, 1959) but, if so, it is not clear what the propulsive force for movement of the filter might be.

If large particles entering the prosopyles are unable to escape into the flagellated chamber around the edges of the collars because of the snugly fitting secondary reticulum, and if they are too large to go through the pores

in the mucous filter, they should be retained and ingested. Given the dimensions of the pores, all objects larger than about $0.1 \mu\text{m}$ ought to be retained and ingested. As noted above, however, *Oopsacas minuta* was unable to retain $0.1 \mu\text{m}$ objects (Perez, 1996). It is clear that more precise data on the mesh structure and dynamics will be needed, along with more experimental data on particle retention, before the role of the mucous net can be properly understood.

On passing into the flagellated chamber, incurrent water is usually free to escape through apopyles to the atrial cavity and thence to the exterior. In some species however, including *F. occa* (Reiswig and Mehl, 1991), *Aphrocallistes vastus* and *Rhabdocalyptus dawsoni* (Leys, 1999), an inner membrane system is present that might further regulate or impede passage of water, or be a site of phagocytosis. In *Rhabdocalyptus dawsoni*, material freshly collected from the natural habitat, inner membranes were found in only 1–10% of the flagellated chambers. The membranes were no more prevalent in one season than another, but in specimens kept in aquaria in the laboratory for 3 weeks the membranes appeared in all the flagellated chambers, forming an elaborate system of internal partitions. Leys (1999) suggests that the membranes are ‘amoeboid extensions of the trabecular reticulum that absorb non-functioning flagellated chambers’. It seems unlikely that they are significant in the normal feeding process.

5.2.2. Translocation

While a role for the collar bodies in nutrient uptake cannot be excluded, the bulk of the evidence points to the trabecular syncytium, in particular the primary and secondary reticula of the flagellated chambers, as the primary site where phagocytosis takes place (Perez, 1996; Wyeth *et al.*, 1996; Wyeth, 1999). The trabecular syncytium is also clearly the transport route for digested nutrients en route to other regions. Vesicles of all sizes can be seen moving in cytoplasmic streams in trabecular strands in pieces of living tissue sandwiched between a slide and a coverslip (Figure 26). Phagosomes containing internalised latex beads have been observed moving slowly in the trabecular syncytium close to collar bodies (Wyeth, 1999) but these movements did not resemble the faster, directional movements of particles moving in cytoplasmic streams, which may mean that primary phagocytic breakdown is largely accomplished locally in the vicinity of the flagellated chambers. In plated aggregates, particles move in streams at a rate of $2.15 \mu\text{m s}^{-1} \pm 0.33 \mu\text{m s}^{-1}$ (Leys, 1996, 2003b), as also in intact tissue.

Nutrient transport in hexactinellids thus appears to resemble the ‘symplastic’ transport seen in plants, where cells remote from sites of nutrient

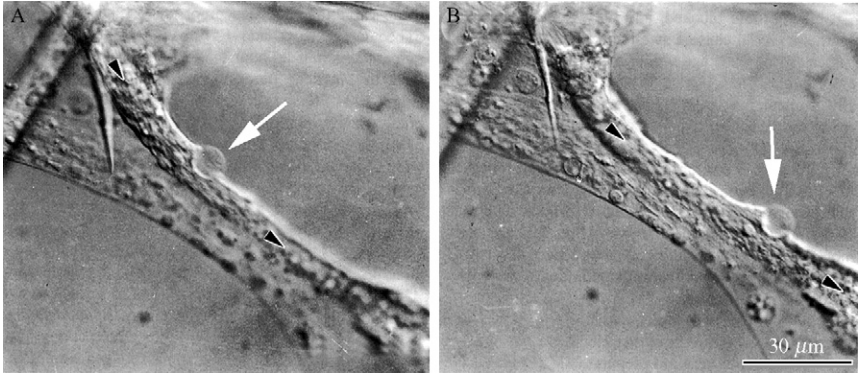


Figure 26 Cytoplasmic streaming in the trabecular syncytium observed in a sandwich culture of living tissue from *Rhabdocalyptus dawsoni* (from Wyeth *et al.*, 1996). A vesicle (white arrow) is seen being transported within a cytoplasmic stream moving from left to right as indicated by black arrowheads. The two pictures were taken 20 seconds apart. Velocity of transport was $2.25 \mu\text{m s}^{-1}$.

uptake are supplied by flow of materials from cell to cell through aqueous intracellular channels. There is no evidence that archaeocytes play a role in hexactinellid nutrient transport by migrating through the mesohyl as described for other sponges (extracellular or ‘apoplastic’ transport). Mackie and Singla (1983) in making the symplastic/apoplastic distinction point to the rounded form and lack of pseudopodial extensions in hexactinellid archaeocytes as evidence that they do not migrate, and to the thinness of the mesohyl as evidence of its unsuitability as a migration pathway. Transfer of nutrients to archaeocytes, cystocytes and other cells would require passage across plugged junctions. Much remains to be determined about the composition of these junctions and what materials can pass through them, but the junction is not a membrane barrier (Section 3.2) and there are structures interpreted as pores in the material of the plug (Mackie, 1981; Pavans de Ceccatty and Mackie, 1982; Mackie and Singla, 1983; Köster, 1997). The central channel through the pore particles is given at ca. 7 nm in diameter in *Rhabdocalyptus dawsoni* and 11 nm in *Rossella racovitzae*. In addition to the pores, ‘transit vesicles’ are frequently seen, apparently caught in the act of crossing plugged junctions, for instance in *F. occa* (Reiswig and Mehl, 1991) and *Chonelasma choanoides* (Reiswig and Mehl, 1994). Both pores and transit vesicles are reported for *Aphrocallistes vastus* (Leys, 1998). Despite the lack of physiological evidence regarding translocation of materials across plugged junctions, it appears reasonable to assume that materials can cross them either directly through the pores or within membrane-enclosed transit vesicles.

5.2.3. *Autophagocytosis*

Electron micrographs of *Rhabdocalyptus dawsoni* tissues kept in sandwich cultures (Wyeth, 1996) show phagosomes containing what appear to be collar bodies in various stages of breakdown. This, along with other evidence, suggests a process of remodelling whereby collar bodies and possibly other components are internalised and digested. Whether such processes are characteristic of healthy, normal animals is not clear. Observations by Leys (1999) on specimens of *Rhabdocalyptus dawsoni* kept in laboratory aquaria suggest that the inner membranes that appear within the flagellated chambers are amoeboid processes involved in absorption of non-functioning tissues. This species undergoes seasonal regression (Leys and Lauzon, 1998), but it is not known if the tissues undergo autophagocytosis during these periods. Cell death as such has not been investigated in hexactinellids, but it should be noted that homologues of mammalian genes involved in apoptosis have been identified in other sponges (Wiens and Müller, 2006).

5.2.4. *Comparison with other sponges*

Contrary to the situation in cellular sponges (Simpson, 1984), there is no evidence that hexactinellids can phagocytise particles in significant amounts in the incurrent canals or in any location other than the primary and secondary reticula of the flagellated chambers. If collar bodies phagocytise particles at all, it is likely that only very small particles are taken up. The arrangement seen in some hexactinellids whereby most or all of the water entering the flagellated chambers is apparently forced to pass through the microvillar mucus net by the presence of tightly fitting rings of secondary reticulum at mid-collar level is apparently unique to this group and has no counterpart in cellular sponges. The inner membranes seen in some hexactinellids may have counterparts in the central cells of certain cellular sponges but the significance of these structures is unclear. In hexactinellids, intracellular digestion occurs in the primary and secondary reticula and transport of phagosomes and food breakdown products almost certainly occurs symplastically by cytoplasmic streaming within the trabecular syncytium and does not involve apoplasmic transport by migratory cells. Bypass routes allowing water to pass directly from incurrent to excurrent canals avoiding the flagellated chambers have been reported in some hexactinellids (Leys, 1999; Bavestrello *et al.*, 2003) and have also been described in demosponges (Bavestrello *et al.*, 1988), but experimental evidence of their functioning in this capacity is still lacking and recent evidence (Section 5.2) suggests *Aphrocallistes vastus* and *Rhabdocalyptus dawsoni* lack such routes.

5.3. Production and control of feeding currents

As viewed by Bidder (1923), hexactinellids were essentially 'inefficient', passive feeders, their bodies interposed like filters in the path of slowly moving water masses in the 'eternal abyss'. He saw flagellar beating as having only local significance in assisting movement of water through the meshes in the choanosome. It is now clear that hexactinellids, like other sponges, can pump water efficiently through the entire body by the beating of the flagella in their flagellated chambers and in the absence of external water currents. This is not to say that passive ventilation may not also play a role. Currents generated by the sponge not only bring in food but also serve for respiratory exchange and removal of metabolic wastes.

5.3.1. Spontaneous and evoked arrests: sensitivity to environmental variables

Flow meter recordings from *Rhabdocalyptus dawsoni* in its natural habitat (Lawn *et al.*, 1981) showed that the sponge usually pumped water at a steady rate but that pumping was occasionally interrupted by spontaneous arrests of variable duration. Arrests were frequently seen when divers were working in the vicinity of the sponge (G. Silver, personal communication), suggesting that seemingly spontaneous arrests may have been due to extrinsic factors, such as sediment in the water. Flow meter recordings from sponges taken into tanks in the laboratory showed a similar pattern of steady pumping interrupted by arrests, occurring both 'spontaneously' and in response to mechanical disturbance (Mackie, 1979; Lawn *et al.*, 1981). Leys (1996) and Leys *et al.* (1999) showed that arrests could also be evoked by sediments introduced into the inhalent water stream. Leys and Tompkins (2004) tested sponges on filtered (25 μm) and unfiltered sediments whose main ingredients were organic debris, clay and silica from diatom frustules. The minimum concentration of sediment causing arrests was 10 mg litre⁻¹. Arrests in *Rhabdocalyptus dawsoni* were typically isolated events (Figure 27). When the sponge stopped pumping the flow rate declined sharply and then started to recover after about a minute, returning to the resting level in another minute. A second arrest occurring before the sponge had recovered from the first resulted in a further downward deflection. Stepped deflections of this sort were seen both at the start of an arrest sequence and at the end, as pumping resumed, as if the sponge was testing the water. In *Aphrocallistes vastus*, such stepped deflections and recoveries were much more common than in *Rhabdocalyptus dawsoni* (Figure 27), and also appeared to be more tolerant of increased sediment loads than the latter.

In *Aphrocallistes vastus*, with continued application of filtered sediment, the resting level baseline, representing maximal pumping, gradually declined,

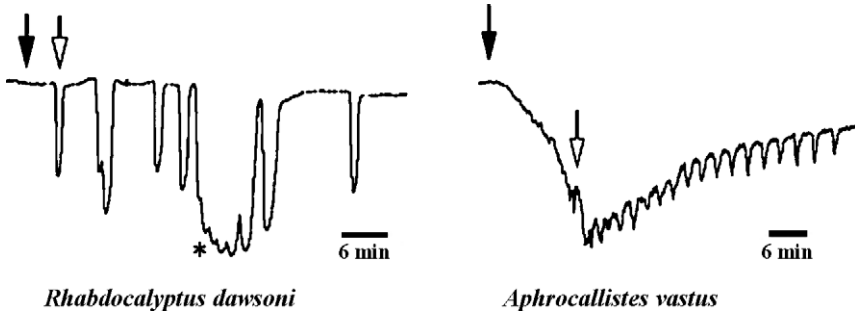


Figure 27 Arrests (downward deflections) induced by addition of 25 μm filtered sediment to the water. Black and white arrows indicate the start and finish of sediment addition. In *Rhabdocalyptus dawsoni*, single arrests are all-or-none events lasting about 2 min. Arrests occurring in sequence at short intervals (asterisk) depress the baseline further, as water flowing through the sponge progressively loses momentum, resulting in a stepped pattern. Arrests in *Aphrocallistes vastus* tend to occur in rapid succession, leading to gradual depression of the baseline, and recovery is often also stepped, as if the sponge was testing the water (courtesy of S. P. Leys and G. J. Tompkins).

presumably because of clogging of the canals. When addition of sediment ceased, pumping gradually returned to normal levels. It is not clear how hexactinellids rid themselves of sediments, but it seems probable that the particles are endocytosed and transported along cytoplasmic exit routes and released into the effluent stream, as discussed in Section 5.2.

Arrests can readily be evoked by mechanical stimuli such as tapping the walls of the tank, pinching a corner of the sponge with forceps or even twanging a single spicule. Electrical stimuli are also effective (Lawn *et al.*, 1981; Mackie *et al.*, 1983; Leys *et al.*, 1999). In each case, arrests spread through the whole sponge; they are never restricted to the vicinity of the stimulus.

There is no clear evidence that hexactinellids are sensitive to changes in light intensity. Sensitivity or susceptibility to ultraviolet (UV) light may seem unlikely in a predominantly deep-water group of animals, but a gene has been isolated from *Aphrocallistes vastus* that shows a high degree of sequence similarity to genes encoding invertebrate (6–4) photolyase (Schröder *et al.*, 2003a). This is a DNA repair gene, and its presence may mean that the sponge is adapted to repair damage caused by UV irradiation. *Aphrocallistes vastus* occurs at <20-m depth in British Columbia waters, where significant amounts of UV penetrate. The gene is expressed chiefly in the upper parts of the body where irradiation damage would be most likely to occur. The photolyase photo-reactivating system may have evolved in hexactinellids early in their evolution when exposure to UV light exceeded present levels and when hexactinellids lived in shallower water. Whether the

sponge can detect UV or light of any sort in the behavioural sense is unknown, and there is no evidence of diurnal rhythmicity in the pattern of spontaneous arrests.

5.3.2. *Nature of arrest events*

All the evidence available at the present time suggests that water current arrests are simply due to cessation of flagellar beating, but this has yet to be confirmed by direct visual observation. Tissues maintained in sandwich cultures should in theory allow visualisation of flagellar arrests, but pieces of *Rhabdocalyptus dawsoni* prepared in this way in tanks at the University of Victoria (Wyeth *et al.*, 1996; Wyeth, 1999) did not show the normal pattern of evoked and spontaneous arrests. In fact, they, like intact sponges in the same water system, lost the ability to arrest altogether and pumped continuously. Even in optimal conditions at Bamfield, sponges often failed to show arrests or started doing so only after many hours or days of continuous pumping. The arrest system is clearly very susceptible to disturbances in the environment. The mechanical trauma involved in setting up a sandwich culture would be relatively severe.

There is no reason to suppose that arrests are brought about by closure of pores such as those in the dermal membrane (ostia) or the prosopyles leading into the flagellated chambers. Observations of ostia in living sponges showed no changes, and electron microscopy showed no aggregations of microfilaments around any of these pores that might function as sphincters. Arrests take place rapidly (within 20 seconds), suggesting flagellar arrest as much the most likely mechanism. Ciliary or flagellar arrests as a means of regulating water flow are well documented in tunicates, bivalve molluscs and other invertebrates (Aiello, 1974).

5.3.3. *Spread of arrests*

Arrests were found to propagate through the sponge on the all-or-none principle at velocities of 0.26 cm s^{-1} (Lawn *et al.*, 1981; Mackie *et al.*, 1983). They can spread along zig-zag paths created by cuts and along thin strips cut vertically and horizontally through the body wall (Figure 28). In specimens bearing asexual buds, arrests evoked in the sponge spread to the bud and *vice versa*.

Lawn *et al.* (1981) proposed that the trabecular reticulum was the histological substrate for conduction of signals causing arrests. As a syncytium, it could 'act as a single neuron', conducting electrical impulses throughout the sponge. Attachment of recording electrodes was made difficult, however,

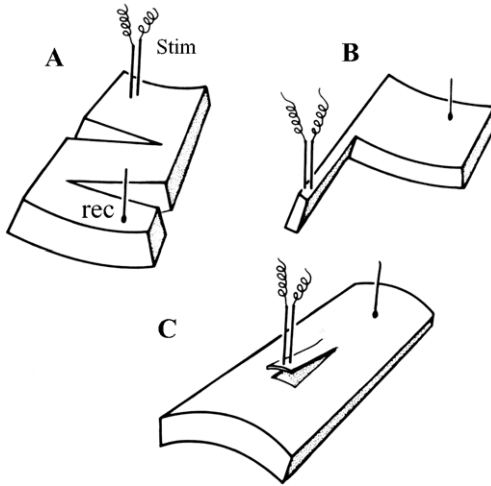


Figure 28 Spread of arrests in *Rhabdocalyptus dawsoni* recorded with a flow meter (rec) following electrical stimuli delivered at distant points (stim) (from Mackie *et al.*, 1983). Conduction can take place along zig-zag pathways (A), in narrow slices through the sponge wall (B) and in flaps of dermal membrane (C).

by the porous structure of the sponge and all attempts to record the suspected electrical signals failed until an approach using aggregates of dissociated sponge tissue grafted on to the sponge was devised (Leys and Mackie, 1997; Leys *et al.*, 1999). The aggregates were placed on the dermal or atrial surfaces of the same sponge from which the tissue was taken, and became attached, evidently fusing with the trabecular syncytium of the host. These provided substantial, non-porous attachments for recording electrodes (Figures 29–31). Impulses were found to propagate into and out from these autografts. With two such grafts, it was possible to record the passage of an impulse directly over a measured distance between recording electrodes (Figure 30). In the example shown, impulse conduction velocity was 0.28 cm s^{-1} at 10°C . This agrees with values for the velocity of spread of arrests as measured on whole sponges with a flow meter. Preparations in which current arrests and electrical impulses were recorded simultaneously showed a perfect correspondence between spread of impulses and spread of arrests (Figure 31). Repeated arrests and long-duration arrests were shown to be triggered by sequences of electrical impulses. An important observation was that conduction could still occur even when the feeding currents were completely arrested (Figure 31C and D). This shows that the conduction and effector systems are independent. It seems very clear that the conduction system is indeed the trabecular

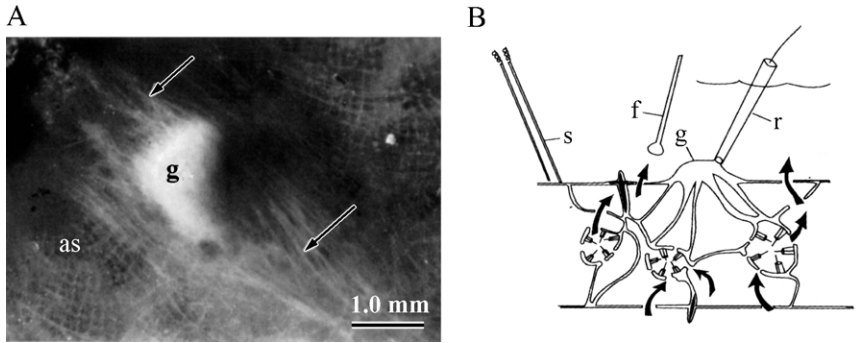


Figure 29 Setup for recording from attached autografts in *Rhabdocalyptus dawsoni* (from Leys and Mackie, 1997). (A) Shows a graft (g) attached to the atrial surface (as) that has fused with the trabecular syncytium. Streams of cytoplasm (arrows) run out from the graft into the sponge tissue. (B) Diagram of a section through the body wall bearing a graft (g). A stimulating electrode on the atrial surface (s) evokes an impulse that propagates to the graft, where it is recorded electrically (r). Arrows show water flow through the sponge, changes in flow rate being recorded by a flow meter (f).

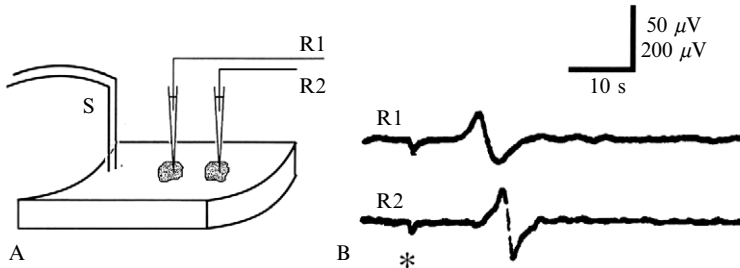


Figure 30 Recording from grafts in *Rhabdocalyptus dawsoni* (from Leys et al., 1999). (A) Stimulus (*) delivered as S evokes an electrical impulse that is picked up in linear sequence by recording electrodes (R1, R2) in grafts (stippled) attached to the atrial surface of a piece of sponge. (B) Shows the time relationships as the impulse passes from R1 to R2, a distance of 1.55 cm, giving a conduction velocity of 0.28 cm s^{-1} in this example.

reticulum, including the flattened dermal and atrial layers, and that impulses spread everywhere on the all-or-none principle through this system.

The effectors are presumably the flagella of the choanocytes. To enter these cells impulses must cross plugged junctions. As noted in Section 3.2, hexactinellid plugs are not membrane barriers, and probably therefore offer little resistance to the forward flow of action currents.

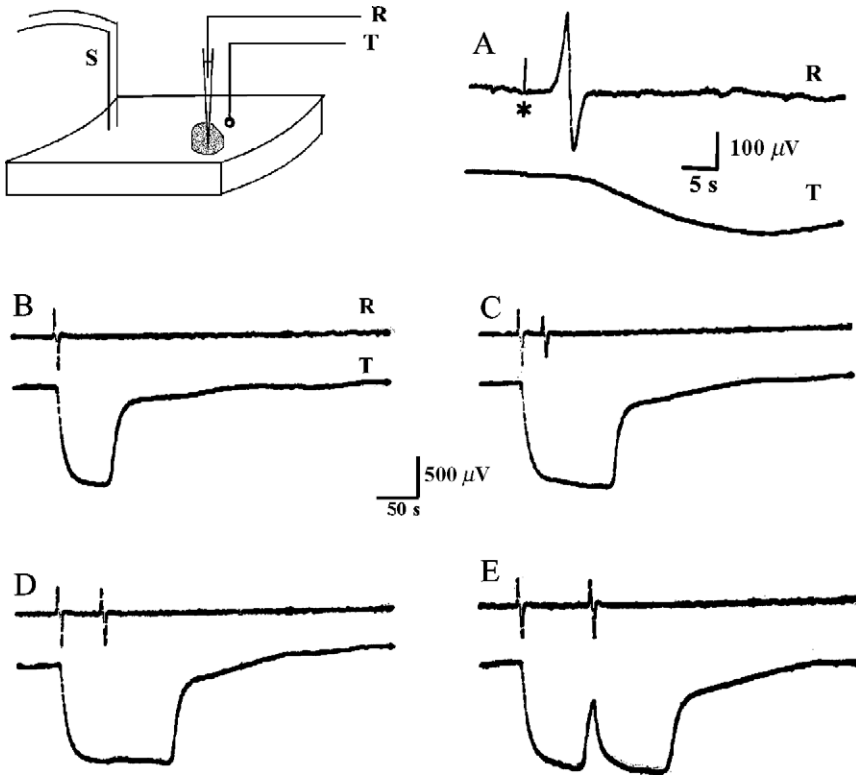


Figure 31 The diagram shows a recording setup where electrical stimuli delivered at S evoked impulses that propagated to a recording electrode (R) in a graft, while an adjacent flow meter (T) recorded arrests (*Rhabdocalyptus dawsoni*). A single evoked impulse and accompanying arrest are shown on an expanded time scale in A (asterisk indicates moment of shock). Responses to single (B) and paired shocks (C–E) are shown on a compressed time scale. In C–E, shocks were delivered 35, 57 and 93 seconds apart, respectively. The second shock prolonged the arrest (C, D) or evoked a second, longer arrest (E), where the sponge had started to pump again when the second shock was delivered (from [Leys et al., 1999](#)).

The system shows the typical characteristics of an electrical conduction system such as fatigue, chronaxie and refractoriness, but compared with excitable tissues in other animals the absolute and relative refractory periods are very long (29 and 150 seconds, respectively). The conduction velocity of 0.27 cm s^{-1} is also slow compared with conduction in excitable epithelia, muscles and nerves in animals, though it falls within the same range as action potential propagation in some plant systems, for example $0.1\text{--}0.4 \text{ cm s}^{-1}$ in tomato seedlings ([Wildon et al., 1992](#)). Impulses propagating through the sponge probably do not travel in straight lines ‘as the crow flies’ owing

to the branching, reticulate character of the substrate and the actual conduction velocity within individual strands is probably considerably higher. The system is unusually temperature sensitive. Conduction velocity varied with temperature showing a peak at 10°C (Figure 32), a temperature which corresponded well with the temperature at the collection site. Above 12.5°C propagation was usually lost, although flagellar beating continued. Below 7°C flagellar beating ceased, but this does not mean that impulses necessarily ceased to propagate. Between 7 and 10°C the Q_{10} was about 3. In later tests, some individuals were found that were able to function at considerably higher temperatures, but the same Q_{10} value applied to the pooled sample used in these tests. The sensitivity of the system to temperature is probably a reflection of the sensitivity of calcium channels on which the action potential depends. Action potentials based on sodium are much less temperature sensitive. These results with *Rhabdocalyptus dawsoni* suggest that temperature may well be a limiting factor affecting hexactinellid distribution in other habitats (Leys and Meech, 2006).

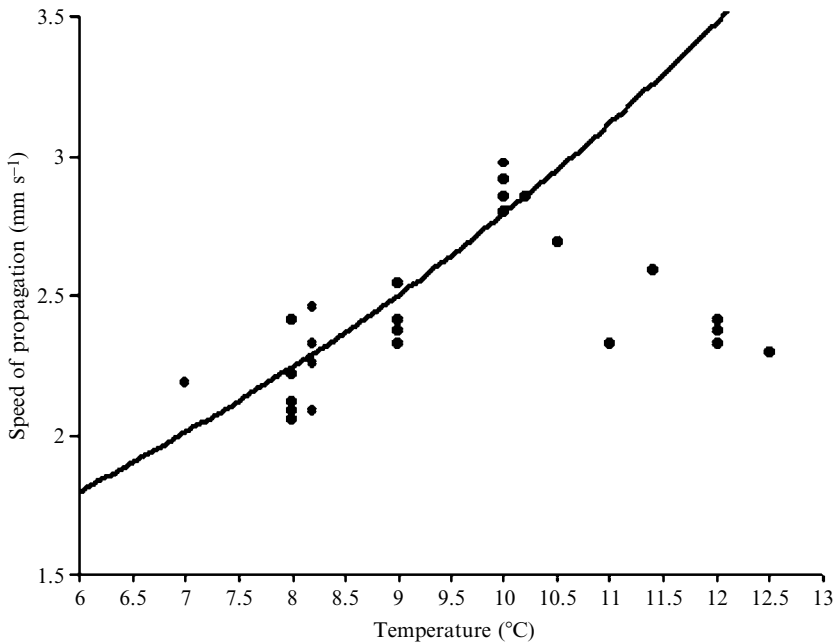


Figure 32 Effect of ambient temperature on the speed of propagation in *Rhabdocalyptus dawsoni*. The line through the points shows the slope of the relationship expected for a Q_{10} of 3 (courtesy of R. W. Meech).

5.3.4. The action potential

Experiments with drugs and ions affecting membrane channels strongly suggest that the electrical impulses are calcium spikes (Leys *et al.*, 1999). Sodium-deficient solutions had little effect on the wave form of the action potential, but propagation was blocked in solutions containing elevated levels of cobalt and manganese ions known to block calcium channels (Figure 33A and B). Nimodipine, a calcium channel antagonist, blocked conduction in relatively low concentrations. Cessation of flagellar beating—the effector response triggered by impulses arriving in the choanocytes—is

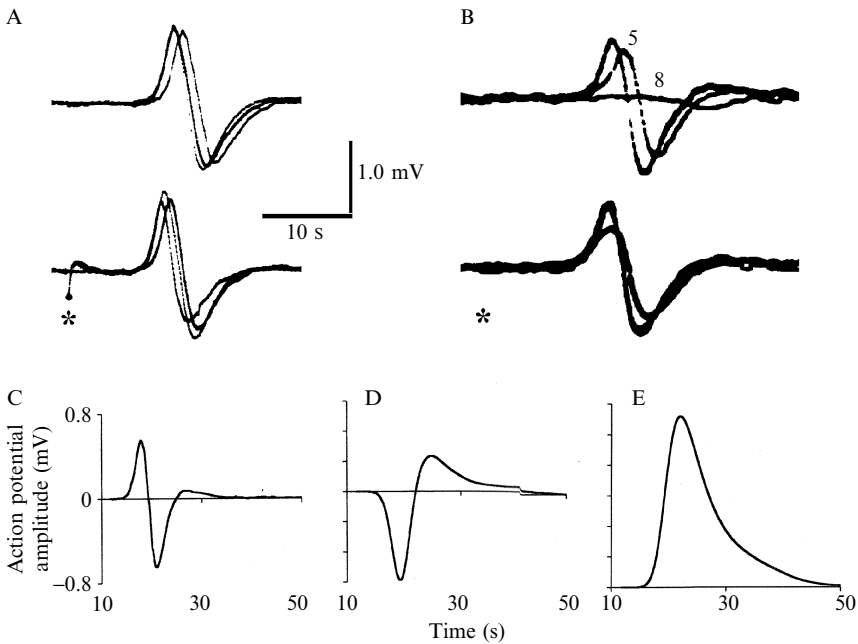


Figure 33 The action potential in *Rhabdocalyptus dawsoni* (from Leys *et al.*, 1999). (A) Lack of sodium dependency. The picture shows the effect of a 50% reduction (upper) and 75% reduction (lower) in $[Na^+]$. The superimposed traces show the reduced $[Na^+]$ trace along with sea water controls made before and after the experiment. The amplitude of the potentials was not significantly decreased. (B) Addition of 10 mmol of Co^{2+} to the sea water. In the upper set, the first trace is a sea water control. The second shows the reduced amplitude of the potential after 5 min, the third after 8 min (complete block). In the lower set, addition of 5 mmol Co^{2+} reduced but did not abolish the event. (C–E) Integration of the externally recorded action potential (C) produced the curve shown in D, and a further integration produced E, which approximates to the shape of the spike as it would appear in an intracellular recording.

presumably due to influx of calcium ions accompanying spiking, as in other ciliated cells. Beating would start again when the normal intracellular calcium levels were restored by ion pumping.

Intracellular and patch recordings have not yet been attempted on this preparation, so interpretation of the underlying events is based on evidence from extracellular recordings alone. Integration of the bipolar wave form of the impulse recorded with a suction pipette revealed the diphasic external current associated with propagation. A further integration produced a monophasic signal which may be taken as an approximation to the action potential as it would appear in an intracellular recording (Figure 33C–E).

5.3.5. Functional significance of arrests

The ability to turn off the feeding current is assumed to be adaptive in terms of preventing entry of sediments with the incurrent water stream. Sediments could be stirred up by any natural disturbance in the locality, as by the activities of interlopers such as crustaceans moving on or near the sponge. The response finds a close counterpart in the behaviour of ascidians, which arrest the feeding current when disturbed in any way, including when there is excessive sediment in the water (MacGinitie, 1939; Takahashi *et al.*, 1973).

5.3.6. Comparison with cellular sponges

An ability to arrest the feeding current is reported for some tropical demosponges (Reiswig, 1971b). In some cases contraction of exhalant water channels is held to be responsible while in others cessation of flagellar beating is thought to take place along with contractile movements. Other workers have described spreading waves of contraction in various sponges but such responses are typically local, though in some cases (e.g. *Tethya lyncurium*, described by Pavans de Ceccatty *et al.*, 1960) they affect the whole sponge. They are also usually very slow compared with *Rhabdocalyptus dawsoni*. In *Ephydatia muelleri*, for example, contraction waves run up the osculum at 30 to 350 $\mu\text{m s}^{-1}$, while those spreading through the canals in the choanosome travel at 4 $\mu\text{m s}^{-1}$. An exception is *Phorbis amaranthus*. This demosponge drops flaps over its ostial fields when stimulated, with a latency of <1 second (Reiswig, 1979b). The mechanism is unknown. All these phenomena and the possible mechanisms underlying them are discussed by Leys and Meech (2006). Cellular sponges lack not only nerves (Pavans de Ceccatty, 1989) but also gap junctions (Green and Bergquist, 1982), and in the

absence of these or any other known aqueous channels interconnecting the cells, it is hard to see how electrical signals could propagate through their tissues. Indeed, all attempts to record electrical correlates of the contractions have failed. What distinguishes hexactinellids such as *Rhabdocalyptus dawsoni* is that purely local stimuli such as twanging a single spicule can send an electrical signal through the entire animal that causes an immediate, all-or-none effector response affecting all parts of the body within a few seconds. This is possible because the trabecular syncytium, lacking internal membrane barriers, can act as a conduction pathway. No counterpart to this tissue exists in cellular sponges.

6. THE SILICEOUS SKELETON

6.1. Discrete spicules

The taxonomy of Hexactinellida has historically been, and still is, based on their siliceous skeletons. Indeed, distinction between the two primary subclasses, Amphidiscophora and Hexasterophora, is on the form of their smaller spicules, amphidiscs versus hexasters. The skeleton supporting the thin network of living tissues is a delicate scaffold of siliceous spicules, some of which may be fused together by secondary silica deposition to form a rigid framework. Silica is deposited in the form of amorphous opal, $\text{SiO}_2 \cdot n\text{H}_2\text{O}$, in production of a variety of distinct types of structures, one, some or all of which may be present in different species at various stages of growth: (1) discrete spicules that remain as loose elements throughout life of the sponge; (2) rigid siliceous networks formed by fusion of the main supporting spicules and extending through parts or all of the main body tissue mass (choanosomal or parenchymal position) and (3) rigid networks or thin lacework plates of fused minor spicules and synapticalae, formed commonly at contacts with hard foreign objects (basidictyonal plates) and more rarely on free exposed outer surfaces (surface crusts or external capsules).

As a group, hexactinellids secrete an amazing array of spicules of various shapes and sizes, but any one specimen or species produces repetitive copies of only a few (2–12) types of spicules. Here we introduce only those names of spicule types needed to follow general discussion. The first naming system for sponge spicules developed by [Bowerbank \(1858\)](#) was unwieldy, little used and supplanted for hexactinellids by a more comprehensible system, based on spicule shapes, developed by [Schulze \(1887\)](#). Since then, as new species and spicule shapes were discovered, new names for spicule types, often without definitions, were added to hexactinellid nomenclature. Hexactinellid

taxonomists, not immune from occasional failure of logic, have proposed some unfortunate names for spicule groupings that should be allowed to disappear by disuse. There is no single complete and authoritative illustrated list of hexactinellid spicule names available. Several sources provide names and illustrations of part of the variety (Koltun, 1967; Hooper and Wiedenmayer, 1994; Boury-Esnault and Ruetzler, 1997), and Tabachnick and Reiswig (2002) provide text definitions of spicule names but without illustration. The complete range of hexactinellid spicule forms and their nomenclature can be surveyed by perusal of the Hexactinellida section of *Systema Porifera* (Hooper and Van Soest, 2002, pp. 1201–1509).

The spicule types produced by any single species are generally consistent across a wide range of specimen sizes, compelling evidence that spicule form and size are genetically controlled. They are thus used as primary characters for species descriptions. During juvenile development, however, expression of the different spicule types occurs as a succession of stages and the first spicules of a type may be smaller than the corresponding spicules in mature adult specimens. In addition, while the fidelity of shape and size of any spicule type formed by a specimen is impressive, considerable variation is always present within a sample of every spicule type. Furthermore, there are always some spicules produced that are obvious aberrancies or mistranslations of a shape/form programme. These are usually ignored in descriptions unless they occur at a frequency that assures they will be found by an observant investigator.

6.2. Megascleres and microscleres

6.2.1. Size

Spicules of Hexactinellida, like those of Demospongiae, are generally divided into megascleres and microscleres based on the features of size, shape and function. Megascleres, as larger components, usually with largest dimension 0.2–30 mm, obviously include the major supporting skeletal elements. The largest megascleres are those that project from the body surface and serve as protective lateral spines or basal attachment roots—the single basal spicule of *Monorhaphis* can attain a size of about 3 m in length and 1 cm in diameter (Schulze, 1904). Microscleres are usually less than 0.1 mm in diameter and are commonly astral in form, here meaning having more than six terminal rays. They are clearly accessory skeletal elements by their small size, but some astral microscleres attain diameters of 1 mm, overlapping significantly with megascleres in size. When encountering unusually large spicules of a type that is elsewhere small in size, astral

in form and assigned to the microsclere fraction, they are likewise considered to be simply large microscleres. In practice, distinction between megascleres and microscleres is subjective for intermediate spicule types, has changed over time, and is best decided by consensus of practicing specialists. Microscleres are usually not fused to skeletal elements except for their rare and apparently accidental incorporation in frameworks and the common insertion of small oxyhexactins throughout the frameworks of many Hexactinosida. [Reiswig's recognition \(1992\)](#) of medium-sized, surface-associated and non-supporting spicules as 'mesoscleres' has not been consistently applied by that author nor followed by other recent authors.

6.2.2. *Form*

All spicules of hexactinellids, both megascleres and microscleres, have either the form of a regular hexactin or can be considered derivations of that basic form ([Figure 34A](#)). The regular hexactin has six rays (actins) of equal length and shape, intersecting at a point where each ray is normal to the centre of a circumscribing cube (cubic symmetry), and each ray intersects four others perpendicularly and is in line with the remaining fifth ray extending out from the opposite side of the intersection point. Since the spicule consists of three axes or axons (two rays per axis), the spicules are also called 'triaxons' and the class has been referred to in the past as the 'Triaxonia', a junior synonym of Hexactinellida. Every hexactinellid spicule has a system of internal organic axial filaments developed to varying degrees. Each ray consists of an organic axial filament surrounded by a cone of silica, sometimes as a single unit but conspicuously concentrically layered in larger spicules. Early suggestions that organic material is either incorporated in each layer or a thin sheet of spiculin is deposited between layers of silica have not been supported by spicule analysis ([Sandford, 2003](#)). Collagen fibrils have been demonstrated in the layered matrix of *Hyalonema sieboldi* root spicules ([Ehrlich et al., 2005](#)), but whether this organic matrix material is a general feature of siliceous spicules remains as yet unknown. In the regular hexactin, the six axial filaments, one running axially in each ray, intersect perpendicularly at the centre of the spicule in cubic symmetry. The intersection of the axial filaments is known as the 'axial cross' ([Figure 34A](#)) and that point is considered the 'spicule centre'. Those spicules where the axial filaments typically extend distally to the tip of each ray are known as 'holactins' ([Kirkpatrick, 1910](#))—antonym 'heteractin' (new term) with some distal rays lacking axial filaments (see below). If the filament remains open and exposed at the tip, lengthening of the ray can continue. When the filament is closed off at the ray tip by silica deposition, extension of that ray by primary growth cannot continue.

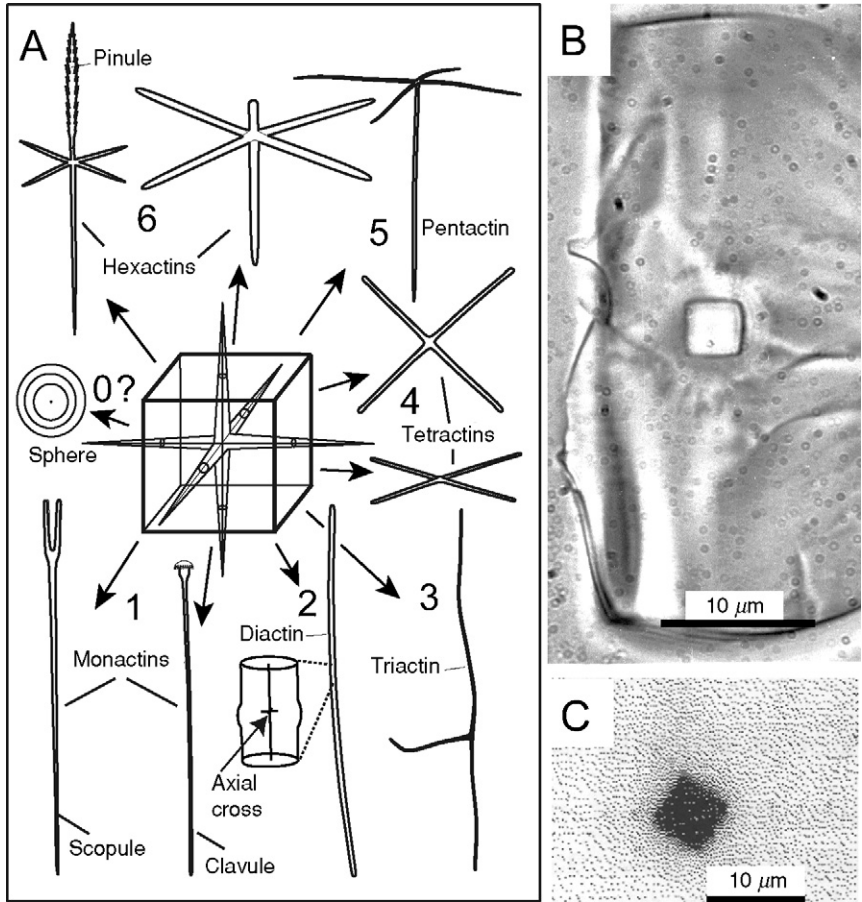


Figure 34 (A) Derivation of hexactinellid megascleres with undeveloped rays from a basic hexactin of cubic symmetry. (B) Cross section of a pentactin of *Crateromorpha* sp. with square axial canal (from Reiswig, 1971). (C) Atomic force microscope image of the square axial filament in a polished cross section of a spicule of *Rossella racovitzae* (from Sarikaya *et al.*, 2001).

There has not yet been a systematic study of open versus closed spicule tips within or between hexactinellid species or even spicule types.

The organic axial filament of Hexactinellida is square in cross section (Figure 34B and C) while that of Demospongiae is either hexagonal or triangular. The square sectional shape is retained in uneroded spicules when the axial filaments are artificially removed by treatment with nitric acid, bleach or hydrogen peroxide. The exposed space is called the axial canal. Walls of axial

canals of spicules from non-living sources in nature (sediments, spicule pads or mats, dead fused skeletons and so on) erode more rapidly than the rest of the spicule and the canal is thus enlarged and rounded in section. This occurs in spicules of museum specimens stored for extended periods in acidic fluids. The axial filament consists mainly of a mixture of proteins previously known as 'spiculin' as well as a small fraction of inorganic minerals. The main proteins in axial filaments of both hexactinellids and demosponges have been sequenced; they have been more specifically renamed as 'silicateins' indicating their presumed enzymatic activity in silication (see silication below).

The impressive diversity of spicule forms in Hexactinellida can be ascribed to variation of only a few features of the basic regular hexactin. Derivations from the regular hexactin involve: (1) modification of one or two of the six rays by elongation, shortening, formation of special spination and so on to form a variety of irregular hexactins (Figure 34A); (2) complete reduction of one or more rays (Figure 34A, 1–5) and (3) addition of secondary rays on the tips of one, some or all of the developed rays or on the undeveloped spicule centre (Figure 35). In addition to these major sources of form variation, all spicules may be modified by ray curvature (rare in hexactinellids) or formation of small to large spines or thorns in various patterns on some or all ray surfaces. Modification of one or both rays of a hexactin axon are common in surface-related spicules (Figure 34A, 1), producing spicules known as pinules with a single long bushy ray projecting from the sponge surface, or reduction of the projecting ray from slight to nearly complete. Total ray reduction from the basic hexactin results in five-rayed pentactins, four-rayed tetractins (called stauractins if all developed rays lie in two axes and one plane), three-rayed triactins (called tauactins if all developed rays lie in two axes and one plane), two-rayed diactins (rhabdodiactins if both rays lie in one axis) and single-rayed monactins (Figure 34A).

Virtually all of the irregular variants that can be imagined for each general form occur as well. Although these general spicule forms are listed and typified as discrete, continuity exists between forms such that only arbitrary distinction can be applied to some spicules, for example hexactins with one very short ray and pentactins with a short nub as a rudiment of a sixth ray. With some exceptions, the axial filament system of these derived spicules contains an axial cross with the normal six filaments emanating from it, but those of the undeveloped rays are only rudiments, a few micrometres long. This is considered strong evidence that these forms are indeed modifications of the basic hexactine spicule. Some pentactins and most stauractins, however, do not develop even the rudiments of the undeveloped rays, the significance of which is unclear. Since examination of the axial system requires tedious, careful microscopy, a survey of rudiment patterns has not been made for the various spicule types across taxonomic groups. The exceptional spicules that characteristically lack an axial cross are:

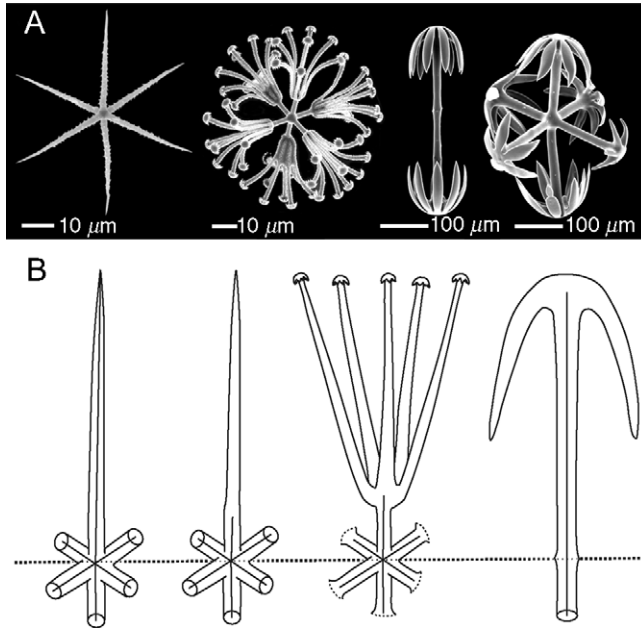


Figure 35 (A) Hexactinellid microscleres, from left to right: oxyhexactin from *Chonelasma lamella*, discohexaster from *Euryplegma auriculare*, macramphidisc and hexadisc from *Hyalonema populiferum* (SEM). (B) Transparency drawings of microscleres (centres and one of the primaries with terminal rays) showing axial filament system, left to right: holactine oxyhexactin from Amphidiscophora, heteractine oxyhexactin and discohexaster from Hexasterophora and amphidisc from Amphidiscophora (redrawn from Kirkpatrick, 1910).

(1) the common thorned diactin known as the ‘uncinate’, with an axial filament extending tip to tip; (2) the amphidisc of Amphidiscophora in which a slight swelling of both the axial filament and first layer of silica gives clear indication of the spicule centre and (3) the rare non-actine sphere or pearl with only a formless central granule as a presumed axial rudiment (Figure 34A). The likelihood that the amphidisc is indeed derived from a hexactin is strongly supported by rare reports of a visible axial cross (Mehl, 1992, Plate 5, Figure 1) and occurrence of hexactine variants, the hexadisc (Figure 35A, right), among typical amphidisc spicules.

Secondary or terminal rays (‘pseudoactines’ of Reid, 2003) lacking detectable axial filaments are commonly added to microscleres but rarely to megascleres. Microscleres have secondary rays appended to the distal ends of all six or only some primary rays, resulting in the attractive complexity and symmetry of these hexactinellid spicules. These structures, sometimes

numbering only one per primary ray (more usually three to five), or occasionally as many as one hundred, are identical or proportionately similar to silica extensions arrayed in definite patterns on simple or variously inflated primary ray tips. Additional variation in form and nomenclature stems from the moderate variety of shape of the secondary rays—straight, sigmoid, hooked and so on—and shape of the terminal tip—sharp-pointed, digitate, serrated disc, group of thorns and so on. Secondary structures carry no detectable axial filament and are referred to as anaxial rays by Reid (2003). The overall form of microscleres bearing more than one secondary ray per primary ray is suggestive of ray branching, but indeed the primary rays and their axial filaments never branch. Such anaxial secondary rays are not appended to the ends of regular megasclere rays, but similar anaxial structures borne on the central knob of monactine megascleres (tines of scopules, Figure 34A, 1 left) can be considered equivalent to secondary rays of microscleres. Spicules bearing both primary axial rays (all spicules) and secondary anaxial rays may be called ‘heteractins’ to distinguish them from holactins that consist only of primary axial rays. The term ‘astral’ proposed by Kirkpatrick (1910) as antonym of holactin is inappropriate for inclusion of scopules and clavules. Although it is, in practice, extremely difficult to ascertain presence of primary versus secondary rays in microscleres with only six pointed rays (microxyhexactins), this distinction has major taxonomic and phylogenetic importance. All such spicules in Amphidiscophora are holactins, while all such spicules in Hexasterophora are heteractins (Figure 35B).

Other structures such as the whorls of anaxial spines or teeth on the ends of the diactine amphidisc microscleres characteristic of the subclass Amphidiscophora are generally not considered equivalent to secondary rays, since they do not exhibit complexity of tip form, and are equivalent to the tip ornaments (spines) of secondary rays of Hexasterophora. An extensive analysis of anaxial ornamentation structures with the aim of determining their equivalence or homology has not yet been made. Likewise, it is not entirely certain that axial filaments are totally absent from secondary rays, spines, thorns and other structures simply because they cannot be perceived with standard light microscopy. As has been shown by Drum (1968), some demosponge microscleres have submicroscopic axial filaments in secondary structures, and for hexactinellids, such a possibility remains unexplored. A general ‘rule’ for hexactinellid axial filament patterns is that, although these structures intersect at the spicular centre of most spicules, they never branch as occurs in dichotriaenes of some demospoges. A corollary of this restriction is that axial rays can never be added to a spicule after silication has begun and no hexactinellid spicule can have more than six axial rays unless such occurs through an accident during its early development.

6.3. Spicule locations

Different spicule types often have precise locations in hexactinellids, attesting to specificity of function, although this is not always apparent. The original positional designations made by Schulze (1887) are still used, with a few modifications, for original descriptions of spicule locations and diagnoses of patterns for higher taxa (Figure 36). There are basically three types of location recognised—spicules associated with surface membranes (dermalia, atrialia, canalaria), spicules distributed through the main body wall between the surfaces (parenchymalia), and spicules partly projecting from the outer body surface (prostalia). Dermal spicules supporting the outer living tissue layer are generally distinct types and sizes of pentactins, hexactins or sometimes tetractins and diactins. When an additional larger spicule type supports these immediately below the surface, the dermalia are termed autodermalia and the larger supporting category, usually large pentactins but sometimes diactins, are called hypodermalia. In Recent hexactinellids, surface-related spicules almost always remain as loose skeletal elements, presumably to allow movement of surface tissues during expansion, by hydrostatic inflation, and collapse, by elastic tissue rebound, of fluid spaces circumscribed by the trabecular syncytium. They are rarely interconnected by silica fusion to form networks, although in many fossil forms they were fused to the main framework (Mehl, 1992). A similar nomenclature is applied to equivalent spicules lining the atrial cavity and larger canals.

Parenchymalia include several distinct types of spicules with different distributions and roles. The major spicules providing primary physical support for the sponge are the principalia, usually large, robust hexactins or diactins (rhabdodiactins), sometimes pentactins, tetractins or triactins. They are often very intimately entwined by much thinner diactin spicules, the comitalia, which presumably provide fabric-like resiliency to the combined network. All other spicules, both megascleres and microscleres, distributed throughout the parenchyme without detectable pattern (so far), are collectively called intermedia. Unlike dermalia, the parenchymal principalia and comitalia are sometimes fused by secondary silication to form a rigid skeleton. In lyssacine Hexactinosa, such fusion of parenchymal megascleres is an informal process, but in the dictyonine Hexactinosa, hexactin principalia are often (not always) regularly arranged at fusion to form intricate lattices—the principalia then known as dictyonalia.

The remaining positional designation, prostalia, includes three groups of megascleres usually in the form of monactins, pentactins or sometime diactins. The most well known are the basalia extending from the lower body, for example the basal spicule tuft of *Hyalonema*, that provide support of the body over the benthic surface but also enable anchorage in soft muds and grapple attachment to irregular hard substrates. Basalia are typically

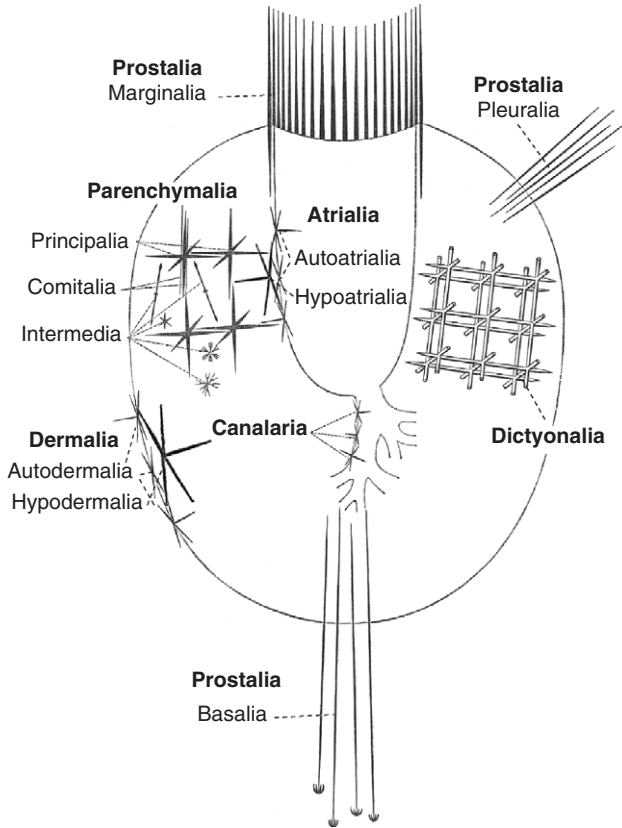


Figure 36 Nomenclature of spicule locations in Hexactinellida (redrawn and modified from Schulze, 1887).

monactins or diactins with specialised toothed anchors or pentactins or rough diactins serving as very effective grapnels. Prostalia which project from the lateral surface, known as pleuralia, are mainly diactins or monactins, but some hypodermalia are erected from their positions of origin below the dermal surface to extend as a veil several millimetres over the outer surface. Pleuralia presumably provide protection of the lateral surface from large predators and support that surface above the substrate should the sponge fall over (prevent occlusion of ostia and potential burial). Special prostalia around the oscular margin, the marginalia, likewise protect that delicate growing edge and prevent easy entrance to the osculum by larger crawling invertebrates. The distal projecting parts of prostalia listed above are bare siliceous structures freely colonised by epibionts (Boyd, 1981; Beaulieu, 2001a,b). Large uncinates, the barbed diactins or monactins present in

many groups, may project from lateral surfaces and are then considered by most practicing hexactinellid specialists as prostral megascleres, although they always remain totally covered by a thin film of living tissues. We find no support, neither in size nor form, for their historical assignment as inter-medial microscleres. Likewise, the special surface-related monactin group called scepstrules (clavules and scopules and related forms) were historically regarded as microscleres but by size and form they are clearly megascleres. By position, they are best considered comitalia of dermalia and gastralia.

6.4. Fused silica networks

Spicules of hexactinellids can be physically joined (fused or ankylosed) by deposition of secondary silica in several ways: by simple spot-soldering with a very thin siliceous film at points of contact between spicules, by formation of anaxial bridges or synapticula (silica filaments of Reid, 2003) between surfaces of spicules not in direct contact or by enclosure of rays or entire spicules in a continuous layer of secondary silica. These are best-considered stages of a continuous series. Spot-soldering is differentiated from synapticular bridging only by visible gaps between the original spicule surfaces adjacent to the connection. Synapticula may also extend from spicule surfaces as free-ended filaments; these may be unconnected distally or join to other such filaments, occasionally forming anaxial networks. Although small, completely anaxial networks have been reported in a few cases, it is uncertain whether they originate free of other skeletal elements or are out-growths of simple synapticula that have broken free of their original location on axial spicule surfaces.

Hexactinellids that form fused skeletons are much more likely than those with only loose spicules to be found as fossils. While spicule fusion is common among hexactinellids, it is equally important to appreciate that this process is completely unknown among the subclass Amphidiscophora where all spicules remain loose throughout life. Even in those groups where fusion is well known or ubiquitous (orders Hexactinosa and Lychniscosa of Hexasterophora), specific types of spicules (microscleres, scepstrules, uncinates and so on) always remain loose or are only occasionally incorporated by apparent accident.

6.4.1. *Lyssacine parenchymal networks*

While some members of all three families of Recent Lyssacinosida may form fused basal skeletons, fusion of parenchymal megascleres is known to occur in only two families, Euplectellidae and Rossellidae; it remains unknown in

Leucopsacidae. In Euplectellidae, the often regularly arranged principalia and the more irregularly interlaced comitalia and intermedia are typically found to be entirely loose spicules, and in many species parenchymal spicule fusion is unknown. However, in some species of many genera, for example *Euplectella* and *Corbitella*, spicule fusion appears to begin from the base and spread upwards, ultimately involving the entire suite of parenchymal megascleres, including those of the sieve plate. Some specimens have only patches of spot-soldering between megascleres of the lower body, but fusion in other specimens is extended to include synapticular bridges and, in some, expanded to full enclosure of the entire parenchymal skeleton into a rigid glassy network. The fused skeletons are quite irregular (Figure 37A) since the connected spicules are of mixed types, diactins to hexactins, and remain in their original orientations relative to one another. The fusion process appears to be informal in the sense that it does not seem to be a predictable result of an early developmental programme. It may be related to aging since specimens with completely fused skeletons are unable to grow in length or width, but wall thickening remains possible. A detailed study relating the extent of spicule fusion with size, a surrogate for age, has not yet been carried out for any species of this family. Note that fusion of parenchymalia remains unknown for many species of Euplectellidae.

6.4.2. *Dictyonal parenchymal frameworks*

Four orders of Recent hexactinellids, Hexactinosida, Aulocalycoida, Fieldingida and Lychniscosida, have fused siliceous parenchymal frameworks composed primarily or exclusively of hexactins connected by secondary silica enclosure. Framework forms are fairly regular and predictable in all of these except Fieldingida where the irregular structural pattern remains unresolved. The component hexactins are known as dictyonalia and the frameworks as dictyonal. Dictyonalia of the first three orders are simple hexactins (Figure 37B), but those of the Lychniscosida have 12 synapticular struts developed equidistantly and symmetrically around each dictyonal centre, outlining a regular octahedron (Figure 37C). Such dictyonalia are known as lychniscs. Interconnection of hexactins in all these orders is a normal and necessary part of growth and occurs at or just behind the free margin, resulting in longitudinal extension of the fused framework. Hexactinellid specialists have long known that basic differences exist between dictyonal frameworks of various groups, but to date there has been little progress in understanding and communicating those differences. Only four types of differences are now appreciated: presence and absence of various types of skeletal channelisation (canals of palaeontologists), how adjacent

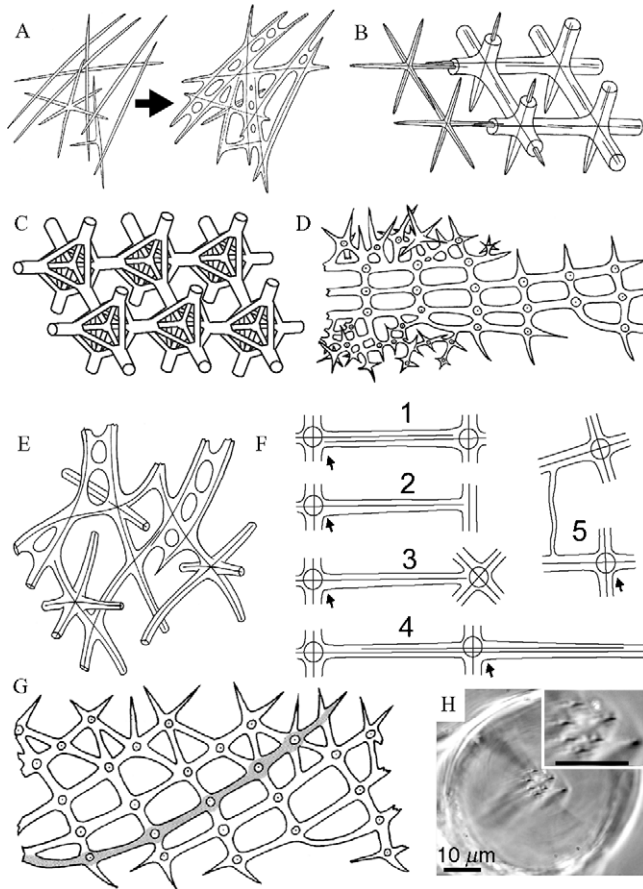


Figure 37 Parenchymal-fused silica networks of Hexactinellida. (A) Loose (left) and fused (right) networks of parenchymalia in lyssacine hexactinellids (from Reid, 1958). (B) Part of a dictyonal framework of hexactinosan showing classic, but erroneous, terminal addition of hexactin dictyonalia (from Reid 1958). (C) Part of a dictyonal framework of a lychniscosan with characteristic lychnisc nodes. (D) Longitudinal section through the wall of a hexactinosan with cortices developed on both dermal (upper) and atrial (lower) surfaces of the primary framework which alone extends as a series of longitudinal strands to the growing margin (right) (from Reid, 2003). (E) Portion of the irregular parenchymal dictyonal framework of an aulocalycoid hexactinellid (from Reid, 2003). (F) Transparency views of five methods of fusion of dictyonalia including relationships of axial filaments; new appended dictyonalia indicated by arrow. (G) Longitudinal section through hexactinosan dictyonal framework showing longitudinal dictyonal strands (one emphasised in grey) curving to dermal surface (from Reid, 2003). (H) Oblique section of longitudinal strand of *Farrea occa* with central bundle of six axial canals plus one from the most recently added dictyonium.

dictyonalia are connected, primary and secondary layers in frameworks and dictyonal strands.

Skeletal channel types were first described by [Ijima \(1927\)](#) and later refined by [Reid \(1958\)](#) when only two groups of Recent dictyonal Hexactinellida, the Hexactinosa and Lychniscosa, were known. These consisted of simple tubular channels, in the size range of one-half to a few millimetres in diameter, termed epirhyses when passing vertically but shallowly into the body wall from the dermal (inhalant) surface, aporhyses from the atrial exhalant surface, diplo-rhyses when the two channel types deeply overlapped through the middle of the wall, diarhyses when passing completely through the wall, schizorhyses when interconnected to form a single labyrinthic system of channels within the wall and a special form termed amararhyses when channels branch in slits on the atrial side and open on projections on the dermal side. These macroscopically obvious gaps in framework structure are still used as major characters in defining families of Hexactinosa. They are, however, negative characters in the sense that they indicate patterns where addition of dictyonalia is suppressed, presumably to enhance water flow to deeper wall layers, and thus add little or nothing to show how the different frameworks are actually constructed. These different types of skeletal channelisation may, however, be attained convergently in different families.

Distinction of primary and secondary components of dictyonal frameworks, informally recognised by [Ijima \(1927\)](#), was formalised by [Reid \(1958\)](#). The dictyonal framework formed at the growth margin is considered the primary framework, and can be traced back to earlier stages through the entire skeleton. Dictyonalia may be added onto the outer and inner surfaces behind the growth margin (radial accretion), resulting in body wall thickening. The patterns of connection and mesh geometry of these added superficial dictyonal layers are usually strikingly different from those of the primary framework, and such layers are called secondary or cortical layers ([Reid, 1958](#)) ([Figure 37D](#)). All dictyonal frameworks thus have a primary framework, with or without cortical layers on dermal and atrial surfaces. This distinction of layers allowed recognition that channelisation may be restricted to only the cortical layers or involve the primary layer as well, adding another method of distinguishing pattern in skeletons of different taxa. Empowered with this recognition of dictyonal layers, [Reid \(1958\)](#) recognised and defined farreoid (two-dimensional sheet), euretoid (three-dimensional sheet) and aulocalyoid (irregular, [Figure 37E](#)) types of primary frameworks among Hexactinosa.

Details of how dictyonalia are individually inserted onto or into an existing framework remain elusive for all Hexactinellida. Nonetheless, five basic patterns of dictyonal fusion have been identified so far ([Figure 37F](#)): (1) parallel ray fusion, (2) tip-to-ray fusion, (3) tip-to-centre fusion, (4) axon-to-ray fusion

and (5) synapticular bridging. The first pattern appears to be the most common for connection of dictyonalia in primary frameworks and was regarded by Ijima (1927) as the original and basic process of dictyonal framework formation, as seen in *Farrea*. Here the resulting internodal beams have two axial filaments, one from the component rays of each of the two hexactins. In tip-to-ray and tip-to-centre fusions, beams have a single axial filament. Mixtures of these indicate a haphazard attachment process, perhaps best interpreted as a lack of pattern. In axon-to-ray fusion, the axial centre and both axial filaments of one axon are appended to another ray so the two beams in question have two or more axial filaments, one of which is continuous throughout the two beams (Reiswig, 2002a). Synapticular bridging is rare but is an important method of connection in Aulocalycoid skeletons (Reiswig and Tsurumi, 1996).

Longitudinal dictyonal strands were undoubtedly recognised by early hexactinellid specialists, but their existence was first formulated by Reid (1958). Here the longitudinal rays of dictyonalia are aligned in a continuous series to form major longitudinal structural components of the primary framework. In basic farreoid and euretoid frameworks, strands are more or less straight (Figure 37B and D), but in groups with thicker body walls, strands curve smoothly to dermal or atrial or both surfaces (Figure 37G). Reid (1958) presumably accepted Ijima's statement (1927) that all beams in the basic two-dimensional *Farrea* framework resulted from parallel ray fusion and thus carried two axial filaments. Hence, the relatively straight path of strands was thought to be due only to the sequential step-by-step alignment of each dictyonallium in series. No one has questioned Ijima's statement for 85 years. One of us (H.M.R.) has recently inspected the axial filaments in beams of *F. occa*, the type species of *Farrea*, which was the basis of Ijima's claim, and found transverse beams to have the expected two axial filaments but longitudinal beams contain numerous (five to eight or more) closely bunched axial filaments passing entirely by the axial centre of all added dictyonalia (Figure 37H). It is clear that dictyonalia are added here in axon-to-ray fusion, not parallel ray fusion, and linearity of longitudinal strands here, and likely in all taxa with such structures, is due to dictyonalia being attached to the side of an existing continuous silicified axis composed of a bundle of rays. This finding suggests that present hypotheses about how dictyonal frameworks with longitudinal strands are constructed must be completely rethought and casts doubt on the distinctness of the order Aulocalycoida. Several groups of hexactinellids lack dictyonal strands and their methods of framework construction also need detailed examination in light of this discovery. Unfortunately, determination of axial filament patterns requires very careful examination of framework elements with high magnification oil immersion objective, a necessarily destructive process.

6.4.3. *Basidictyonal frameworks*

Special fused basal skeletons have long been known in a few dictyonine hexactinellids (Schmidt, 1880; Weltner, 1882), but recognition of their general occurrence in all basiphytous (attached to hard substrate) dictyonine and lyssacine forms was delayed until many species had been surveyed. Ijima (1901) introduced the term ‘basidictyonalia’ for frameworks composed of small, thick-rayed hexactins (Figure 38A and B) in the basal regions of lyssacines. Since its earliest recognition, the basidictyonal framework was known to consist of two distinct components—the main three-dimensional mass composed of fused hexactins and the thin lattice network of a quite different structure apposed to the substrate (Figure 38C). A broad range of names has been applied inconsistently to the entire framework and its component parts. We suggest ‘basidictyonal mass’ for the hexactine skeleton, ‘limiting basal plate’ for the superficial surface membrane and ‘basidictyonal framework’ for the entire structure; the term ‘basidictyonal plate’ often used for the structure is often physically inappropriate and is easily confused with the macroscopic ‘basal plate’ used to describe a spreading body part at the attachment site.

The basidictyonal mass is mainly or totally composed of simple, stubby hexactins, sometimes pentactins, of ray length 30–120 μm , fused together directly at contact points or by synapticula. Even in *Lychniscosa*, the basidictyonalia never have lantern nodes. Junctions are tip-to-tip unlike those of most true dictyonalia (see above). This structure may be a single layer or may be several millimetres in thickness. In most lyssacines, the main parenchymal spicules (diactins) may insert loosely into this lattice, but fusion between parenchymals and basidictyonalia occurs only in those forms that have extended secondary fusion. Details of the relationship between the basidictyonal mass and the main fused parenchymal framework of dictyonal hexactines is poorly known but they are probably joined in early development. Basiphytous hexactinellids settle on two basic types of substrate relative to the structural components of the limiting basal plate—flat surfaces of rocks, shells and so on, and cylindric surfaces of proctal spicules and dictyonal frameworks of dead hexactinellids. On flat substrates, the limiting basal plate, where known in detail, consists of stauractins (basidictyonalia?) joined by synapticula to form a thin porous silica sheet with 20–40 μm pores (Figure 38D). On curved surfaces, stauractine, pentactine and/or hexactine dictyonalia appressed to the surface form the building elements for encompassing substrate curvature by synapticular junctions and threads (Figure 38E). The plate is not in direct contact with the substrate, as is the case with calcareous or organic spongin deposition in other sponges, but attachment is attained by encompassing (grasping around) substrate

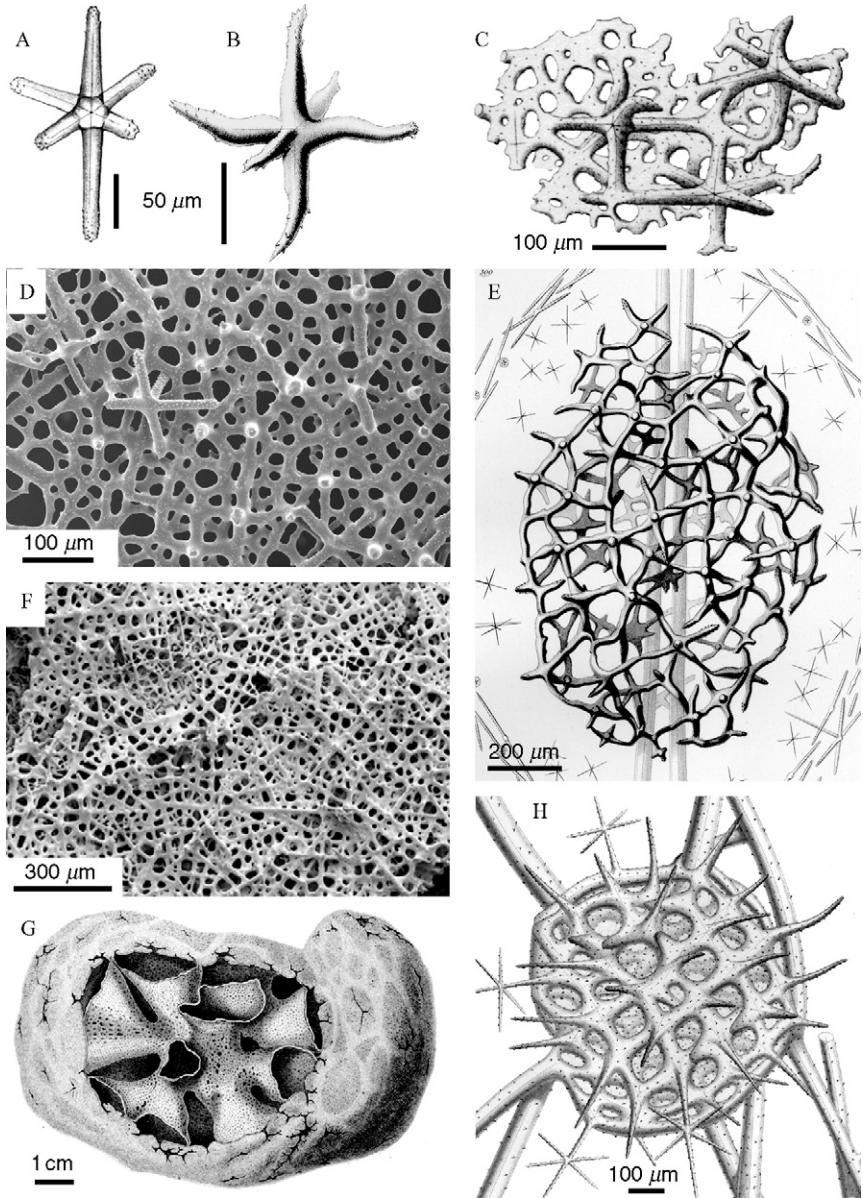


Figure 38 Non-parenchymal siliceous networks of Hexactinellida. (A, B) Stout, small basidictyonalia from lysaccinosans, (A) *Regadrella okinoseana* (from Ijima, 1901) and (B) *Rhabdocalyptus mirabilis* (from Schulze, 1899). (C) Basidictyonal skeleton of *Rhabdocalyptus unguiculatus* from sponge side showing limiting basal plate with fused hexactins of the basidictyonal mass above them (from Ijima, 1904).

irregularities with a closely conforming rigid plate. The limiting basal plate is fused to the network of basidictyonal hexactins above by direct fusion and synapticula. Although the basidictyonal skeleton is characteristically formed at the site of larval attachment, indistinguishably similar structures are apparently formed at sites where adult tissues contact foreign objects and form secondary attachments. In the two known series of post-larval development, basidictyonal elements in the dictyonine, *F. sollasii*, have begun formation in the earliest stage encountered (0.53-mm body length; 67-nl volume) (Okada, 1928), but develop later in the lyssacine, *Leucopsacas scoliodocus*, where they are first seen in juveniles (1.85-mm body length; 1650-nl volume) (Reiswig, 2004). In both cases, parenchymal megascleres appear later than the basidictyonal elements.

6.4.4. Surface networks

Networks of fused spicules and synapticula, variously referred to as cover layers, cortices, tunics, capsules, rinds, Hüllschichte and so on, were characteristic of several groups of fossil dictyonine hexactinellids (Reid, 1958) but are known in only three Recent dictyonine genera: *Lychnocystis* and *Neoaulocystis* of the order Lychniscosida and *Fieldingia*, the only Recent genus in the new order Fieldingida (Tabachnick and Janussen, 2004). These structures are composed of stauractin and pentactin spicules, with a few hexactins, interconnected by an extensive network of anaxial synapticula, forming finely porous lamina, always fused to the underlying dictyonal frameworks. In the two lychniscid genera, the spicules of the networks differ from normal dictyonalia in always having simple nodes. In *Lychnocystis* and *Fieldingia*, the surface networks are rigid, up to 1 mm thick, and multilayered, containing stacks of laminae joined by occasional fusions with the unpaired ray of constituent pentactins stretching between them (Figure 38F). In these genera, every specimen so far encountered has well-developed surface networks; hence the process of development is unknown. In *Neoaulocystis*, most specimens lack any surface networks, but some have early plates extending laterally from the outer margins

(D) Margin of a flat basidictyonal framework of *Rhabdocalyptus dawsoni* from sponge side showing limiting basal plate with only a few rays of constituent pentactins projecting up a sites for future hexactin attachment. (E) Basidictyonal framework of a *Rhabdocalyptus mirabilis* juvenile settled on two proctal spicules (vertical rods) of an adult; note the lack of direct basidictyonal cohesion with the proctal spicules (from Schulze, 1899). (F) Surface network of *Fieldingia valentini* from internal side; compare to basidictyonal limiting plate, D (from Tabachnick and Janussen, 2004). (G) Body of *Neoaulocystis zitteli* partially enclosed in surface network (from Schulze, 1887). (H) Weltner body from *Lychnocystis superstes* (from Schulze, 1887).

of tube walls (Figure 38G). The soft, flexible polygonal plates meet adjacent plates, circumscribing stellate clefts which are eventually closed to cover the entire outer surface excepting large oscular openings in a continuous 0.3 mm thick membrane of porous silica. Multilayering has not been noted in *Neaulocystis*. Without clear definitions, the few data on mesh and beam dimensions are incomparable, but pore sizes generally range from 2 to 45 μm . While porosity of the structures seems adequate for inhalent water flow through these rigid structures, formation of an unexpandable surface shell seems mal-adaptive in blocking further growth. However, it is not known whether these structures are permeated or covered with living tissue and generally entire body forms are unknown for the species bearing these structures. Most workers (Schmidt, 1880; Schulze, 1887; Ijima, 1904) have commented on the similarity of surface networks with basidictyonal frameworks, especially those formed at new contacts with foreign objects, but a direct comparison has not yet been carried out.

6.4.5. Weltner bodies

Sharply delineated spherical knots, skeletal nodes or spheres known as Weltner bodies in recognition of Weltner's detailed descriptions (1882) of them are known sporadically from many dictyonines, but occur predictably in only a few species, *Lychnocystis* (earlier *Cystispongia*) *superstes*, *Neaulocystis zitteli* and both known species of *Fieldingia*. These tight condensations of the regular internal dictyonal framework, liberally covered and sometimes filled with fused small spiny hexactins (Figure 38H), are commonly 0.7–2.0 mm diameter and visible to the naked eye. They are regularly spaced and probably provide stress focal points in the very loose skeleton of *Fieldingia* species, but it is doubtful that they contribute to strengthening the sturdy lychnisc skeletons of the other species. They have been considered products of local stimulus (irritation) by foreign organisms (Schulze, 1900) and possible basidictyonal skeletons of internal buds that have been later integrated into the parental skeleton (Ijima, 1927). These and a variety of other less well-described networks of silica deserve detailed study, but lack of availability of specimens is a continuing deterrent.

6.5. Silication

6.5.1. Basic process and forms of siliceous structures

It has long been assumed that initial silica deposition in hexactinellids occurs as spicule formation as in demosponges by polymerisation of silicic acid on

an organic axial filament deposited within an intracellular vacuole in a cell, generally termed a scleroblast, and specifically called a silicoblast. The specialised limiting membrane of such vacuoles is known as a silicalemma, but the space in which silica deposition occurs remains unnamed. We propose 'silica deposition space' (sds) for this, avoiding "vacuole" since in some or all cases it may be confluent with extracellular spaces. Silica deposition has not been directly observed in hexactinellids, but morphological details of preserved hexactinellids and direct observation of the process in living freshwater demosponges (Weissenfels and Landschoff, 1977) offer strong support that initial silication is similar in both sponge groups. In hexactinellid megascleres, additional layers of silica are added either over the entire surface of the primary spicule or only onto the ends of the longer ray in very large prostaia. Such layers are easily seen due to presumed variations in refractive index as 'ghosts' of earlier spicule surfaces, in lateral view as complete outlines or serially stacked elongate cones and in cross sections as concentric rings surrounding the primary spicule. The initial siliceous cylinder immediately around the axial filament is known as the adaxial zone (Hartman, 1983) or axial cylinder (Claus, 1868) and the added secondary layers are collectively referred to as the peripheral zone. Since basic morphology of both the initial spicule and added layers appears to be determined by the geometric form of the axial filament system, these can best be termed primary and secondary stages of actinal silication (Reid, 2003).

Ornamentation added either to megascleres as spines, hooks, anchor teeth of basalia or long tines of scopules, or to microscleres as unbranched or extensively branched terminal rays, are often considered results of a distinct silication process ('anactinal' in Reid, 2003) since such structures bear no axial filaments resolvable by light microscopy. At our present stage of understanding silica deposition, there seems to be no basic difference 'in kind' between inconsistent variable development of thorns on rays of pentactine megascleres and consistent, channelised formation of terminal rays on hexaster microscleres. Spine formation on megascleres clearly occurs as part of secondary layering of the primary spicule, but whether layer addition occurs on microscleres has not been determined. In both cases, ornamentation does not seem ascribable to the templating function of the axial filament system since that element is quickly enclosed in an impermeable (?) silica sheath.

Additional forms of silica deposition such as spot-soldering of spicules, enclosure of part or entire spicules by silica layering in dictyonal and lyssacine frameworks, formation of synapticular bridges and networks between spicules, all appear to be aspects of anaxial silication since silica deposition here cannot be patterned directly by axial filament geometry. Deposition here appears to differ only qualitatively from the simplest layer addition on primary spicules. Thus, the process of silica deposition in fusion of spicules and synapticular formation, though generally known as

'secondary silication' is unlikely to differ from that involved in layer addition to basic axial spicule structures. In addition to the rules of hexactinellid spicule form noted earlier (axial filaments never branch and new rays cannot be added on to pre-existing spicules), two additional features of silica deposition require consistency testing: silica deposition is irreversible (notwithstanding discovery of a silicase gene in a demosponge, Schröder *et al.*, 2003b) and silica can only be deposited directly on autochthonous axial filaments or on autochthonous siliceous surfaces deposited on autochthonous axial filaments.

6.5.2. Silica constituents and characteristics

Spicules of hexactinellids are nearly indistinguishable from those of demospoges in most measured characteristics. They have the general formula of opaline silica, $\text{SiO}_2 \cdot n\text{H}_2\text{O}$, where n varies from 0.33 in *Monorhaphis* to 0.25 in *Rossella* and most other hexactinellids, reflecting the bound water (water of hydration) of 7–12% dry weight driven from 'dry' spicules when heated to 900°C (Minchin, 1909; Sandford, 2003); some water continues to be evolved at least to 1400°C (Sandford, 2003). Sandford (2003) found that bound water bonds, as indicated by Fourier-transform infrared spectra, are generally similar for silica gel and spicules of both hexactinellids and demospoges. He found an anomalous endothermic event in glass transition temperatures at 425–500°C in *Hyalonema* (amphidiscophoran) spicules that was absent in hexasterophoran spicules. In addition to bound water, hexactinellid spicules consist of 83.8–88.3% SiO_2 and 1.7–4.2% of other minerals, including sulphur, aluminium, potassium, calcium and sodium as major elements (Sandford, 2003). The amount of organic matter in hexactinellid spicules remains unknown and can only be inferred as less than (part of) the weight loss on combustion, given as 2.9% of dry weight in *Poliopogon amadou* by E. Fischer (Schulze, 1904). The refractive index is reported as 1.49 in *Rossella racovitzae* (Sarikaya *et al.*, 2001), 1.467–1.47 in four hexactinellid species (Sandford, 2003, with reservation on accuracy) and 1.425–1.48 in basal spicules of *Euplectella aspergillum* (Aizenberg *et al.*, 2004), values slightly higher than those of demospoges. The long held notion that the microscopically visible layering in spicules is due to variations in refractive index caused by differences in bound water (Schwab and Shore, 1971 in demospoges) were rejected for spicules of *Rossella racovitzae* by measurements of Sarikaya *et al.* (2001), but substantiated by interferometric measurements of spicules of *Euplectella aspergillum* by Aizenberg *et al.* (2004). Density of hexactinellid spicules is 2.03–2.13 (Sandford, 2003), encompassing most values reported from demospoges.

Sarikaya *et al.* (2001) provided additional measurements on spicules of *Rossella racovitzae* for which comparative data on demosponge spicules is unavailable. Hardness is 3.22 ± 0.33 GPa and elastic modulus is 38 ± 3 GPa, both measured by atomic microforce indenter and both about one-half the values for glass fibres and silica rods. Hexactinellid silica is thus softer and less elastic than glass. In three-point bends, these authors found hexactinellid spicules to be exceptionally tough and flexible, with fracture strength of 900 mPa, fracture toughness of 2–5 mPa (both five times the values for glass rods) and fracture energy 15 times that of glass rods, ascribed to energy storage in spicule layers prior to general rupture of the entire spicule. Mechanical properties of individual spicules and the entire skeleton of *Euplectella aspergillum* were elegantly explored in terms of engineering design by Aizenberg *et al.* (2005). They concluded that details of construction at seven levels of hierarchy provided a supporting framework of outstanding mechanical rigidity and stability for the basically brittle silica-building material.

6.5.3. Microscopy of silica deposition

Observations of sections of fixed hexactinellid tissues have led to a series of conclusions on spicule formation. Ijima (1901, 1904) combined observations on adult tissues of many hexasterophorans and concluded that microscleres were formed in dense, multinucleate scleroblast masses which he interpreted not as discrete cells as in demospoges, but as local condensations of the general trabecular syncytium. The earliest stages had only the six basal rays of the spicule and no definite number of associated nuclei. He discerned a repeating pattern of expansion, condensation and differentiation of the scleroblast mass with microsclere maturation, with its eventual disappearance or transformation to a diffuse tissue network identical to, and continuous with, the general trabeculum. Ijima's conclusions were entirely supported by studies of Woodland (1908). Okada (1928), in his description of hexaster development in larvae and juveniles of *F. sollasii*, reported prospective scleroblasts to be discrete mononucleate cells of the embryonic dermal epithelium that move below the outer layer and become multinucleate scleroblast masses when the first hexactine stages of the siliceous primordium are encountered. Nuclear numbers of this tissue, which we now recognise as a sclerosyncytium, increase as spicules mature and scleroblast nuclei differ from regular nuclei of the trabeculum in being larger, more spherical, packed with chromatin granules, often possessing nucleoli and staining more deeply with borax carmine. Okada concluded that the scleroblast mass (sclerosyncytium) became part of the general trabeculum when spicule formation was complete.

Development of larval stauractins (megascleres?) has been reported by Okada (1928) in *F. sollasii* and by Leys (2003a) in *Oopsacas minuta*. In *F. sollasii*, stauractin scleroblasts are specific columnar epithelial cells that move under the outer epithelium and begin spicule formation, but remain discrete mononucleate cells throughout spiculogenesis. Using transmission and scanning electron microscopes, Leys (2003a) concluded that the 14 larval stauractins in *Oopsacas minuta* begin development by formation of typical hexactinellid axial filaments in intracellular sds of discrete sclerocytes and deposition of silica on these axial structures. The sclerocytes are first mononucleate cells rich in mitochondria, clear vesicles and pseudopodia and connected to other tissues by plugged junctions. As spicule maturation proceeds, the sclerocytes become multinucleate and then known as sclerosyncytia, but after completion of spicule formation, the ultimate fate of these sclerosyncytia remains unknown.

Few observations on development of megascleres in adult tissues or their relationship to living tissue have been published. In *F. sollasii*, Okada (1928) described formation of clavules and hexactine dictyonalia in multinucleate scleroblast masses that are distinct from the general trabeculum only by nuclear form. Mackie and Singla (1983) summarise observations on tissues of adult *Rhabdocalyptus dawsoni*, without making distinction between conditions in microscleres and megascleres, that spicules are formed intracellularly in multinucleate giant sclerocytes (sclerosyncytia) which are the only large tissue components differentiated from and connected to the trabecular syncytium by plugged cytoplasmic bridges while silica is being deposited. These authors also found mature spicules within the general trabecular syncytium, but whether they are formed there remains an open question. They also report electron-dense materials remaining in/on the walls of the cavity left when spicules are dissolved from tissues by hydrofluoric acid.

Several questions on tissue–spicule relationships remain incompletely resolved. Does silication take place only in sds lined by a special silicalemma membrane? Many authors have taken this to be a general rule for all siliceous sponges because it has been repeatedly verified (or unfalsified) in freshwater demosponges where spicule deposition has been monitored in special living microscopic preparations. Extracellular secretion of spicular silica has been reported only by Uriz *et al.* (2003) in the demosponge, *Crambe crambe*. Although it may be extremely difficult to demonstrate continuity between silicalemma and plasmalemma in ultra-thin sections and transmission electron microscopy, it should be obvious that, in hexactinellids, silica secretion and often axial filament extension must occur at sites which are bordered by membranes that are continuous with the plasmalemma of either the scleroblast or the general trabecular syncytium. These include all projecting prostaia, including the conspicuous basal anchors of Hyalonematidae, which are mostly emergent from the living tissue but remain embedded in trabecular

syncytium at one end where axial filament and silication continues. Extension of the axial filament and silication must take place here in spaces that are continuous with the external milieu, but that are presumably functionally isolated by close apposition of membranes to spicule surfaces. The same situation must hold for dictyonal skeletons in general where living tissues have retracted from any part of the skeleton, most commonly the basal attachment. Initial formation of axial filaments and silica secretion may take place within closed intracellular sds, but lack of continuity with the plasmalemma would be difficult to prove. Many spicules may be enclosed in intracellular sds during their entire development, but some, as just noted, cannot remain so, even during their development, which may continue as long as the sponge lives and never be completed.

Do spicules that have completed development remain within intra-syncytial sds or are they exocytosed and thus freely exposed to the exterior milieu? Again, as noted, some spicules and dictyonal structures are clearly exposed at least in part. Observations by several workers suggest most spicules remain entirely coated (enveloped within) the trabecular syncytium (Woodland, 1908; Okada, 1928; Wyeth *et al.*, 1996), but others have suggested that most megascleres are attached to or enclosed by strands of the trabecular syncytium only at discontinuous points (Mackie and Singla, 1983).

Do spicules have an organic spicular sheath or organic matrix? The fibrillar organic material found by Travis *et al.* (1967) on/in *Euplectella* spicules may be part of the collagenous mesolammella appended to outer spicule surfaces when in extra-syncytial position, but the electron-dense lining remaining on cavities of *Rhabdocalyptus dawsoni* spicules in intracellular locations (Mackie and Singla, 1983) might represent an organic sheath involved in the process of silica deposition. The undissolved amorphous electron-dense matter remaining after spicule dissolution with hydrofluoric acid (HF) (Travis *et al.*, 1967; Mackie and Singla, 1983; Leys, 2003a) may be the remains of matrix molecules, but this material has yet to be completely characterised. Aizenberg *et al.* (2004) interpreted gaps formed between outer layers of basalia of *Euplectella aspergillum* after NaOCl exposure, but other interpretations for this effect were not explored. An energy dispersive X-ray analysis (EDX) carbon map of a spicule section, likewise, interpreted to document organic matter within the spicule matrix was not convincingly portrayed. This may be the same fibrillar collagen demonstrated by Ehrlich *et al.* (2005) in root spicules of *Hyalonema sieboldi* using a novel method of silica extraction.

6.5.4. Axial filaments

Early history of observations and nomenclature of hexactinellid spicules and their parts is summarised by Schulze (1904), but he omits his own earlier

fanciful interpretation (Schulze, 1887) of axial filaments as channels to supply nourishment to the living distal parts of root spicules of *Hyalonema* and *Euplectella*. While most studies of axial filaments have been carried out on demosponges, conclusions obtained there can be generally assumed to apply also to those of hexactinellids pending their falsification in that group. Axial filaments of hexactinellids vary in size (width of side) from 0.3 to 0.5 μm in larval stauractins of *Oopsacas minuta* (Leys, 2003a) to 7 μm in pentactins of *Rossella racovitzae* (Sarikaya et al., 2001, Figure 34C). Bütschli (1901) concluded from staining characteristics that axial filaments of demosponges were mainly protein. Dendy (1926) proposed that axial filaments were a group of microbes, his 'sclerococci', which induced host sponges to encapsulate them in silica, thereby forming their skeletons. This hypothesis attracted no support by other biologists. The nature of filaments of the demosponge *Haliclona rosea* was convincingly settled by Garrone (1969) through use of electron microscopy, X-ray diffraction and pepsin digestion. He concluded that these filaments were composed primarily of a hexagonally crystallised protein. Subsequent studies on demosponges showed that filaments undergo submicroscopic branching, extending fine cores as small as 0.05 μm diameter into spines and thorns of megascleres and microscleres (Garrone et al., 1981; Simpson et al., 1983, 1985). The filaments were also shown to be more heterogeneous, both within a single spicule and between species, than previously thought, with occasional repeating surface beading, less dense centres and refractile cores (perhaps containing silicates) or voids. The crystalline protein figured earlier by Garrone (1969) was considered only a small part of the mature filament.

Shimizu et al. (1998) purified three main structural protein subunits from axial filaments of the demosponge *Tethya aurantium*, cloned and sequenced the cDNA of the most abundant one and determined that these were similar to members of the cathepsin L and papain family of proteases. Since axial filaments were already suspected of serving as templates for silica deposition (Imsiecke et al., 1995), and Shimizu et al. (1998) found that the purified protein filaments and subunits promoted polymerisation of silica and silicenes from corresponding silicon alkoxide precursors at room temperature and neutral pH, they named the three protein subunits as silicatein α , β and γ to emphasise their enzymatic properties. Although axial filaments and silicateins of hexactinellids and demosponges are no doubt derived from a common ancestral source, Croce et al. (2003) found significant differences between them in small angle X-ray diffraction studies. Filaments of the hexactinellid *Scolymastra joubini* have two different two-dimensional lattices due to protein units repeating at $+50^\circ$ and -50° relative to the spicule axis and consistent with a hexagonal packing of spirally oriented cylindrical protein units elongated along the filament axis (Figure 39B and C). This contrasts to the hexagonal protein lattice of the demosponge *Geodia*

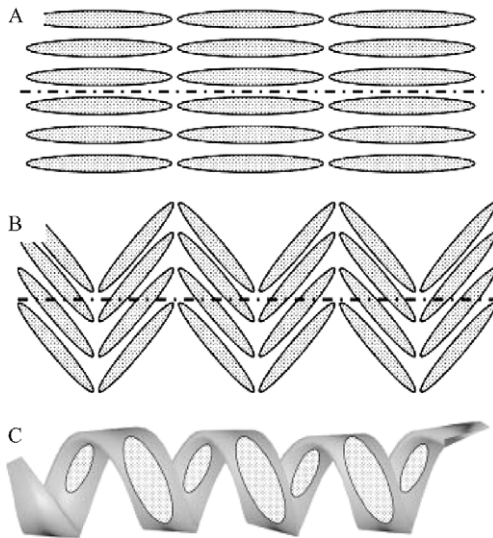


Figure 39 Comparison of two-dimensional structural models of protein (silicatein) units in axial filaments of the demosponge *Geodia cydonium* (A) and the hexactinellid *Scolymastra joubini* (B), with longitudinal spicule axes represented by dot-dashed lines. (C) Three-dimensional representation of the model of spirally oriented cylindrical protein units along the axial filament axis of *Scolymastra joubini* (from Croce *et al.*, 2003).

cydonium with units oriented parallel (apparently erroneously reported as perpendicular) to the spicule axis and packed more densely than in hexactinellid filaments (Figure 39A). Spacing between units also differs in the two filaments, 8.4 nm in the hexactinellid and 5.8 nm in the demosponge. A more detailed comparison of the silicateins of Hexactinellida and Demospongiae awaits sequence determination of hexactinellid silicateins.

6.5.5. Molecular processes and silication model

Results of experiments on silication in demospoges, summarised here, have led to proposed models that probably apply also to hexactinellids. Silication rate *in vivo* is influenced by silica concentration, temperature, particulate organic matter concentration and Fe^{3+} concentration (Uriz *et al.*, 2003). Silicateins are not entirely restricted in their distribution to the axial filament but have also been shown by immunofluorescent labelling to occur on the outer surfaces of developing spicules (Cha *et al.*, 1999) and may be the same material seen lining outer spicule surfaces after spicule extraction

(Mackie and Singla, 1983; Leys, 2003a). Spicules dissociated with HF expose axial filament silicateins which remain active in polymerisation of silicon alkoxides but lose their templating function (Shimizu *et al.*, 1998). Silicatein *in vitro* catalyses deposition of 70 nm diameter particles (nanospheres) on axial filaments several layers thick (Cha *et al.*, 1999). A similar process probably occurs *in vivo* since atomic force microscopy has shown that HF-etched spicules of the demosponge *Tethya aurantia* have nanoparticles of 50 to 80 nm diameter in alternating layers about one particle thick (Weaver and Morse, 2003). Similar nanospheres 50 to 200 nm in diameter have been shown to be the basic form of building material in the spicules of *Euplectella* sp. (Aizenberg *et al.*, 2004, 2005). Nanospheres as small as 17 nm diameter have been detected in demosponge spicule formation *in vivo*; these apparently fuse to form particles 100 to 1200 nm in diameter and intervening spaces are then smoothly filled with amorphous silica (Uriz *et al.*, 2003). Layering in spicules may indicate pauses in nanosphere deposition and smoothing (filling in) steps. High silica concentrations have been found in the cytoplasm near developing spicules (to 50%) and in the spicule space between spicule and bounding silicalemma (50–65%) (Uriz *et al.*, 2003).

The following model of silication in sponges is derived from these observations and propositions put forth by Croce *et al.* (2003), Müller *et al.* (2003), Weaver and Morse (2003) and Uriz *et al.* (2003). Sclerocytes secrete axial filaments composed mainly of silicateins but other organic molecules are included. Silicatein acts as a structural template for formation of the highly organised mesoporous axial filament. Inorganic silicate diffuses or is actively taken up into the sclerocyte and complexed with specific proteins to form an as yet unidentified organo-silica substrate. The organo-silica complex is transported across silicalemma to the sds. Silica from organo-silica substrate is polymerised on the outer surface of the mesoporous axial filaments as nanospheres, perhaps at serine and histidine catalytic centre sites, and the complexing protein is released and possibly recycled to the sclerocyte cytoplasm. Growth of the axial filament continues at spicule tips, providing primary patterning of the spicule, while at the same time transport and deposition of silica continue on lateral spicule surfaces between the tips. Once the first few layers of silica nanospheres encase the axial filament, enzymatic activity can no longer be expressed by silicateins of the axial filament. Continuing deposition of silica on the outer surface of spicules is facilitated and controlled by silicatein at active sites on the silicalemma, resulting in production of specific patterned morphologies of spicules.

Several elements of this model remain unverified. Other unknowns include the roles of the minor non-silicatein organic compounds incorporated in axial filaments, whether silicateins associated with the silicalemma are the same forms as those in the axial filaments and how the final high-fidelity sub-microscopic external patterning on spicule surfaces is genetically controlled.

7. ECOLOGY

7.1. Habitats: distribution and abundance

Glass sponges are found in deep water (greater than 500 m) in all oceans of the world, but only inhabit shallow waters (up to 20 m) in four known locations: Antarctica, southern New Zealand, submarine caves in the Mediterranean and coastal waters of the North Pacific. Their restriction to deep waters is shared with only one other sponge group—lithistid demosponges—which, like glass sponges, have a heavily fortified glass spicule skeleton (Pisera and Lévi, 2002). It has been speculated that silica limitation in shallow waters forms the upper limit for both of these groups (Austin, 1983, 1999; Maldonado *et al.*, 1999), but light, temperature, food availability and turbulence (current or wave-driven) may also restrict the distribution of glass sponges in particular to deeper waters (Leys *et al.*, 2004). Currently, there is no experimental evidence to support or reject any one of these hypotheses.

Although in many regions glass sponges appear sparsely distributed, in some localities, both deep and shallow, glass sponge populations are very dense (Figure 40A and B). High densities (1.5 m^{-2}) of *Pheronema carpenteri* occur within a narrow depth range (1000–3000 m) in the Porcupine Seabight, southwest of Ireland (Bett and Rice, 1992). Stalks of *Hyalonema* can be found every 5 m ($\sim 2\text{--}3$ per 10 m^2) at 4100 m in a bathyl basin off California (Beaulieu, 2001a,b). The benthos at 100–300 m in the Weddell Sea, Antarctica is heavily occupied by sponges (Barthel and Gutt, 1992; Barthel and Tendal, 1994). Although demosponges are most abundant (up to 200 per 10 m^{-2}), some sites are dominated by seven species of hexactinellids; of these *Rossella racovitzae* was the most abundant with up to 23 individuals in 10 m^2 . Some hexactinellids like *Scolymastra joubini* can obtain substantial sizes of over a metre in height and breadth (Figure 40C).

The tiny 3 to 7 cm long cave sponge *Oopsacas minuta* occurs at a high density of up to 100 m^{-2} (Vacelet *et al.*, 1994). But the most abundant glass sponges in terms of number and biomass are found in NE Pacific fjords and continental shelf waters where dictyonine forms (those with a fused skeleton) each up to a metre in breadth, reach individual abundances of up to 250 individuals per 10 m^2 on vertical walls and form solid reefs up to 160 km^2 on continental shelf habitats (Conway *et al.*, 1991, 2001; Krautter *et al.*, 2001; Conway *et al.*, 2004; Leys *et al.*, 2004) (Section 7.3). Glass sponges tend to have a patchy distribution in all regions studied which could suggest that they either have very particular ecological requirements or larval dispersal is only local (Barthel and Gutt, 1992; Bett and Rice, 1992; Leys and Lauzon, 1998).



7.2. Succession: glass sponge skeletons as substrates

Except for a few species such as the minute cave sponge *Oopsacas minuta*, most glass sponges tend to be large, conspicuous inhabitants of the benthos. When these large animals die, their spicule skeletons, whether loose (lyssacine) or fused, form a firm mat or scaffold which dramatically alters the landscape for other animals.

In a study of sponge associations at Kapp Norvegia, Antarctica (Barthel and Gutt, 1992), glass sponge skeletons of lysaccine forms were found to be intertwined in such a way that when the tissue disappeared the skeleton was still resistant to tearing (Barthel, 1992). As few demosponges contribute similar distinct spicule masses, Barthel (1992) suggests that the spicule mats of hexactinellids restructure soft substrates, which then allows colonisation by demosponges and a host of other invertebrates (Figure 41).

At the Porcupine Seabight, spicule mats were found to cover one-third of the sea floor (Bett and Rice, 1992). Principal component analysis of abundance of organisms in box core samples suggests that most variation in abundance of organisms is related to the presence of spicules. Specifically, of the 10 most abundant taxa found in the cores, 7 increased in abundance with increased spicule mat density. What remains unclear is how these soft sediment substrates are initially colonised. Possibly, disturbance caused by other conditions, such as anchor ice (Dayton, 1989), can cause sufficient variation in sedimentation and food availability to allow the first hexactinellid larvae to settle.

Hyalonema is able to colonise soft substrates. Every individual of this remarkable genus lives suspended on a tall shaft of spicules anchored in 20–40 cm of sediment (Beaulieu, 2001a,b). The bulk of the body forms a thick disc or cone whose upper surface is oriented away from the prevailing current. The spicule stalk of live specimens may have some tissue coating, but once grown, the adult sponge withdraws to its high-rise habitat, thus leaving the spicules free for settlement of other animals (Beaulieu, 2001a). When the sponge dies, the disc disappears leaving an upright stem of long glass shards (Figure 42). Of 2105 *Hyalonema* stalks studied photographically in an abyssal plain at 4100 m near California, only 14% supported a living sponge on top. The remaining 1810 stalks were inhabited by a huge array of predominantly filter feeders (Beaulieu, 2001b). Common colonisers on the stalk are zoanths (which also inhabit 30% of live stalks), but other

Figure 40 Abundance and distribution of glass sponges. (A, B) Dictyonine sponges, *Aphrocallistes vastus* and possibly *Heterchone calyx*, at 160 m in the fjords of British Columbia, Canada (Leys, unpublished data). (C) *Scolymastra joubini* with crinoids attached and a nearby diver at 50 m at McMurdo Sound, Antarctica (courtesy of G. Bavestrello).

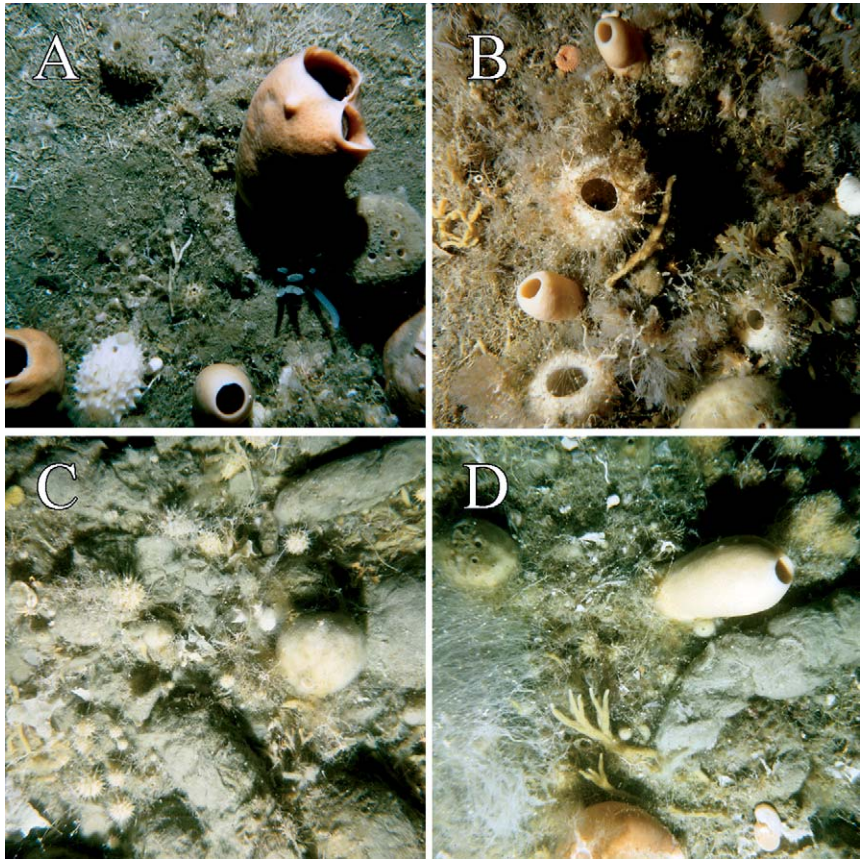


Figure 41 Glass sponges and spicule mats formed by glass sponges in the Weddell Sea (A, B are from 71°06,211'S11°39,032'W, 194-m depth; C, D are from 71°38,2'S12°09,5'W, 112 m. All photos represent 0.56 m². Courtesy of J. Gutt, copyright: J. Gutt, AWI). (A) *Rossella nuda*, a tube-shaped, smooth-sided, cream-brown sponge (top right and bottom left and middle); *Rossella racovitzae*, the white sponge bottom left; two demosponges, probably *Cinachyra barbata*, right below *Rossella nuda*. (B) Several specimens of *Rossella racovitzae* (white with projecting spicules) and *Rossella nuda* (cream with smooth exterior) on a mat of bryozoan skeletons. (C) A dense glass sponge spicule mat supporting the growth of several demosponges, including the small round white sponge *Cinachyra antarctica*. (D) *Rossella nuda* (right) and *Cinachyra barbata* (left middle) on a mat of glass sponge spicules.

inhabitants included tunicates, ophiuroids, anemones, bryozoans, other sponges (as well as other hexactinellid sponges) and even a benthic ctenophore. So many organisms inhabit these stalks that within the slim 20 to 50 cm vertical habitat all the ecological interactions of competition for space,

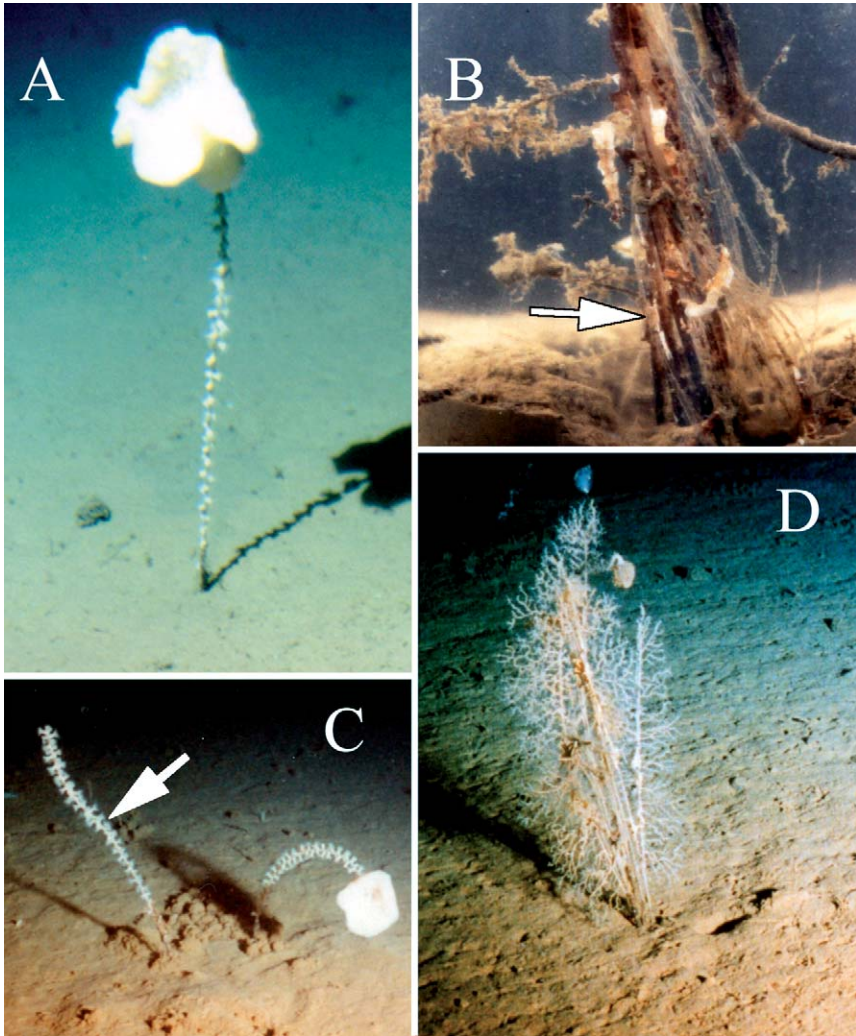


Figure 42 Live and dead stalks of *Hyalonema* at 4100-m depth in the NE Pacific (A, from Beaulieu, 2001a, with kind permission of Springer Science and Business Media; B–D, Beaulieu, unpublished data). (A, B) The sponge forms a disc of living tissue on the end of a shaft 25 to 50 cm long of spicules that are twisted together (B, arrow). In time, tissue covering the stalk recedes, allowing other animals colonise it (C, arrow). (C, D) Eventually, the disc-shaped body also dies, but the stalk remains for many years as a substrate for colonisation by other invertebrates.

flow and food, predation and succession can be found. Clearly, even the smallest collection of glass sponge spicules can structure the benthos of abyssal and shallow water habitats.

7.3. Reefs or bioherms

7.3.1. Structure of the reefs

Vast sponge reefs are at the other extreme of sponge skeleton habitats. Reefs and mounds are formed by the accumulation of generations of glass sponge skeletons. Massive mounds of spicules (biostromes) are found in locations of high densities of glass sponges, such as Antarctica, and have a structuring effect on the other biota as described above. But sponge reefs (bioherms) are formed by only three species of hexactinellid whose skeleton is fused or dictyonine. The rigid scaffold formed by the dictyonine skeleton remains after the tissue has died allowing juveniles to settle on the exposed skeletons of adults, but to form the reef the base of the skeletons must also become locked into a rigid structure by the accumulation of sediment (Conway *et al.*, 2001; Krautter *et al.*, 2001; Conway *et al.*, 2005b). It is presumed that the sponges need to grow just fast enough to keep ahead of sedimentation.

During the Jurassic, dictyonine sponges thrived and left a record that can be found throughout the world in outcrops of weather resistant rock. The first sponge reefs are known from the Atlas Mountains of Morocco, a region that formed the southern margin of the Tethys Sea. In the Middle Jurassic, bioherms are known from India, Spain, France and Hungary (Mehl and Fürsich, 1997; Pisera, 1997). The reefs reached their maximum in the Late Jurassic, when siliceous sponges formed a discontinuous deep-water reef belt over 7000-km long spanning the northern margin of the Tethys Sea, a region that now covers much of Europe (Ghiold, 1991; Leinfelder *et al.*, 1994; Krautter *et al.*, 2001). Although the reefs declined during the Cretaceous, sponge mounds with a high diversity of hexactinellids persisted throughout that period in regions now part of northern Germany and Spain, and then disappeared entirely world-wide. No modern analogues were thought to exist until the discovery in 1987–1988 of several bioherms and biostromes in Queen Charlotte Sound and Hecate Strait on Canada's western continental shelf (Conway *et al.*, 1991). Continued surveying of Canadian waters including southern locations using multibeam and side-scan sonar have now revealed at least seven reefs. In the north there are four discrete reefs, the largest nearly 160 km², which together form a discontinuous band covering some 425 km² at 165–240 m. In the Strait of Georgia three more reefs have been identified, one very close to the city of Vancouver, directly under the outflow of the Fraser River (Conway *et al.*, 2004) (Figure 43).

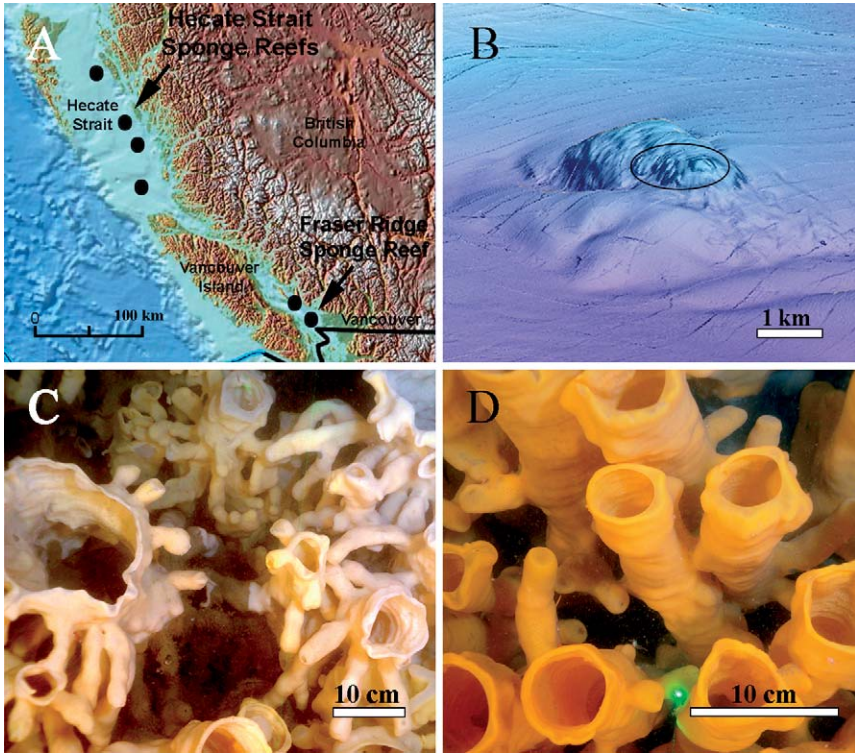


Figure 43 Sponge reefs. (A) The location of sponge reefs on the continental shelf of the Northeast Pacific. (B) A multibeam image showing the southernmost 1 km long reef (black oval) on the Fraser Ridge near Vancouver, Canada (courtesy of K. Conway). (C, D) The 5000-year-old Fraser Ridge Reef supports the growth of *Aphrocallistes vastus* and *Heterochone calyx* (courtesy of V. Tunnicliffe and VENUS).

It is quite remarkable that the presence of the reefs was not known earlier, especially considering the proximity of the Fraser Ridge to Vancouver. Although grab sampling from much earlier surveys did reveal abundances of glass sponges in a region of the Strait of Georgia 40 km northwest and southeast of Nanaimo (Fraser, 1932), the region under the Fraser River plume was not sampled. Development of modern benthic survey technology was certainly key to their discovery and description and multibeam data sets combining elevation and backscatter data can precisely delimit reef areas (Conway *et al.*, 2005a), but by far the best way to view the reefs is by submersible or remote operated vehicle. As shown in videos by these researchers, the reefs loom out of the dark waters as a forest of yellow and orange bushes. Some species have vast, gaping oscula (e.g. *Heterochone calyx*) while others have undulating and billowing palm-like extensions

(*Aphrocallistes vastus*), yet others are a mass of snow white frills (*F. occa*); four lyssaccine sponges are also found on the northern reefs (Krautter *et al.*, 2001). Detailed information on the fauna of the southern reefs is not yet available.

The living sponges on the reef surface are only about 1 to 2 m high, but cores have shown that the average depth of reef mounds is 5–8 m high, but they can be as tall as 19 m, an estimated 6000–9000 years old (Conway *et al.*, 2001), which suggests that initial colonisation occurred shortly after the retreat of glaciers on Canada's West Coast. Reefs range from symmetrical and circular in plan view biohermal forms to steep-sided elongate ridges. The first sponge larvae to settle encountered a surface of glacially derived boulders concentrated and piled high at the edges of iceberg scours (Figure 44) (Krautter *et al.*, 2001). Bottom currents are thought to keep surfaces of these mounds sediment free for the continued attachment of new sponges (Krautter *et al.*, 2001).

7.3.2. *Organisms associated with the reefs*

Common macrofauna on the reefs are several species of rockfishes, crustaceans and echinoderms that live in and around the sponges (Krautter *et al.*, 2001). Although a variety of annelid worms (terebellids and serpulids) and bryozoans encrust the dead sponge skeletons, endobenthic and semi-infaunal organisms are rare. The presence of two bivalve species that are adapted for low oxygen and for reducing conditions (*Thyasira fouldi* and *Thyasira flexuosa*) in cores of the reef sediment suggests this is not a thriving infaunal habitat (Cook, 2005). On the other hand, the reef supports a remarkable diversity of foraminifera (Krautter *et al.*, 2001; Guilbault *et al.*, 2006).

7.3.3. *Fisheries and conservation of the reefs*

Side-scan sonar data collected in July 1999 revealed numerous sets of parallel tracks traversing many mounds within several of the British Columbia sponge reefs (Conway *et al.*, 2001; Krautter *et al.*, 2001). The tracks—usually 70–100 m apart—are suspected to be carved by the heavy (2 tons) doors of the otter trawl, which fishers use to indiscriminately harvest fish and invertebrates. Trawl marks were not evident in the same area in 1988. Observations by submersible in 1999 showed piles of sponge skeletal debris (Conway *et al.*, 2001). A startling summary of observations from the British Columbia groundfish bottom trawl fishery has shown that between 1996 and 2002 about 253 tons of corals and sponges were harvested as bycatch; however,

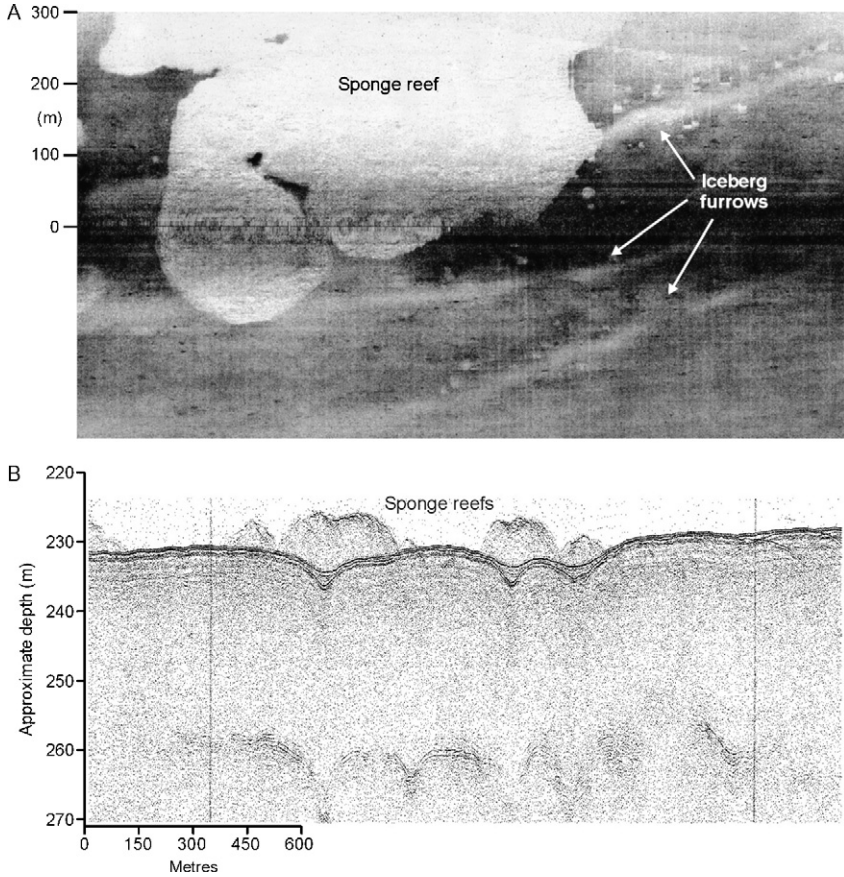


Figure 44 Side scan (A) and bathymetry (B) show profiles of one of the sponge reefs discovered in Hecate Strait in 1990 (courtesy of K. Conway). The 9000-year-old reef grows on the edges of iceberg scours at approximately 200-m depth.

because these are non-commercial species it is thought that many additional observations were unreported (Jeff Ardon, personal communication). An analysis of the regions in which most bycatch occurred suggests there are 12 patches in which 97% of all coral/sponge bycatch was observed, many adjacent to and on the sponge reefs. Voluntary avoidance of the reefs was agreed on by groundfish trawlers in 1999, but although fishing was reduced, landings continued within these areas and over the reefs (Jamieson and Chew, 2002). In 2002, the areas directly over reefs were officially closed to fishing by the Department of Fisheries and Oceans, Canada, and the long-term goal is to implement Marine Protected Areas covering an additional 9-km buffer zone around each reef (Jamieson and Chew, 2002).

7.3.4. Chemical oceanography of the reefs

The uniqueness of the Canadian sponge reefs in the modern world has prompted attempts to define the key oceanographic characteristics that delimit the distribution of glass sponges in general and of reef-building sponges in particular (Maldonado *et al.*, 1999; Leys *et al.*, 2004; Whitney *et al.*, 2005). The principal factor thought to be critical for glass sponge existence is silica, because of the massive amounts of the nutrient they require for skeleton formation (Austin, 1983, 1999; Maldonado *et al.*, 1999; Krasko *et al.*, 2000), but high levels of biogenic materials must also be necessary. The Canadian West coast sponge reefs occur in a high silicate (43–75 μm) and low oxygen environment at 140–240 m (Whitney *et al.*, 2005). Oceanographic surveys of bottom currents, nutrient and oxygen levels and particulate materials in waters near and over the Hecate Strait sponge reefs suggest that both silica and nutrients are enhanced in waters surrounding the reefs during summer months (Whitney *et al.*, 2005). As deep ocean water crosses the shelf during weak summer upwelling, silica levels increase and oxygen levels are depleted due to remineralisation of waters. Furthermore, the bottom currents around the canyons in which the reefs occur trap particulates keeping them within the reef for up to 6 days at a time. The particulates are suggested to provide nutrients to the sponges as well as enhance reef construction (Yahel *et al.*, 2007).

7.4. Growth rates and seasonal regression

Growth rates of glass sponges have been difficult to determine because of their preferred deep sea habitat and because of the unusual shapes that some species have. Dayton (1979) carried out the first long-term growth study on three species in McMurdo Sound, Antarctica, using underwater photography of marked specimens at 60 m depth. He found that while two species, *Scolymastra joubini* and *Rossella nuda*, showed only slight growth over 10 years—one specimen increasing in diameter from 75 to 77 cm and the other from 34 to 37 cm—others showed no measurable change in size. A third species, *Rossella racovitzae*, grew considerably. Because this species regularly forms buds, joins with other individuals and normally lives within the mat of spicules of previous generations of sponges, growth rates were particularly difficult to determine from photographs. Linear growth rates of portions of 13 sponges, caged and uncaged, ranged from 11 to 16 cm in 10 years (Figure 45). Small individuals, however, showed a massively faster growth rate. Of 40 individuals caged in 1974 for 3 years, 15 sponges increased their volume by 100–300%, 12 increased in volume by up to 100%, 5 died and 5 showed negligible (1–10%) growth.

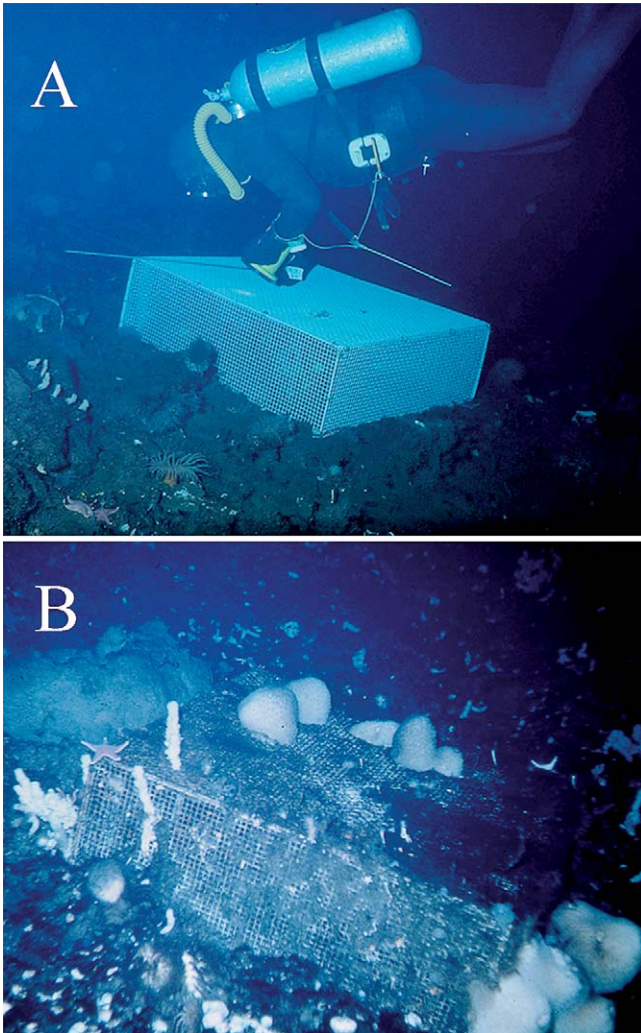


Figure 45 During the 1960s and 1970s, P. K. Dayton and colleagues used cages to prevent predation on sponges by asteroids at 54 m depth in McMurdo Sound, Antarctica. (A) P. K. Dayton carrying a cage. (B) Cages had no inhibitory effect on growth of the demosponge *Mycale* which grew right through the mesh (courtesy of P. K. Dayton).

The trend to slower growth in larger animals appears to be also true for the NE Pacific species, *Rhabdocalyptus dawsoni*. Growth rates in these tube-shaped sponges were measured by underwater photography for 3 years (Leys and Lauzon, 1998). The average linear rate of growth of sponges 5–95 cm in

length was nearly 2 cm year^{-1} , and the average increase in volume was 167 ml year^{-1} , but larger sponges grew marginally less during the observation period than smaller sponges. Since much larger sponges occur in other inlets on the British Columbia coast, it is suggested that the maximum size obtainable depends on local environmental conditions and that in general these sponges can be considered to show indeterminate growth as do corals (Sebens, 1987).

Attempts have been made to quantify growth rates in the aptly named 'cloud' sponge *Aphrocallistes vastus*, a principal component of the massive sponge reefs in the NE Pacific. Austin (cited in Krautter *et al.*, 2001) reported many individuals of *Aphrocallistes vastus* growing on a cable that had been submerged in the Strait of Georgia 10 years earlier. Surveys in 1991 revealed no sponges; thus animals that were 67 cm in length in 2000 may have grown $3\text{--}7 \text{ cm year}^{-1}$ or even more depending on when they settled. Recent *in situ* measurements of small specimens of *Aphrocallistes vastus* at Senanus Island in Saanich Inlet suggest linear growth rates of $1\text{--}3 \text{ cm year}^{-1}$ (Austin, 2003). Preliminary results from an *in situ* study of multiple photographs of marked animals on fjord walls taken with the remotely operated vehicle ROPOS (ropos.com) also suggest linear growth rates of $1\text{--}3 \text{ cm year}^{-1}$ in small specimens. However, these images also illustrate the massive shape changes that accompany growth: increased width of the base, width of the apex and remodelling of the 'flanges' or projections that will subsequently form the characteristic 'mittens' or palm-shaped projections of this species (Figure 46). Throughout the remodelling process the osculum changes location.

7.5. Predation, mortality and regeneration

Two studies suggest that the skeleton accounts for almost 90% of the animal by dry weight; only 10% being organic material (Barthel, 1995; Whitney *et al.*, 2005). Barthel's calculations of the calorific values of glass sponge tissue suggest there is not much of a meal to be had in a glass sponge, but that does not seem to deter either asteroids or nudibranchs, the typical sponge predators.

The most significant study of predation on glass sponges is by Dayton and colleagues (Dayton, 1979, 1989; Dayton *et al.*, 1974). The asteroids *Odontaster meridionalis*, *Acodontaster conspicuus*, *A. hodgsoni*, *Perknaster fuscus antarcticus*, and the nudibranch *Austrodoris mcmurdensis* were the main predators of *Rossella racovitzae* and *Rossella nuda* (the 'volcano' sponge), but the extent of predation (by predators on different species) is highly variable. On one hand, up to 18 *Austrodoris* nudibranchs can feed on a

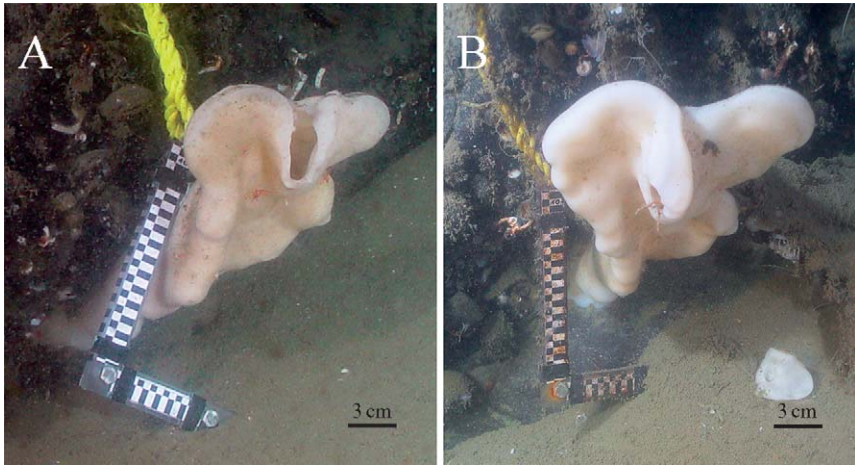


Figure 46 Growth rates in glass sponges are difficult to determine accurately because of the unusual shapes of the animals. These two images taken 1 year apart show the increase in breadth and depth of a 20-cm tall individual of *Aphrocallistes vastus*. Scale markings are 0.5 cm. The linear growth rate of this specimen is approximately 1 cm year^{-1} (Leys, unpublished data).

single *Rossella nuda* without significant damage to the sponge, yet it takes only one to four *Acodontaster* asteroids to kill a large *Rossella nuda*. Attacks by asteroids are not always fatal. Field observations showed that all large individuals of *Scolymastra joubini* had depressions and grooves indicative of browsing by nudibranchs and asteroids (Dayton, 1979). By caging freshly wounded individuals of *Scolymastra joubini*, Dayton's team was able to show that sponges could regenerate if no more than 10% of the sponge volume was wounded (Dayton, 1979); a larger wound usually caused the sponge to die. They concluded that large sponges could tolerate occasional attacks over several years, but survival was unlikely if several asteroids converged on the same individual (Figure 47).

In the NE Pacific, glass sponge populations observations of predation are scarce. Few asteroids are ever seen directly on the hexactinosan (reef-building) sponges, but three species of asteroid—*Pteraster tessellatus*, *Henricia* sp. and *Mediaster* sp.—are typically found on *Rhabdocalyptus dawsoni*. *Henricia* is thought to feed on bacteria and tiny particles that it captures in mucous (Morris *et al.*, 1980), thus it may feed on detritus in the shaggy 'spicule jungle' of *Rhabdocalyptus dawsoni*. *Pteraster* is certainly after the sponge tissue, however, since individuals pulled off the sponge come away with stomach everted and spicules and tissue attached (Leys, unpublished observations; Figure 47C).

The ability of *Rhabdocalyptus dawsoni* to rapidly recover from small wounds appears to be similar to that of *Rossella nuda*. Experimental wounds

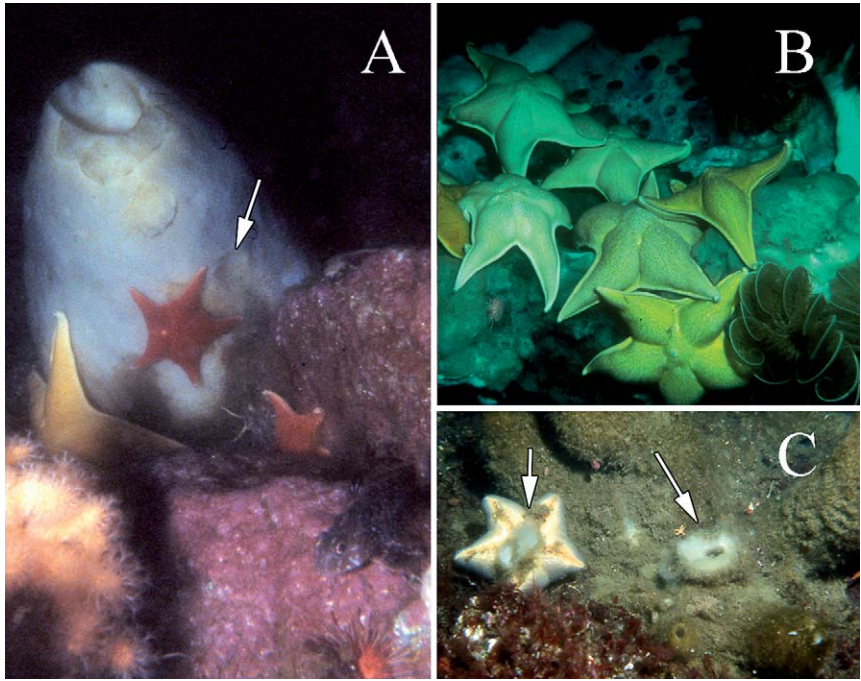


Figure 47 Asteroid predators of glass sponges (A, B, courtesy of G. Bavestrello; C, Leys, unpublished data). (A, B) The asteroid *Acodontaster* on a specimen of *Scolymastra joubini* in Antarctica. Depressions in the outer surface of the sponge (A, arrow) can be seen where the asteroid was previously feeding. (C) *Pteraster tessellatus* was pulled off the outer wall of *Rhabdocalyptus dawsoni* inhabiting North-east Pacific fjords. Spicules are still attached to the everted gut (arrows) of the asteroid.

inflicted by removing a 5 cm² core from 33 sponges at 20 m depth in Barkley Sound, British Columbia, regenerated at 0.05 ± 0.03 cm² day⁻¹, filling in the open wound within 5 months (Leys and Lauzon, 1998). These rates are in close agreement with those from an earlier study also on *Rhabdocalyptus dawsoni* by Boyd (1981), who found the oscular lip region regenerated at an average of 0.08 cm² day⁻¹. Several interesting observations merit note: first, several of the wounds increased in size before beginning to regenerate; second, 4 of the 33 sponges wounded died; third, regeneration of tissue targeted the atrial side of the wound first so that a thin cover was formed over the opening before the wall of the sponge was thickened. As with the Antarctic sponges observed by Dayton (1979), in most cases the site of the wound was visible as a scar for several years afterwards. The process of tissue remobilisation is presumed to involve cytoplasmic streaming (Section 4.4), rather than the

crawling of individual cells as occurs in cellular sponges, but histological studies are lacking.

Hexactinosan sponges have also been found to readily regenerate soft tissue when kept in flow through sea water tanks at the Bamfield Marine Sciences Centre. Because rates of regeneration for *Rhabdocalyptus dawsoni* in laboratory tanks were identical to rates achieved *in situ* (Leys, unpublished data), it is likely that hexactinosan tissues do regenerate easily in the field, although it is not known how long it takes to reconstruct the fused skeleton once damaged.

An interesting phenomenon that Dayton noticed during his studies in Antarctica was the mortality of very large and presumably very old sponges over relatively brief periods (Dayton, 1979). Similar mortality of *Rhabdocalyptus dawsoni* has been observed in British Columbia (Leys, unpublished observations). No concrete cause of the mortality could be determined in either case, but for *Rhabdocalyptus dawsoni* it is possible that some sponges are not able to recover from the observed seasonal sloughing or shedding of the outer tissue coat that may be caused by lack of food during winter months (Leys and Lauzon, 1998).

7.6. Recruitment

Knowledge of recruitment of glass sponges varies greatly depending on what is known of the reproductive periods (Section 8), population dynamics and size class distributions of different species. To find the smallest juveniles a microscopic survey of hard substrates is necessary, but because juveniles can often be found attached to the skeleton of adults, surveys of the adult skeleton have produced the bulk of information on recruitment.

For both *Oopsacas minuta* and *F. occa* which reproduce year round (Okada, 1928; Boury-Esnault and Vacelet, 1994), juveniles are readily found. In *Oopsacas*, juveniles as small as 200 μm have been found attached to rock that was chiseled from the wall of the 3PP cave near Marseille, France. Sponges smaller than 1 cm long are already reproductive and the bulk of the population in the cave is approximately 3 cm long. Since the largest adults can be 7 cm long, the population (after several years of disturbance and collecting by divers) is considered to be young.

In *Farrea*, juveniles were found attached to the base of adults in all the collections Okada (1928) made (Figure 48), but nothing is known about population dynamics. In Antarctica, numerous small specimens of *Rossella racovitzae* were found by Dayton's team (1974), but as this species regularly formed buds, recruitment was considered to be from asexual reproduction. A few juveniles (<1 cm) of *Rhabdocalyptus dawsoni* can be found among the

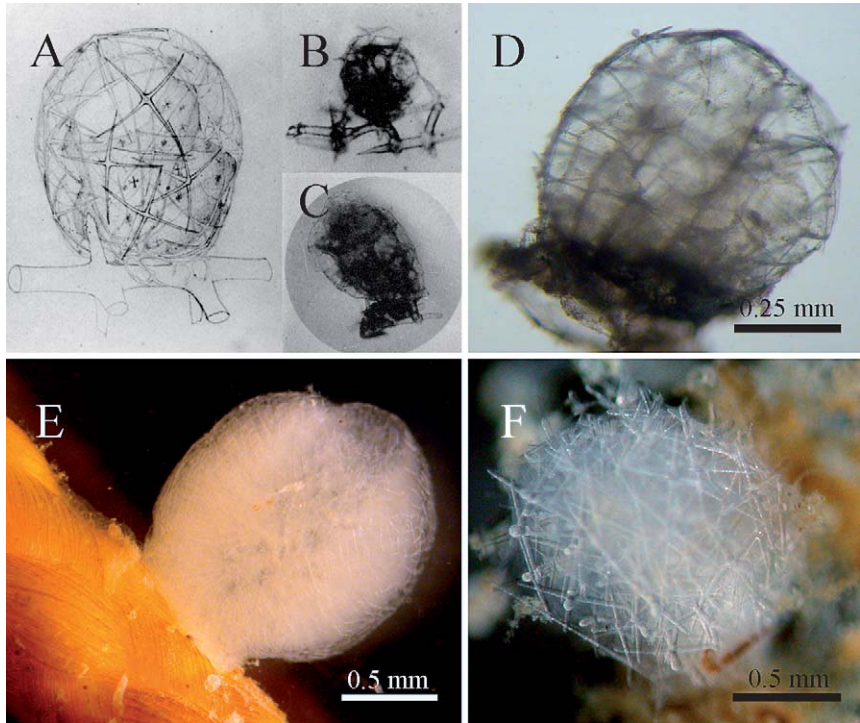


Figure 48 Juvenile glass sponges. (A–C) *Farrea sollasii* juveniles (A: Plate 2, Figure 14; B: Plate 2, Figure 10; C: Plate 3, Figure 1; from Okada, 1928). Dimensions of the juveniles are: (A, $0.6 \times 0.7 \text{ mm}^2$; B, $0.53 \times 0.49 \text{ mm}^2$; C, $1.02 \times 0.76 \text{ mm}^2$. (D) A juvenile of *Oopsacas minuta* approximately 2 weeks old chipped from the rock wall of the 3PP cave in Marseille, France. (E) A juvenile of *Oopsacas minuta* attached to rope in the cave. (F) A juvenile dictyonine sponge found on the skeleton of a dead sponge collected from 160 m depth in Barkley Sound, Canada (D–F, S. P. Leys, unpublished data).

spicule coat of adults (Leys and Lauzon, 1998), and Reiswig (personal observation) has also found them on the hairy tunicate *Halocynthia*.

Young individuals, slightly more than 2 weeks old of *Oopsacas minuta*, can be readily found on the walls and on plastic ropes suspended from the roof of the 3PP cave near Marseille (Figure 48D and E). Juveniles of hexactinosan dictyonine sponges also settle on the skeleton of adults, thus forming the reef framework. Krautter *et al.* (2001) found 1 mm diameter ‘globular’ skeletons of young sponges attached to the larger skeleton of adults. The juvenile appears to attach initially with very fine, tendril-like spicules (some 10–50 μm in diameter), which wrap around the adult’s spicule (Neuweiler, 2000; Krautter *et al.*, 2001). In the smallest specimens there is a

space between the spicules of the new sponge and the substrate; as the sponge gets larger the space is filled in with what appear to be 'pillar-like' attachment structures. Larger juveniles (2–3 mm) also have hexactin spicules, which are joined to the previous skeleton by fine siliceous tendrils. Live juvenile glass sponges (possibly *Heterochone calyx*), 1–2 mm in diameter, were found on the skeletons of dead sponges (also *Aphrocallistes vastus*) collected from fjord walls in Barkley Sound, British Columbia in early July 2003 (Leys *et al.*, 2004).

7.7. Symbioses: animal–plant associations

It appears that glass sponges lack the kinds of secondary metabolites found in so many demosponges and which have generated interest among bioprospectors (P. Anderson, University of British Columbia, personal communication). It is unknown whether the absence of chemical deterrents makes glass sponges more vulnerable to predation or less able to resist infection after wounding (Section 7.5). Glass sponges do form associations with bacteria and other invertebrates and even algae, but while some associations appear positive, others cause the degeneration of the sponge.

Although many organisms are associated with the dead spicule skeleton of glass sponges (Sections 7.2 and 7.3.2), the live tissue of most species is pristine. In fact, considering that many of these species live in regions of high productivity, remarkably little marine detritus remains on the surface tissues. While the surfaces of dictyonine hexactinosan sponges are particularly 'clean', the long projecting spicules common to lyssacine species can trap some of the detritus, but usually in a very minor way, such that the sponges appear for the most part to be 'clean'. One NE Pacific species differs. *Rhabdocalyptus dawsoni*, the shallowest and thus most accessible of the British Columbia glass sponges, is completely covered with 'sediment' and a veritable 'jungle' of invertebrates (Figure 49A and B). In his study of the associates inhabiting this 'spicule jungle', Boyd (1981) found 56 different species from six phyla; he counted a total of 2163 associated invertebrates on 13 sponges. The most abundant epifauna by far were the polychaete worms, *Syllis* sp., *Harmathoe multisetosa* and *Harmathoe extenuata*, and the terrellids *Eupolymnia heterobranchiata* and *Polycirrus* sp. which together composed 58% of the inhabitants, but brittlestars were also very numerous, with *Amphipholis* sp. alone counting for 15% of the associates. Some of the species were ubiquitous to all sponges (e.g. *Harmathoe* sp., *Syllis* sp., *Polycirrus* sp., *Eupolymnia heterobranchiata*, *Pugettia richii* and *Eualus pusiolus*), and yet other combinations were correlated with the depth that the sponge was collected from. Boyd determined that the majority of the macrofauna were

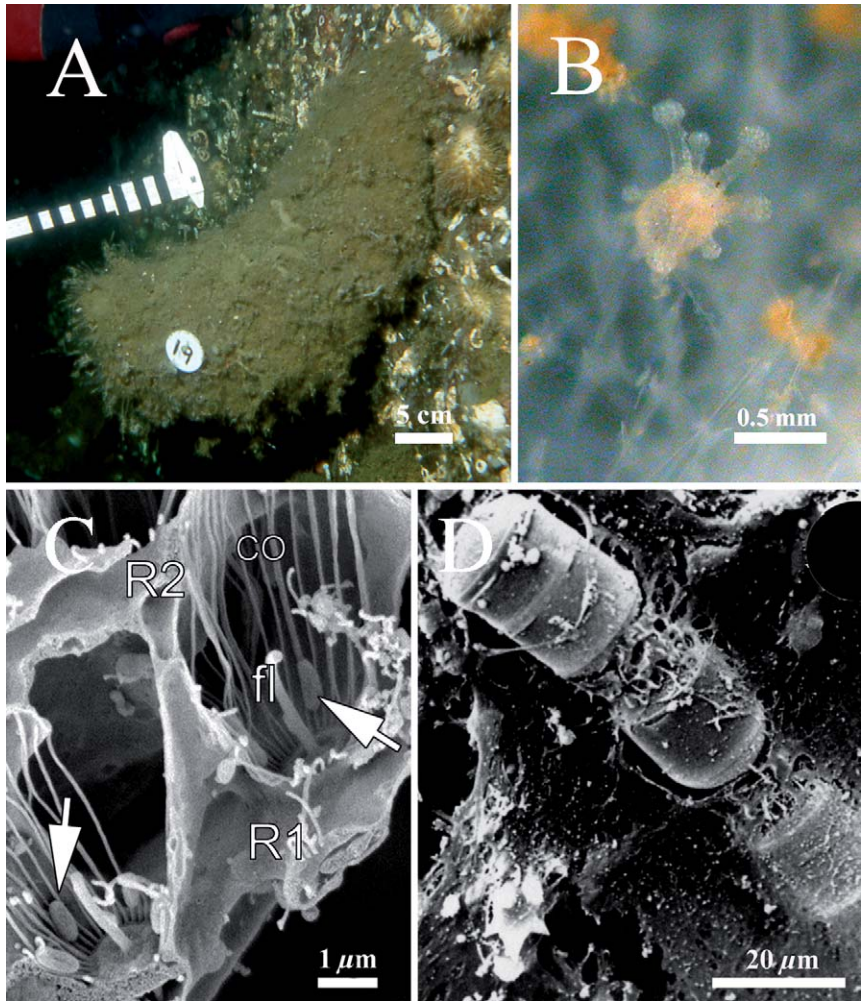


Figure 49 Symbionts in glass sponges. (A) The brown coat of *Rhabdocalyptus dawsoni* hosts a great diversity of invertebrate species. (B) A colonial hydroid lives entwined in the atrial tissue of *Rhabdocalyptus dawsoni* (light micrograph). (C) Symbiotic bacteria live along the inner surface of the collar (co) microvilli in *Aphrocallistes vastus*. Primary and secondary reticula, R1, R2; flagellum, fl. (D) Scanning electron micrograph of a diatom embedded in the tissue of *Scolymastra joubini* (D. Courtesy of G. Bavestrello).

inquilines, simply using the sponge as a substrate. Several species that were 'built in' to the sponge spicule habitat (e.g. terebellid worms and ascidians) were considered facultative commensals, based on their ability to benefit from the sponge's feeding current. Apparently, Boyd did not find any

juvenile glass sponges in his survey of the spicule jungle. He did, however, find a number of juvenile echinoderms, polychaetes, gastropods and bivalves, and suggested that the presence of a 'tangled web of sharp glass fibres combined with the continual accumulation of organic matter create a nutrient-rich habitat free from the threat of predation (aside from other associates)'.

Whereas autotrophs are common associates of demosponges and are considered to contribute to the sponges' nutrition (Sarà *et al.*, 1998), sections of glass sponges rarely reveal bacteria or algae among the tissues, with only a few notable exceptions. In *Oopsacas minuta*, a rod-shaped bacterium is harboured within the circle formed by the collar microvilli and within the mesohyl of the adult sponge (Section 5, Figure 23) (Boury-Esnault and Vacelet, 1994; Vacelet, 1996). Similar bacteria lie along the inside of the collar microvilli in *Aphrocallistes vastus* (Figure 49C). Although it is unclear what beneficial exchange may occur between the two organisms, the bacterium does not appear to be detrimental to the sponge tissue.

Diatoms are found in or on the atrial surface of some individuals of lyssacine sponges in Antarctica and have been suggested to have formed a symbiosis with the sponge by benefiting from the light-transmitting properties of the glass spicules (Cattaneo-Vietti *et al.*, 1996). A similar alga-sponge symbiosis has been observed in a few individuals with upward facing oscula in shallow (<20 m) water in British Columbia. In British Columbia waters, however, less than 20% of the surface light reaches depths of 15 m at any time in the year (Sancetta, 1989). Given the direction of the rays of light, very little luminance would strike a spicule protruding from the dermal side and even less would be transmitted through to the atrial side of the sponge. The situation with respect to light is not much different in Antarctic waters, which suggests that the alga found on *Rossella racovitzae* is more likely to receive light that directly hits the surface of tissue facing upwards.

Diatoms have also been found embedded in the tissue of the Antarctic sponge *Scolymastra joubini*. Four of 15 sponges studied by Cerrano *et al.* (2000) had irregular green-brown spots 0.5–1.5 cm² in size. In an extreme case, green areas covered up to 40% of the sponge. Scanning electron microscopy of the tissues revealed chains of the diatom *Melosira* partially embedded in the dermal tissue of the sponge (Figure 49D). Although the dermal tissue appeared normal, vast regions of the choanosome were absent where dense aggregates of the diatoms were wedged in among the spicule skeleton.

Colonial hydroids are common associates of demosponges, but associations with hexactinellids are less documented (Puce *et al.*, 2005). Schuchert and Reiswig (2006) described a new species of hydroid *Brinckmannia hexactinellidophila* from *Heterochone calyx*. The hydroid lives entwined within the tissues of the sponge at densities of up to 10 individuals per square millimetre. A different, yet unidentified species lives in *Rhabdocalyptus*

dawsoni. The hydroid tentacles and mouths are visible among the spicules and tissue of the atrial surface, while their stolons are completely entwined among the other tissues of the sponge (Figure 49B). The species inhabiting *Rhabdocalyptus dawsoni* is quite distinct from that in *Heterochone* and curiously, hydroid symbionts are absent from all individuals of *Aphrocallistes vastus* studied to date (H.M.R. and S.P.L., unpublished data) even though the sponges inhabit exactly the same environment.

8. REPRODUCTION

8.1. Sexual reproduction

8.1.1. Reproductive periods

Reproductive periods for hexactinellids vary depending on the species and possibly even the population. Records are scant and most stem from early collection expeditions in which scientists were focusing specifically on morphology and thus carried fixatives to preserve tissues and larvae (Schulze, 1880, 1887, 1899; Ijima, 1901, 1904; Okada, 1928). There are three recent studies (Boury-Esnault and Vacelet, 1994; Leys and Lauzon, 1998; Leys *et al.*, 2006).

Ijima (1901) made a special search at different seasons for reproductive cells in *Euplectella marshalli* but found neither developmental stages nor larvae. In subsequent collections of rossellid hexactinellids (Ijima, 1904), he still only found developmental stages and larvae in very few specimens. In *Vitrollula fertilis*, he found larvae in April, larvae and various developmental stages in July but only archaeocyte congeries in November, and from this presumed that the main active reproductive period is in early summer.

Okada (1928) probably carried out the most extensive survey of reproduction in a single population by collecting specimens of *F. sollasii* (Farreidae, Hexactinosida) monthly from the Nakanoyodomi (about 600 m deep) in the Sagami Sea. After Ijima's work, he was surprised to find reproductive specimens every month, and suggested that the breeding season was likely year-long because of the fairly constant temperature and uniform environmental conditions that exist at that depth. Other surveys have not had the same luck as Okada, however. Although deep sea expeditions do occasionally report finding a reproductive glass sponge, a survey of tissue collected monthly from the NE Pacific rossellid species *Rhabdocalyptus dawsoni* failed to turn up anything but archaeocyte congeries (Leys and Lauzon, 1998). However,

a study of samples of *Heterochone calyx* collected in October 1982 by one of us (H.M.R.) has revealed one specimen with numerous spermatocysts (accounting for approximately half of the congeries), some of which appeared to have emptied their contents, thus possibly having spawned, and many early embryos in various stages of cleavage. Of the many specimens of the NE Pacific reef-building sponge *Aphrocallistes vastus* that have been collected since the early 1980s, developing embryos were only found in one specimen collected in November 1995. Despite extensive work on glass sponges in Antarctic waters, there are no reports of sexually reproductive individuals. Thus, it is likely that shallower populations (those in the NE Pacific and Antarctica) are affected by seasonality of the surface waters more than deep-water populations. The hint from the two *Heterochone* and *Aphrocallistes* individuals is that reproductive period occurs in the autumn.

8.1.2. Gametogenesis

The bulk of our knowledge on reproduction in glass sponges stems from studies on two animals: *F. sollasii* (Okada, 1928) and *Oopsacas minuta* (Boury-Esnault and Vacelet, 1994; Boury-Esnault *et al.*, 1999; Leys *et al.*, 2006). This section of development will draw heavily from these accounts and from that information provided in Ijima's description (1904) of larvae in *V. fertilis*. The genera used below refer to the species used in these studies.

Gametes—both sperm and eggs—arise within archaeocyte congeries that are suspended within the trabecular reticulum between flagellated chambers (Okada, 1928; Boury-Esnault *et al.*, 1999). Spermatocysts are first identifiable as dense groupings of archaeocytes up to 30 μm by 23 μm in *Oopsacas minuta* surrounded by a thin (0.5 μm) layer of the trabecular reticulum (Figure 50A and B). In young spermatocysts, cells are larger in the centre than at the periphery of the cyst, ranging from 2.7 to 5.3 μm in diameter with a nucleus 1.6–2.6 μm and a nucleolus 0.5–1 μm (Boury-Esnault *et al.*, 1999). Each cell has a flagellum that coils around the cell. All spermatocytes cells are connected by plugged cytoplasmic bridges, and cells at the periphery of the cyst are connected to the surrounding trabecular envelope by plugged cytoplasmic bridges. At this point, the characteristics of free sperm remain unknown.

Oogenesis also occurs within archaeocyte congeries. The first oocyte is identifiable as a large cell (10 μm in diameter) within the congerie that has begun to accumulate yolk and lipid inclusions (Okada, 1928; Boury-Esnault *et al.*, 1999) (Figure 50C and D). Archaeocytes are connected to one-another by plugged cytoplasmic bridges and are suggested to act as nurse cells providing the lipid and yolk to the developing oocyte. But at some point the oocyte presumably breaks this connection because the mature oocyte is a

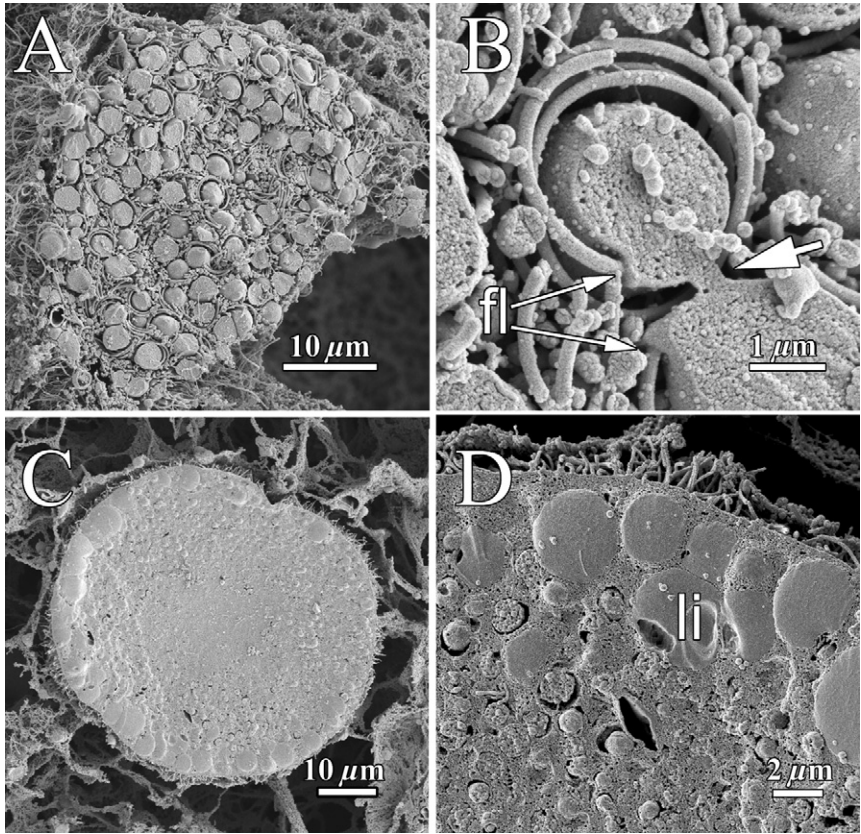


Figure 50 Gametogenesis. (A) Scanning electron micrograph of a spermatocyst in the adult tissue of *Oopsacas minuta*. (B) Higher magnification of two spermatids connected by a cytoplasmic bridge (arrow) in the spermatocyst shown in A. The flagellum (fl) is coiled around each cell body. (C) Scanning electron micrograph of an oocyte fractured in half. (D) Higher magnification of the oocyte in C showing lipid-dense inclusions occupy the periphery and the surface has numerous microvilli (Leys, unpublished images).

completely independent ovoid cell 100–120 μm in diameter in *Oopsacas minuta* (Boury-Esnault *et al.*, 1999) and 70–130 μm in *F. sollasii* (Okada, 1928), with large lipid inclusions (3.2- to 6.7- μm diameter) at the periphery and membrane-bound yolk inclusions (1.3–2.7 μm) and very small vacuoles more centrally. Boury-Esnault *et al.* (1999) describe a 45 to 50 μm diameter nucleus with a 10 μm nucleolus within the oocyte, but although a subsequent study (Leys *et al.*, 2006) found identifiable nuclear regions at the light microscope level, a nuclear membrane was not visible in any thin section

studied by transmission electron microscopy. This may be what Okada referred to as a 'vesicular' nucleus (Okada, 1928, p. 3). The presumed nuclear material forms a dense osmiophilic region that occupies the centre of the cell and radiates out into the peripheral regions of the cytoplasm, not unlike the chromatin in the nucleoids of some bacteria (Robinow and Kellenberger, 1994). The surface of the oocyte has numerous short pseudopodia. Okada found most oocytes at the outer trabecular layer of *F. sollasii* and suggested that after fertilisation they migrate in to the inner trabecular layer to lie beside a flagellated chamber. In *Oopsacas minuta*, however, oocytes and developing embryos can be found throughout the body wall, from just under the dermal membrane to just under the atrial membrane, where they lie adjacent to flagellated chambers.

8.1.3. Embryogenesis

Cleavage is total and equal, but asynchronous, for the first five cycles until the embryo has approximately 32 cells (Figures 51 and 54). The embryo remains of the same size during these divisions, partitioning cytoplasm, yolk and lipid into daughter blastomeres. Early blastomeres retain all the characteristics of the oocyte, with pseudopodia extending from their surface, a dense nuclear region, large lipid inclusions at the periphery and membrane-bound yolk inclusions more centrally. It is not until the 32-cell stage (blastula) that a distinct nucleus can be seen in individual blastomeres (Leys *et al.*, 2006). This feature may reflect the fact that divisions are rapid, leaving little time for re-assembly of the nuclear membrane between cycles. If so, the appearance of nuclei at this stage—concurrent with the change to unequal cleavage—could reflect slowing of the cell cycle.

Boury-Esnault *et al.* (1999) were able to see polar bodies in some embryos and determined that the first cleavage is meridional, presumably in relation to the polar body and flagellated chambers. The second cleavage may be meridional or rotational (Leys *et al.*, 2006). The third cleavage is asynchronous, producing first six and then eight blastomeres. New blastomeres in the six-cell embryo are placed just above the cleavage plane of the first tier; similarly future blastomeres are lodged compactly over each previous cleavage plane giving the appearance of a type of spiral cleavage. Cells in the 16- and 32-cell blastula are thus geometrically arranged around a hollow centre.

The next cleavages are unequal producing small cells (micromeres) on the outside and larger cells (macromeres) on the inside. While some micromeres inherit yolk and lipid inclusions, most of the inclusions are retained by the macromeres. Some of the micromeres take up stains more intensely than others, possibly depending on their position within the new 'outer' layer of

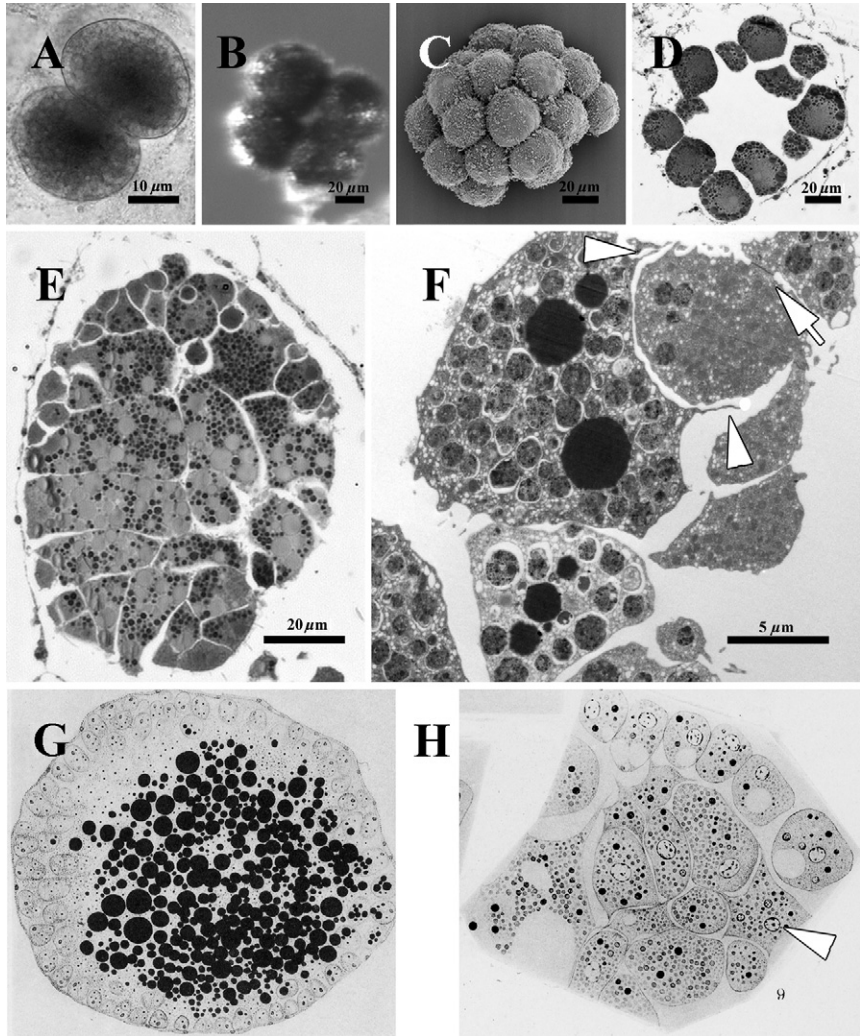


Figure 51 Embryogenesis. Stages in development of *Ooprococcus minuta* as seen by light microscopy (A, B, D, E), scanning (C), and transmission electron microscopy (F) and as drawn by Okada (1928) (G, H) (A–F, Leys, unpublished data). (A, B) Two- and four-cell embryo. (C, D) Thirty-two cell blastula. (E) Macromeres fuse to form increasingly larger cells and eventually a single syncytial tissue, the trabecular tissue. (F) Macromeres envelop micromeres (arrowheads), which are connected to one-another by plugged cytoplasmic bridges (arrow). (G) Okada's drawing of an embryo from *Farrea sollasii* at approximately the same stage as E (Plate 5, Figure 7). (H) Okada's drawing of cells at the periphery of the embryo in G. Cells are enveloped by a reticulate tissue (arrowhead by S.P.L.).

the embryo. Some micromeres remain wedged between macromeres, while others truly form an outer layer. All embryos are polarised at this stage: one pole lacks micromeres altogether while the opposite pole has a large number of micromeres; thus the embryo is not exactly bilayered at this point.

At this stage several remarkable developments occur that are quite unique to hexactinellids.

First, as soon as they are formed, the micromeres are connected to one-another by plugged cytoplasmic bridges (Figures 51F and 54G and H). Cytoplasmic bridges may occur parallel or perpendicular to the surface of the embryo. The first micromeres (i.e. at the sixth cycle) are connected to others by cytoplasmic bridges and have already differentiated a cilium. Second, the macromeres extend out filopodia and pseudopodia which interact and eventually fuse with filopodia from other macromeres. Third, macromeres extend filopodia apically to surround and eventually completely envelop the micromeres above them, thus forming the surface membrane or epithelium of the new larva. Finally, the newly formed syncytial tissue forms cytoplasmic bridges with each micromere. Thus, from this point on the entire embryo is cytoplasmically connected; it consists of a reticular syncytial tissue—the ‘inceptional trabecular system’ (Ijima, 1904)—and a collection of uninucleate cells all of which are linked cytoplasmically by plugged junctions. Unequal cleavage of the 32-cell stage blastula has been termed ‘gastrulation by delamination’ (Boury-Esnault *et al.*, 1999), but epithelialisation of the embryo and future larva occurs by the fusion of macromeres and their amoeboid envelopment of the micromeres; this is then the moment at which the larval tissue layers are formed.

8.1.4. Cellular differentiation

Interpretation of the continued differentiation of cellular components from thick or thin sections is difficult and varies depending on the perspective of the observer. In *F. sollasii*, Okada (1928) describes an outer layer of cells that surrounds a central mass of ‘clear, transparent, jelly-like substance’ containing amoeboid cells that have migrated in from the outer layer. We know from *V. fertilis* (Ijima, 1904) and *Oopsacas minuta* (Boury-Esnault *et al.*, 1999) that the outer cells are multiciliated cells, which differentiated cilia in the early ‘gastrula’, as described above, and continue to produce cilia until there are some 50 per cell. The cilia are eventually completely surrounded by the newly formed trabecular epithelium so that they ‘pierce’ or project through the smooth syncytial epithelium. The multiciliated cells remain connected to one-another and to the trabecular tissue below them by plugged cytoplasmic

bridges. According to Okada's description, the inner cells that lie among the trabecular tissue differentiate into the sclerocytes, skeletogenic cells and the choanocytes of the future flagellated chambers (Figures 52 and 54H). Sclerocytes are first evident at the periphery of the central mass. They have a large intracellular vacuole in which silica is deposited around a square axial filament (Leys, 2003a). Young sclerocytes have numerous filopodia, suggesting that they may, as Okada described, have wandered in to their present location. Alternatively they may use these filopodia to anchor themselves during spicule development and elongation. Boury-Esnault *et al.* (1999) suggest that sclerocytes in *Oopsacas minuta* originate from macromeres in the inner mass, but sections showing early sclerocytes at the periphery of the embryo (Leys *et al.*, 2006) indicate that they more likely originate from micromeres, as in *F. sollasii*. Without cell-tracing experiments we remain unsure about their precise origin. The sclerocytes are originally uninucleate, but become a multinucleate sclerocyncytium (Section 3.5) as they elongate the larval stauractin (four-rayed) spicule. At all times plugged cytoplasmic bridges connect sclerocytes to the trabecular tissue.

The last cell type to differentiate is the choanocyte. Although Boury-Esnault *et al.* (1999) suggest that choanoblasts arise from the yolk-rich tissue at the posterior pole, subsequent work (Leys *et al.*, 2006) concurs with Okada that they develop from the same population of amoeboid cells as do the sclerocytes. These amoeboid cells take up a central-posterior location when the embryo is still spherical. As the posterior pole extends with the elongation of spicules at the periphery of the embryo, the remaining amoeboid cells become rounded and arranged in small groups. In *Oopsacas minuta*, the first choanocytes possess a collar, flagellum and single nucleus in a cell that is connected to the neighbouring cells and to the reticular tissue by plugged cytoplasmic bridges. Okada (1928) did not see either collars or flagella in the embryo of *F. sollasii* and concluded that these structures differentiate after the larva leaves the parent sponge, but given the minute size of collar and flagellum at this stage it is possible that they were not visible in his sections. He also described an invagination at the surface of the larva near the flagellated chambers, which he suggested could represent the start of canal formation; no equivalent invagination has been found in *Oopsacas minuta*. Ijima (1904) saw archaeocytes in the posterior region of *V. fertilis*, but did not believe they were the anlagen of flagellated chambers because they were still connected directly to other mesohyl spaces in the larva and because the centre of the presumptive chambers was traversed by the reticular tissue. TEMs show that the reticular tissue traverses the non-functional chambers of *Oopsacas minuta*, thus it is likely that chambers are already present in *V. fertilis* as they are in *F. sollasii* and *Oopsacas minuta*.

Stages in the development of *Oopsacas minuta* are summarised in Figure 54.

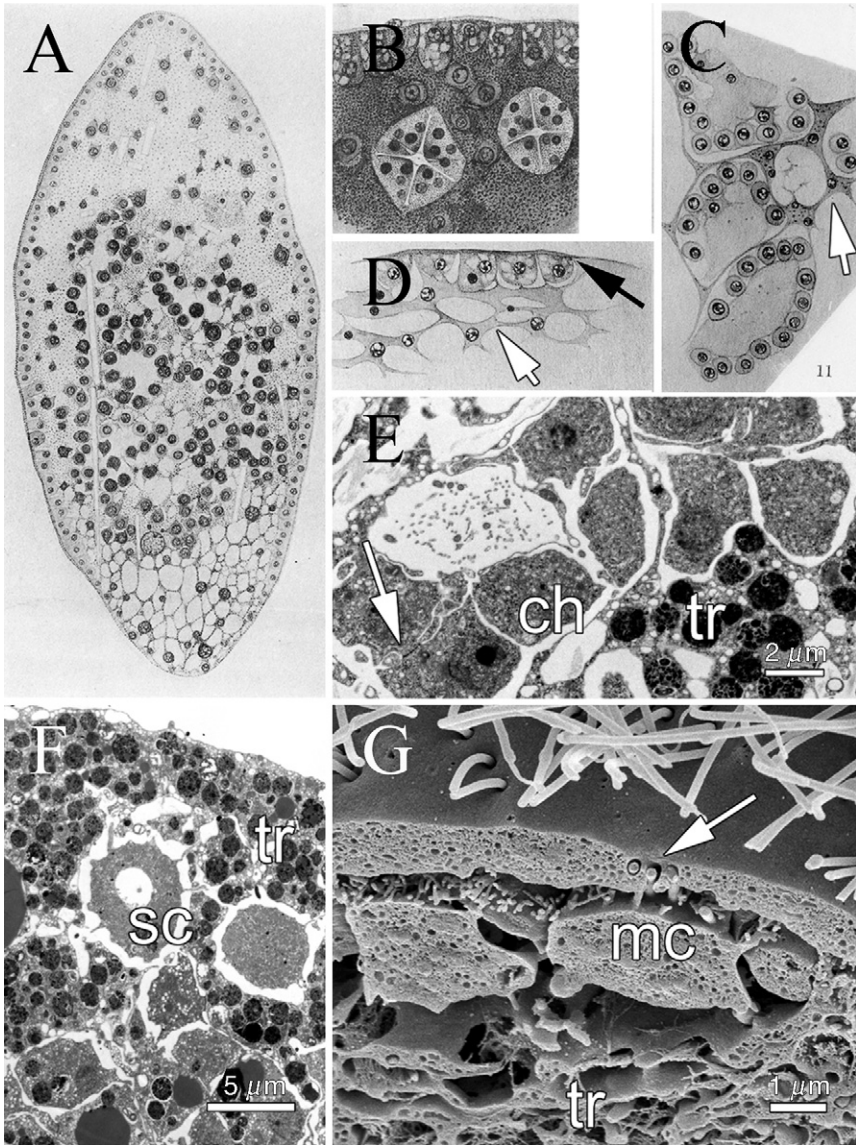


Figure 52 Larval differentiation. (A–D) Drawings of *Farrea sollarisii* embryos from Okada (1928), (E–G) electron micrographs of *Oopsacas minuta* embryos (Leys, unpublished data). (A) Longitudinal section through an embryo approximately 70 μm long (Plate 6, Figure 1) with fully developed stauractin spicules. (B) A peripheral portion of embryo to show micro-scleroblast masses with young disco-hexasters (Plate 6, Figure 10). (C) Choanocytes in a reticular tissue (arrow by S.P.L.) (Plate 6, Figure 11). (D) Peripheral portion of the posterior region of the embryo,

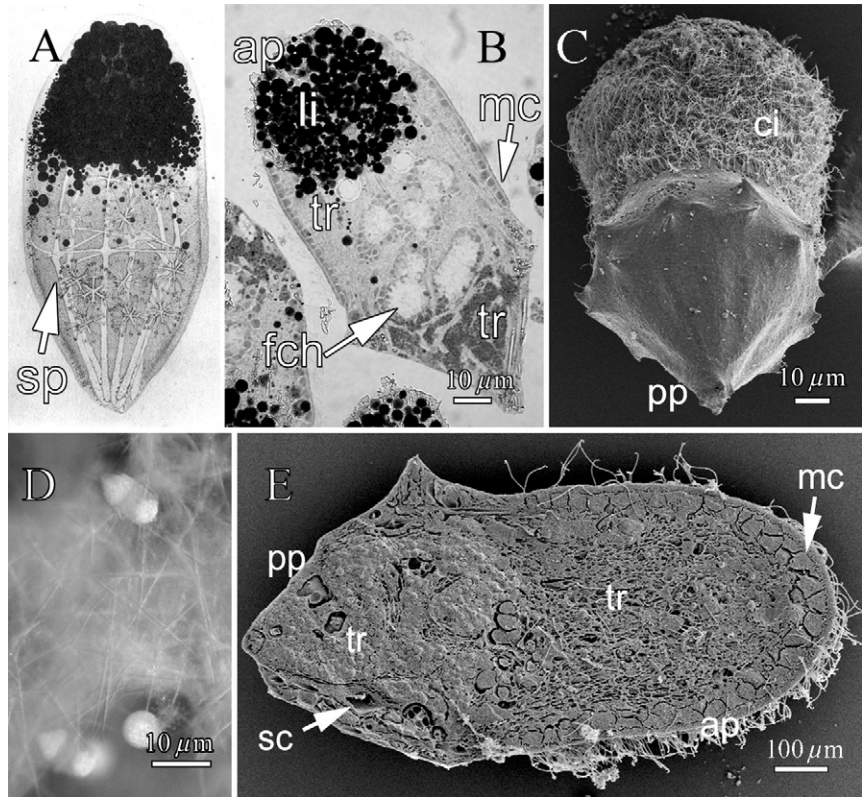


Figure 53 Hexactinellid larvae (A, Okada, 1928; B–D, Leys, unpublished data). (A) Oldest embryo found by Okada (1928) in the parental tissue of *Farrea sollaris* (Plate 2, Figure 6). Sp, spicules. (B) Thick plastic section of a larva from *Oopsacas minuta*. Ap, anterior pole; li, lipid inclusions; mc, multiciliated cells; tr, trabecular reticulum; fch, flagellated chamber. (C) View from the posterior pole (pp) of a larva from *Oopsacas minuta* showing a smooth outer epithelium and a girdle of cilia (ci) at the equator of the larva. (D) Light micrograph showing live larvae (*Oopsacas minuta*) suspended from the trabecular reticulum of the parent sponge. (E) A longitudinal fracture of a larva from *Oopsacas minuta* viewed by scanning electron microscopy. Ap, anterior pole; pp, posterior pole; tr, trabecular reticulum; sc, sclerocyte; mc, multiciliated cell.

showing a reticular tissue (white arrow by S.P.L.) directly beneath the cells. A thin tissue is shown directly over the cells (black arrow). (E) Transmission electron micrograph (TEM) of a newly formed choanocyte chamber. Choanocytes (ch) are connected to one-another by plugged cytoplasmic bridges (arrow) and are surrounded by strands of the trabecular syncytial tissue (tr). (F) TEM of a newly formed sclerocyte (sc) within the trabecular syncytium (tr). (G) Scanning electron micrograph of the peripheral portion of the central region of the embryo showing multiciliated cells (mc) directly over strands of the syncytial trabecular reticulum (tr). The cilia project through the smooth outer layer of the trabecular reticulum (arrow).

8.1.5. Larval structure

The unusual construction of the larva has caused quite a lot of confusion. Early accounts of embryos and larvae from hexactinellids describe a 'cellular' equatorial outer layer, and a 'jelly-like' reticular tissue that forms the inner mass (Ijima, 1904; Okada, 1928). The multiciliated cells were quite distinct in thick sections, but the reticular tissue defied precise definition. Ijima saw that the cellular region was absent from anterior and posterior poles of the larva where the inner mass was exposed to the environment and concluded that the reticular tissue could be traced from anterior to posterior regions. Both Okada and Ijima described additional cells among the reticular tissues at the posterior of the larva. It is likely because of this that Boury-Esnault *et al.* (1999) were inclined to describe the inner region of *Oopsacas minuta* as consisting of two types of cells, one that remains uninucleate, at the anterior end, and one that becomes syncytial and occupies most of the posterior pole. Re-examination of the tissue from *Oopsacas minuta* has shown the reticular tissue to be a single multinucleate syncytium that, as Ijima found, pervades the entire inner mass from anterior to posterior poles and forms the surface epithelium of the larva (Leys *et al.*, 2006) (Figure 53).

The reticular tissue is thicker at the posterior pole of the larva where it has numerous yolk-rich inclusions. It thins out towards the centre of the larva as it surrounds the incipient flagellated chambers, and remains very thread-like in the anterior region where it is no more than a sheath around nuclei and massive lipid inclusions. In all parts of the larva, the strands of the reticular tissue are interlaced with a distinct collagenous mesohyl, the presence of which Ijima inferred from its fluid like consistency (Ijima, 1904). The cellular components of the larva include: (1) the multiciliated cells that form a band around the middle third of the larva, lying directly underneath and piercing with their cilia, the syncytial epithelium; (2) the branched choanocytes, which form two to three flagellated chambers in the posterior–central region and (3) a type of cell with clear vacuolar inclusions. In both *F. sollasii* and *Oopsacas minuta*, sclerocytes are already multinucleate in the larvae (Okada, 1928; Boury-Esnault *et al.*, 1999).

The larva possesses a skeleton that is distinct from the adult. In *F. sollasii*, there are 12 oxystauractin (four-rayed) megascleres that lie 'paratangentially' to the surface of the larva as well as an unknown number of microscleres—discohexasters—that appear just under the multiciliated cells at the posterior pole of the larva (Okada, 1928). The anterior portion of stauractin longitudinal ray is 90 μm and the posterior portion is 50 μm ; the transverse rays are each 20 μm . The *Oopsacas minuta* larva has up to 14 stauractin spicules but lacks microscleres altogether (Leys, 2003a). Measurements of the rays were made after dissolution of the larval tissue in nitric acid, but

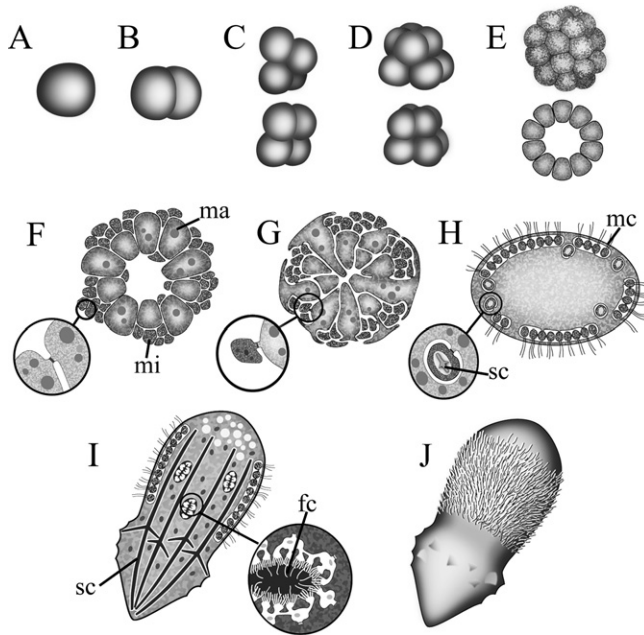


Figure 54 Stages in embryogenesis and larval development of *Oopsacas minuta* (after Leys *et al.*, 2006). (A) Oocyte, (B) two cells, (C) four cells, rotational or equatorial cleavage, (D) eight cells, (E) hollow blastula, (F) unequal cleavage to form micromeres (mi) and macromeres (ma), (G) gastrulation: fusion of macromeres (ma) to form the trabecular syncytium, and envelopment of micromeres by this tissue to form the outer epithelium. (H) Cellular differentiation: formation of multiciliated cells (mc) and sclerocytes (sc, inset). (I and J) Larva in longitudinal section (I), and external view (J) with sclerocytes (sc) and flagellated chambers (fc, inset).

lipid-rich material in the anterior pole obscured the ends of spicules in some preparations so that measurements were made from several different preparations. The longitudinal rays of the stauractins in *Oopsacas minuta* are estimated to be 40–80 μm , while the transverse rays are 27–50 μm .

8.1.6. Larval behaviour, settlement and metamorphosis

Until live larvae could be studied, it was thought, based on Okada's and Ijima's work, that the pointed pole was anterior; the contrary is true (Boury-Esnault *et al.*, 1999). The larva swims with the lipid-dense rounded anterior

end upright, rotating in a right-handed direction (clockwise when viewed from the posterior pole). The live larva from *Oopsacas minuta* is white like the adult sponge, but under the optics of a stereomicroscope the lipid-dense region at the anterior pole appears nearly opaque.

Observations on larval behaviour, settlement and metamorphosis stem from work done by one of us on *Oopsacas minuta* (Leys, unpublished observations). In glass dishes in the laboratory, larvae swim slowly upward. If the surface is left open to the air, the larvae quickly get caught in the air–water interface, but if the surface is covered by a piece of Parafilm™ or by a cover slip, the larvae continue to swim at the surface and occasionally turn and swim back down to the bottom of the dish. Larvae will swim for up to 7 days if the dishes are continually disturbed, but most larvae settle and metamorphose into the juvenile sponge within 12–24 hours after release from the parent; they do this in dishes kept on the table top at room temperature and in dishes maintained at 14°C (the temperature in the cave from where the adult sponges live).

Oopsacas minuta larvae attach by the rounded anterior pole. One hour after attachment the anterior pole has flattened, spreading the still visible lipid-filled inclusions over a broad base while the former posterior pole remains conical. After 24 hours, the post-larva has become broader apically (former posterior pole) and the tissue is translucent. Stauractin spicules can still be seen like tentpoles around the circumference of the main body. Thick sections show that the lipid inclusions remain at the base of the post-larva, while the centre and former posterior pole undergo a massive change in density, from being nearly opaque after osmium fixation to nearly transparent. This change appears to be due to the radical reorganisation of the reticular tissue and disappearance of most of the yolk-filled inclusions. The multiciliated cells resorb their cilia, but the fate of these cells within the post-larva is not clear at this time. Flagellated chambers enlarge and become enveloped by the reticular tissue, as in the adult.

The fate of the larval sclerocytes in *Oopsacas minuta* is not yet known, but Okada (1928) reports that in juveniles of *F. sollasii* the stauractins are replaced by pentactins, which then form the dermalia (spicules supporting the dermal membrane). The smallest specimen observed by Okada was a 0.54 mm × 0.36 mm barrel-shaped juvenile found attached to the base of the adult. The choanocyte layer in this individual was a continuous sheet of choanosome, with ‘evaginated protuberances’ that lay suspended between the inner and outer trabecula reticula. Week-old juveniles from *Oopsacas minuta* are approximately 200 μm in diameter and barrel-shaped. Although the choanosome could not be seen in live specimens, the central region appears open and an osculum opens at the apical side (Leys, unpublished observations).

8.2. Asexual reproduction

The asexual production of buds is characteristic of several species of rossellid hexactinellid. Perhaps the most prolific ‘budder’ known is *Lophocalyx (Polylophus) philippinensis* (Schulze, 1887), although budding is also rampant in *Rossella racovitzae*, one of the most abundant of the glass sponges in Antarctica (Dayton, 1979, 1989; Barthel and Gutt, 1992). Buds are also common in the NE Pacific species *Rhabdocalyptus dawsoni*, where they arise from the base of these tube-shaped animals. Although the cavity of the bud is completely separate from the atrial cavity of the parent sponge, physiological experiments have demonstrated that stimuli to the parent tube cause the arrest of flow within that tube and in the bud. Thus, despite the separation of flow compartments, the cytoplasm of the trabecular syncytium connecting parent with bud is continuous (Mackie *et al.*, 1983).

The ability to reproduce asexually probably depends slightly on the morphology of different groups of hexactinellids because species with a fused skeleton are thought not to be able to modify the fused scaffold at their base once it is formed. Nevertheless, other means of ‘budding’ may be possible. Divers monitoring a population of *Aphrocallistes vastus* in Saanich Inlet, British Columbia, have observed that ‘drips’ of tissue arise from the palm-shaped processes of large animals (Austin, 2003). It is speculated that these ‘drips’ could attach and grow into a new sponge in much the way that portions of the tetractinomorph demosponge *Chondrosia reniformis* (Bavestrello *et al.*, 1998) is able to colonise new locations in the Mediterranean.

9. CLASSIFICATION AND PHYLOGENY

9.1. Classification of recent Hexactinellida

First awareness that hexactine sponge spicules might constitute a distinct spicule type is attributed to Bowerbank (1858). He made no proposition to group together the seven relevant sponges which were scattered across several taxa in arrangements of the time. By 1868, 14 species of future hexactinellids had been described when Thomson (1868) recognised their distinction in formal proposal of the taxon “Vitrea” to contain them, including in his definition that their spicules ‘... may all be referred to the hexradiate stellate type’. Thomson’s concept thus served as the basis for Schmidt’s proposal (1870) of the taxon ‘Hexactinellidae’ for sponges with triaxonal spicules. Claus (1872) proposed another formal taxon for this group, ‘Group 6 Hyalospongiae, Glassschwämme’, but he made no mention

of their unique spicule symmetry in the group definition. Although Claus's Hyalospongiae and [Schulze's name \(1886\)](#), 'Triaxonia', introduced in a prelude to his famous 'Challenger' report ([Schulze, 1887](#)), were used by some workers through the 1960s, Schmidt's name ultimately gained favour and he is now universally acknowledged as authority for the class name, Hexactinellida.

Present classification of Recent Hexactinellida ([Table 1](#)) derives from the review of taxonomic literature in Systema Porifera ([Hooper and Van Soest, 2002](#)), recent addition of the order Fieldingida by [Tabachnick and Janussen \(2004\)](#),

Table 1 Classification of Recent Hexactinellida to family level, with number of genera (Gen), number of species (Spec), and main skeletal types (Skel) indicated

Rank	Taxon name	Gen	Spec	Skel ^a
Class	Hexactinellida Schmidt, 1870	119	531	L/D
Subclass 1/2	Amphidiscophora Schulze, 1886	12	158	Ln
Order 1/1	Amphidiscosida Schrammen, 1924	12	158	Ln
Family 1/3	Phoronematidae Gray, 1870	6	42	Ln
Family 2/3	Monorhaphididae Ijima, 1927	1	2	Ln
Family 3/3	Hyalonematidae Gray, 1857	5	114	Ln
Subclass 2/2	Hexasterophora Schulze, 1886	107	372	L/D
Order 1/5	Hexactinosida Schrammen, 1903	37	113	Ds
Family 1/7	Farreidae Gray, 1872	6	24	Ds
Family 2/7	Euretidae Zittel, 1877	16	45	Ds
Family 3/7	Dactylocalycidae Gray, 1867	3	8	Ds
Family 4/7	Tretodictyidae Schulze, 1886	8	23	Ds
Family 5/7	Aphrocallistidae Gray, 1867	2	7	Ds
Family 6/7	Craticulariidae Rauff, 1893	1	1	Ds
Family 7/7	Cribrospongiidae Roemer, 1864	1	1	Ds
Order 2/5	Aulocalycoida Tabachnick and Reisinger, 2000	8	10	Ds
Family 1/2	Aulocalycidae Ijima, 1927	6	7	Ds
Family 2/2	Uncinateridae Reisinger, 2002	2	3	Ds
Order 3/5	Fieldingida Tabachnick and Janussen, 2004	1	2	Ds
Family 1/1	Fieldingidae Tabachnick and Janussen, 2004	1	2	Ds
Order 4/5	Lychniscosida Schrammen, 1903	3	6	DI
Family 1/2	Aulocystidae Sollas, 1887	2	4	DI
Family 2/2	Diapleuridae Ijima, 1927	1	2	DI
Order 5/5	Lyssacosida Zittel, 1877	53	241	Ls
Family 1/3	Leucopsacidae Ijima, 1903	3	16	Ls
Family 2/3	Euplectellidae Gray, 1867	27	89	Ls
Family 3/3	Rossellidae Schulze, 1885	23	142	Ls
	Hexasterophora Incertae Sedis	5	5	L/D

^aSkeleton types, degree of fusion indicated by shading, are designated by Ln, loose lyssacine network of separate megascleres never fused together; Ls, lyssacine network of usually separate megascleres which sometimes is rigidified by spicule fusion at contact points or by synapticulae but never involving fusion of hexactins; D, rigid dictyonine framework of fused simple hexactins (Ds) or lychnisc hexactins (DI); L/D, includes both lyssacine and dictyonine members.

and review by [Reiswig \(2006\)](#). The first division as introduced by [Schulze \(1899\)](#) is based on types of microscleres: amphidiscs and no hexasters in subclass Amphidiscophora; hexasters and no amphidiscs in subclass Hexasterophora. Before 1899 (e.g. [Schulze, 1887](#)), first division of the class was based on pattern of the primary skeleton: spicules either always isolated or subsequently united irregularly in Lyssacina; hexactine spicules fused together early to form a compact and more or less regular, rigid, dictyonal framework in Dictyonina. In spite of additions and discoveries of new types of hexactinellid organisation since 1899, the subclass division seems very secure. Amphidisc-like microscleres occur in some hexasterophorans, but they are accompanied by hexasters and are considered a convergent development ([Tabachnick and Lévi, 1997](#)).

Subclass Amphidiscophora contains only one Recent order and three families ([Figure 55](#)) distinguished by their major choanosomal spicules: pentactins in Phoronematidae, tauactins in Monorhaphididae and diactins in Hyalonematidae. This arrangement, initiated by [Ijima in 1927](#), replaced the two-family scheme used by [Schulze \(1904\)](#). Spicule fusion never occurs, by any method, in this subclass.

Subclass Hexasterophora contains five orders and several still unplaced species. Classification at both order and family level remain unsatisfactory, with several changes having occurred since the overall revision by [Ijima \(1927\)](#) and more expected in the future. Four of the five orders are dictyonines ([Figure 56](#)), which differ in gross structure of their fused rigid frameworks: the Hexactinosa framework is constructed of fused simple hexactins, all rays of which are approximately one mesh in length in regular arrangement with or without longitudinal strands (the pattern of this group requires re-examination and revision); the Aulocalycoida is constructed of simple hexactins with some rays forming longitudinal strands by continuous extension; the Fieldingida have an irregular, large-mesh framework of simple hexactins with Weltner bodies and a surface crust of fused stauractins (regular tetractins); the Lychniscosida have a regular framework of lychnisc hexactins as dictyonalia and lack longitudinal strands. Within Hexactinosida, families are distinguished primarily by distinctive types of gaps (channels) in the rigid skeleton (see chapters in [Hooper and Van Soest, 2002](#) for details), but Farreidae and Euretidae are differentiated by combination of their sceptrule spicules and thickness of framework at the growth margin. The two Aulocalycoida families differ in structure of their longitudinal strands, being composed of single dictyonal rays in Aulocalycidae and of overlapping rays in Uncinateridae. The two Lychniscosida families are distinguished by frontal ranking of lychniscs in Aulocystidae and lack of such ranking in Diapleuridae.

The fifth order of Hexasterophora, the non-dictyonine Lyssacinosida, is both the most abundant and diverse of the orders, containing nearly

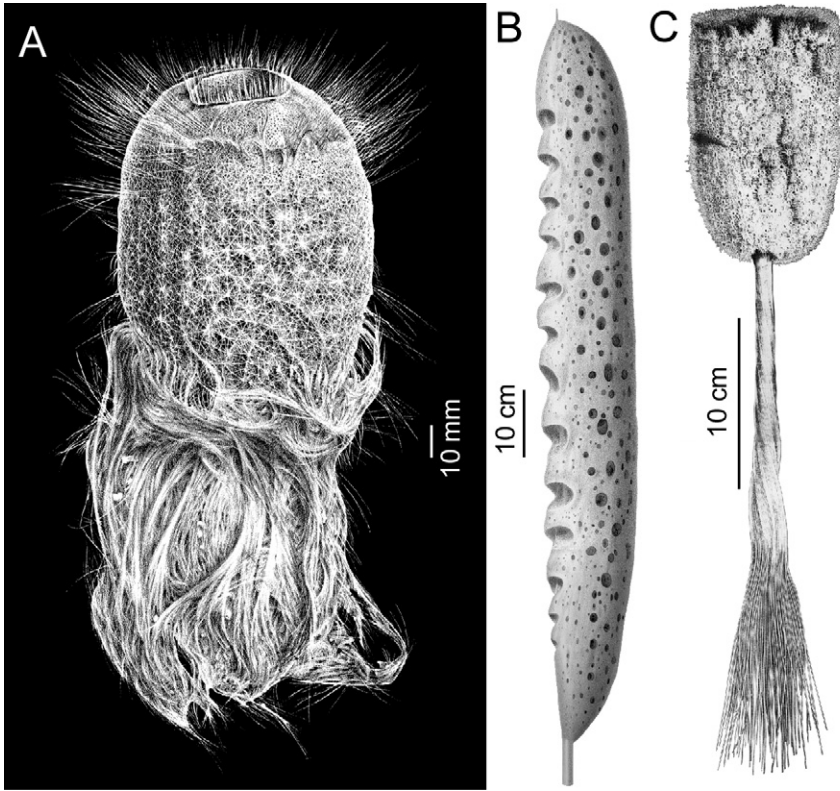


Figure 55 Representative species of the three Amphidiscophora families. (A) *Pheronema carpenteri* (Pheronematidae) from Thomson (1869). (B) *Monorhaphis chuni* (Monorhaphididae) from Schulze (1899). (C) *Hyalonema sieboldi* (Hyalonematidae) from Schultze (1860).

one-half of all known Recent species. Its classification, like that of Hexactinosa, has undergone recent major changes and cannot yet be considered stable. Presently, the group contains three families (Figure 57) differentiated by pentactine hypodermalia and diactine principalia in Rossellidae; no hypodermalia and hexactine principalia in Leucopsacidae; no hypodermalia and stauractine, tauactine and diactine principalia in Euplectellidae.

9.2. Classification of fossil Hexactinellida

Palaeontologists are faced with making order out of material usually far less favourable than that available to neontologists. Specimens of fossils are rare,

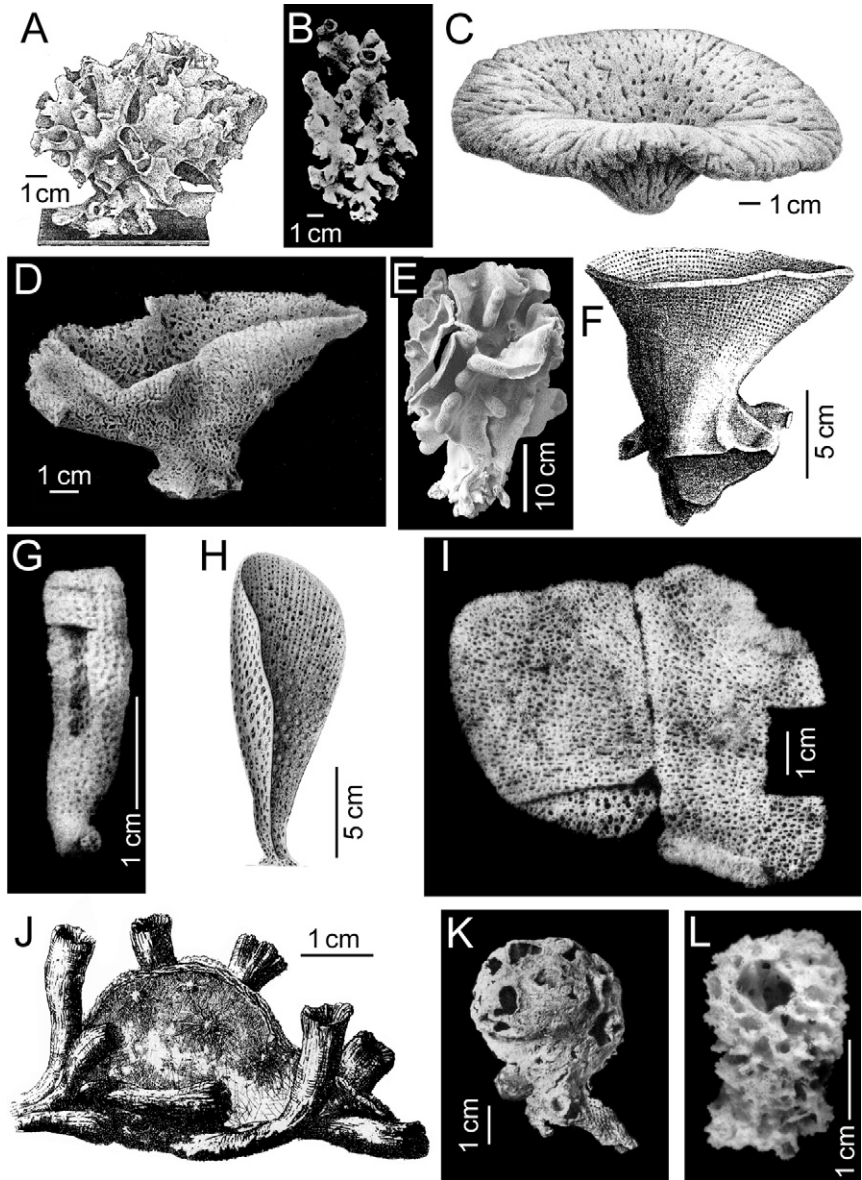


Figure 56 Representative species of the 12 families of dictyonine Hexasterophora. (A–G) order Hexactinosida; (H–I) order Aulocalycoida; (J) order Fieldingida; (K–L) order Lychniscosida. (A) *Farrea occa* (Farreidae) from Carter (1885). (B) *Eurete simplicissima* (Euretidae) from Marshall (1875). (C) *Dactylocalyx pumiceous* (Dactylocalycidae) from Sollas (1879). (D) *Hexactinella ventilabrum* (Tretodictyidae) from Schulze (1887). (E) *Aphrocallistes vastus* (Aphrocallistidae) from Schulze (1899).

fragmentary and often remineralised. Whole body preservations virtually never contain the loose spicules on which Recent classifications are based, and in some strata, the only material that can be obtained are loose spicules extracted from sedimentary rocks. Faced with such limitations, palaeontologists have made astonishing progress in documenting the history of hexactinellids, but still have difficulty in attaining consensus within their own ranks and integrating their results to the classification schemes of Recent hexactinellids. Two classification schemes of fossil hexactinellids have recently been reported. [Krautter \(2002\)](#) gave a non-exhaustive overview that includes recent opinions of mainland European workers ([Table 2](#)). [Rigby \(2004\)](#), with input from Finks and Reid, put together an exhaustive classification in revision of the influential *Treatise on Invertebrate Palaeontology* ([Table 3](#)).

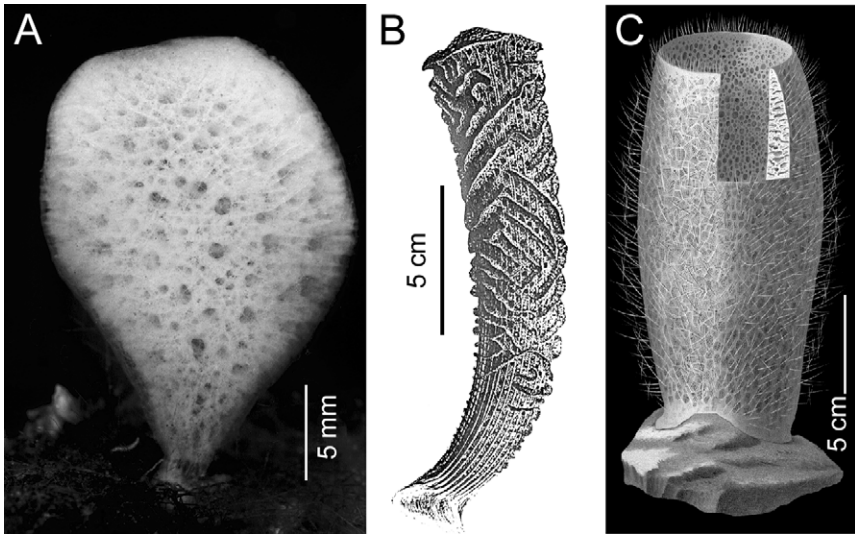


Figure 57 Representative species of the three families of lyssacine Hexasterophora. (A) *Leucopsacas scoliodocus* (Leucopsacidae). (B) *Euplectella aspergillum* (Euplectellidae) from [Owen \(1843\)](#). (C) *Staurocalyptus solidus* (Rossellidae) from [Schulze \(1899\)](#).

(F) *Laocoetis crassipes* (Craticulariidae; fossil species illustrated since the only Recent form is known as fragments) from [Pomel \(1872\)](#). (G) *Stereochlamis incerta* (Cribrospongiidae) from [Ijima \(1927\)](#). (H) *Euryplegma auriculare* (Aulocalycidae) from [Schulze \(1887\)](#). (I) *Tretopleura candelabrum* (Uncinateridae) from [Ijima \(1927\)](#). (J) *Fieldingia lagettoides* (Fieldingidae) from [Kent \(1870\)](#). (K) *Neoaulocystis zitteli* (Aulocystidae) from [Ijima \(1927\)](#). (L) *Scleroplegma lanterna* (Diapleuridae) from [Reiswig \(2002b\)](#).

Table 2 Classification of fossil Hexactinellida to family, from Krautter (2002) (taxa lacking authorities and stratigraphic ranges were inserted from text statements)

“Order Reticulosida” Reid, 1958 ?Neoproterozoic–Permian–?Late Jurassic
 Superfamily Protospongiodea Finks, 1960 ?Neoproterozoic–Middle Cambrian–Permian
 Family Protospongiidae Hinde, 1887 Middle Cambrian–Early Devonian
 Family Dictyospongiidae Hall, 1884 Neoproterozoic ?, Ordovician–Early Carboniferous
 Family Stereodictyidae Finks, 1960 Permian
 Family Hintzespongiidae Finks, 1983 Ordovician
 Family Teganiidae
 Family Hyphanteniidae
 Superfamily Brachiospongiodea Finks, 1960 Ordovician–Permian–?Late Jurassic
 Family Brachiospongiidae Beecher, 1889 Ordovician–Silurian
 Family Stiodermatidae Finks, 1960 Permian
 Family Docodermatidae Finks, 1960 Permian–?Late Jurassic
 Family Stromatidiidae Finks, 1960 Permian
 Family Pileoutidae
 Palaeozoic “Rossellimorpha” ?Late Vendian–Permian
 Order Lyssacinosida Zittel, 1877 Neoproterozoic–Recent
 Order Hexactinosida Schrammen, 1903 Late Devonian–Recent
 Family Euretidae Zittel, 1877 Late Jurassic–Recent
 Family Aphrocallistidae Gray, 1867 Late Cretaceous–Recent
 Family Craticulariidae Rauff, 1893 Middle Jurassic–Recent
 Family Cribrospongiidae Roemer, 1864 Late Jurassic–Recent
 Family Staurodermatidae Zittel, 1878 Late Jurassic
 Hexactinosida *incertae sedis* Early Jurassic–Cretaceous
 Order Lychniscosida Schrammen, 1902 Middle Jurassic–Recent
 Family Cypelliidae Schrammen, 1937 Late Jurassic
 Family Sporadosciniidae Schrammen, 1912 Late Jurassic–Tertiary
 Family Ventriculitidae Smith, 1848 Late Jurassic–Cretaceous
 Family Diapleuridae Ijima, 1927 Late Jurassic–Recent
 Family Neoaulocystidae Zhuravleva, 1962 Late Jurassic–Recent
 Family Becksiidae Schrammen, 1912 Cretaceous
 Family Coeloptychidae Zittel, 1877 Cretaceous
 Lychniscosida *incertae sedis*—Late Jurassic–Cretaceous

Both of these schemes were intended to bring classification of fossil forms into register with that of Recent forms, but they differ in some important ways that reflect the differences in philosophy of the two groups of workers.

Krautter’s scheme, intentionally restricted, was arranged on the cautious premise that those groups of fossil forms that cannot convincingly be related to Recent groups should be maintained separate from those taxa and only those fossil groups that can convincingly be shown to be monophyletic should be retained as taxa. Rigby attempted to assign almost all taxa of

Table 3 Classification of fossil Hexactinellida to family, with number of fossil genera in parenthesis, from Rigby (2004)

Class Hexactinellida Schmidt, 1870 (432) Lower Cambrian–Holocene
 Subclass Amphidiscophora Schulze, 1887 (160) Lower Cambrian–Holocene
 Order Amphidiscosa Schrammen, 1924 (41) Lower Cambrian–Holocene
 Family Hyalonematidae Gray, 1857 (1) Cretaceous–Holocene
 Family Pattersoniidae Miller, 1889 (3) Middle Ordovician–Upper Ordovician
 Family Pelicaspongiidae Rigby, 1970 (24) Lower Ordovician–Triassic
 Family Stiodermatidae Finks, 1960 (13) Lower Cambrian–Permian
 Order Reticulosa Reid, 1958 (118) Ediacaran–Holocene
 Superfamily Protospongioidea Hinde, 1887 (20) Lower Cambrian–Jurassic
 Family Protospongiidae Hinde, 1887 (20) Lower Cambrian–Jurassic
 Superfamily Dierespongioidea Rigby and Gutschick, 1976 (24) M. Cambrian–Holocene
 Family Dierespongiidae Rigby and Gutschick, 1976 (6) Middle Ordovician–Permian
 Family Hydnoctyidae Rigby, 1971 (2) Middle Cambrian–Upper Ordovician
 Family Amphispongiidae Rauff, 1894 (1) Upper Silurian
 Family Multivasculatidae de Laubenfels, 1955 (1) Upper Cambrian
 Family Titusvillidae Caster, 1939 (6) Upper Devonian–Holocene
 Family Aglithodictyidae Hall and Clarke, 1899 (8) Upper Devonian–Carboniferous
 Superfamily Dictyospongioidea Hall and Clarke, 1899 (62) Ediacaran–Upper Triassic
 Family Dictyospongiidae Hall and Clarke, 1899 (55) Ediacaran–Permian
 Family Docodermatidae Finks, 1960 (5) Silurian–Permian
 Family Stereodictyidae Finks, 1960 (2) Carboniferous–Upper Triassic
 Superfamily Hintzespongioidea Finks, 1983 (12) Lower Cambrian–Carboniferous
 Family Hintzespongiidae Finks, 1983 (5) Lower Cambrian–Devonian
 Family Teganiidae de Laubenfels, 1955 (7) Cambrian–Carboniferous
 Order Hemidiscosa Schrammen, 1924 (1) Carboniferous
 Family Microhemidisciidae Finks and Rigby, 2004 (1) Carboniferous
 Subclass Hexasterophora Schulze, 1887 (272) Ordovician–Holocene
 Order Lyssacinosa Zittel, 1877 (36) Ordovician–Holocene
 Family Pheronematidae Gray (2) ?Upper Jurassic, Cretaceous–Holocene
 Family Euplectellidae Gray, 1867 (11) Lower Triassic–Holocene
 Family Asemematidae Schulze, 1887 (1) Palaeogene–Holocene
 Family Rossellidae Schulze, 1887 (1) ?Palaeogene–Holocene
 Family Stauractinellidae de Laubenfels, 1955 (1) Jurassic–Neogene
 Family Leucopsacidae Ijima, 1903 (1) Palaeogene
 Family Uncertain (6)
 Superfamily Crepospongioidea Finks and Rigby, 2004 (1) Triassic
 Family Crepospongiidae Finks and Rigby, 2004 (1) Triassic
 Superfamily Brachiospongioidea Beecher, 1889 (11) Upper Ordovician–Permian
 Family Brachiospongiidae Beecher, 1889 (4) Upper Ordovician–Silurian

(Continued)

Table 3 (Continued)

Family Pyruspongiidae Rigby, 1971 (1) Upper Ordovician
Family Malumispongiidae Rigby, 1967 (5) Upper Ordovician–Carboniferous
Family Toomeyospongiidae Finks, herein (1) Permian
Superfamily Lumectospongioidea Rigby and Chatterton, 1989 (1) Silurian
Family Lumectospongiidae Rigby and Chatterton, 1989 (1) Silurian
Superfamily Lumectospongioidea Rigby and Chatterton, 1989 (1) Silurian
Family Lumectospongiidae Rigby and Chatterton, 1989 (1) Silurian
Order Hexactinosa Schrammen, 1903 (134) Upper Ordovician–Holocene
Family Euryplegmatidae de Laubenfels, 1955 (1)?Cretaceous, Holocene
Family Farreidae Schulze, 1885 (4) Cretaceous–Holocene
Family Euretidae Zittel, 1877 (38) Triassic–Holocene
Family Craticulariidae Rauff, 1893 (30) Triassic–Holocene
Family Cribrospongiidae Roemer, 1864 (15) Middle Triassic–Holocene
Family Staurodermatidae Zittel, 1877 (6) Jurassic–Neogene
Family Aphrocallistidae Gray, 1867 (1) Lower Cretaceous–Holocene
Family Tretodictyidae Schulze, 1887 (9) Upper Jurassic–Holocene
Family Cystispongiidae Reid, herein (1) Upper Cretaceous–Neogene
Family Aulocalycidae Ijima, 1927 (1) Upper Jurassic
Family Emplocidae de Laubenfels, 1955 (1) Middle Jurassic
Family Uncertain (16)
Superfamily Pillaraspongioidea Rigby, 1986 (1) Devonian
Family Pillaraspongiidae Rigby, 1986 (1) Devonian
Superfamily Pileolitoidea Finks, 1960 (9) Upper Ordovician–Holocene
Family Pileolitidae Finks, 1960 (2) Permian–Middle Triassic
Family Wareembaiidae Finks and Rigby, 2004 (2) Upper Ordovician
Family Euretidae Zittel, 1877 (2) Upper Devonian
Family Craticulariidae Rauff, 1893 (5) Upper Devonian
Family Pileospongiidae Rigby, Keyes and Horowitz, 1979 (1) Carboniferous
Order Lychniscosa Schrammen, 1903 (81) Jurassic–Holocene
Family Calyptrellidae Schrammen, 1912 (1) Cretaceous
Family Callodictyonidae Zittel, 1877 (23) Upper Jurassic–Holocene
Family Callodictyonidae Zittel, 1877 (23) Upper Jurassic–Holocene
Family Coeloptychidae F. A. Roemer, 1864 (4) Lower Cretaceous–Upper Cretaceous
Family Ventriculitidae Smith, 1848 (21) Jurassic–Upper Cretaceous
Family Camerospongiidae Schrammen, 1912 (4) Lower Cretaceous–Upper Cretaceous
Family Polyblastidiidae Schrammen, 1912 (2) Upper Jurassic–Cretaceous
Family Dactylocalycidae Gray, 1867 (10) Jurassic–Holocene
Family Sporadopylidae Schrammen, 1936 (3) Upper Jurassic–Cretaceous
Family Pachyteichismatidae Schrammen, 1936 (3) Upper Jurassic–Lower Cretaceous
Family Cypelliidae Schrammen, 1936 (5) Jurassic
Family Uncertain (5)
Order Uncertain (20)

fossil forms to positions within the classification scheme of Recent hexactinellids, even where diagnoses of the fossil groups could not be encompassed in diagnoses of the Recent taxa. Some major disagreements are obvious between the two schemes. In Krautter's arrangement, the order Reticulosa and two included superfamilies, Protospongioidea and Brachiospongioidea, although listed in Table 2, were considered unrelated to Recent forms and, indeed, not even defensible as taxa because of parphyly and/or polyphyly within those groups. Rigby, on the other hand, considered those taxa valid and assigned the order and one of its superfamilies, Protospongioidea, to subclass Amphidiscophora and the other subfamily, Brachiospongioidea, to the subclass Hexasterophora. Krautter included a variety of fossil lyssacine sponges to the very large informal grouping 'Rossellimorpha' (a name introduced by Mehl, 1996) and indicated that convincing monophyletic groupings could not yet be formed within this mixture, and were not yet relatable to Recent taxa. Rigby, on the other hand, assigned almost all genera of lyssacine fossil genera to positions within the Recent classification, leaving no genera unplaced to subclass and only 20 of 432 unplaced to order. Both of the schemes interface well with the Recent hexactinellid classification but perhaps Rigby has gone somewhat beyond credibility in this regard. It is hoped that better communication between the two groups in the near future will produce a consensus arrangement that will identify particular fossil groups or strata that require more intensive examination and facilitate more collaboration between taxonomists working on fossil and Recent hexactinellids.

9.3. Phylogeny of Hexactinellida within Porifera

There is at present no doubt about the monophyly of Hexactinellida; indeed it is the best characterised group of Porifera (Mehl, 1992). Monophyly of Porifera, however, remains hotly contested, with those using morphological evidence, including palaeontologists, accepting monophyly and those using molecular techniques tending to support parphyly of the phylum. Hexactinellids are the first recognisable members of Porifera recorded in the fossil record. Their hexactine spicules have been reported from rocks stratigraphically corresponding to the Ediacaran Period (Neoproterozoic Era) of Mongolia by Brasier *et al.* (1997) and from the similar age Shiobatan Member of South China by Steiner *et al.* (1993). Gehling and Rigby (1996) also reported numerous body impressions of a small, globular sponge, *Palaeophragmodictya reticulata*, from Ediacaran age deposits of South Africa. This species has a surface reticulation reminiscent of two quadrules of spicule impressions which prompted their assignment to Hexactinellida. Mehl *et al.* (1998) questioned

their hexactinellid assignment and suggested that the impressions may not have been of siliceous spicules, but rather of organic skeletal fibres, since the early ground plan of sponges developed by [Reitner and Mehl \(1996\)](#) excluded mineralised spicules. The first certain indications of Demospongiae and Calcarea by calthrops and advanced tetractinellid spicules, respectively, occur in the Lower Cambrian when hexactinellids have already reached a moderate diversity ([Mehl et al., 1998](#)). According to [Mehl et al. \(1998\)](#), mineralised spicules were developed independently in the three classes of Porifera from aspiculate ancestral sponges ([Figure 58](#)), a hypothesis that contradicts the general convention that siliceous spicules of Hexactinellida and Demospongiae represent a shared homologous character.

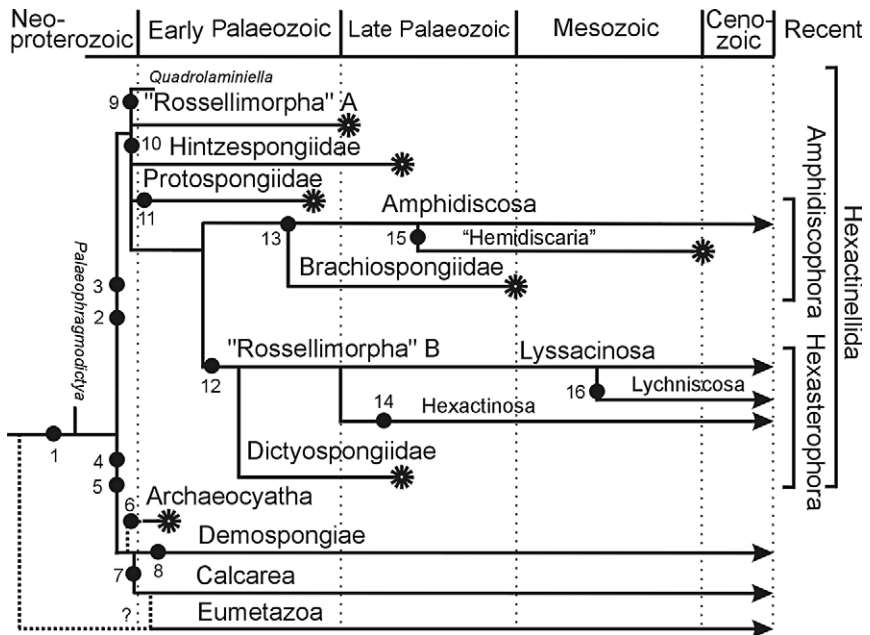


Figure 58 Diagram of the main features of Hexactinellida evolution summarised from [Mehl-Janussen \(1999\)](#), with modifications. Character states and innovations are indicated by numbers: 1, ancestral Ur-poriferan with sessile adult, planktonic larva, choanocytes in leuconoid flagellated chambers; 2, syncytial tissue organisation; 3, triaxial siliceous spicules; 4, pinacocytes; 5, secretion of basal calcareous skeleton; 6, regular archaeocyathid basal skeleton; 7, triactine magnesium–calcite spicules; 8, tetraaxial siliceous spicules; 9, spicules reduced from triaxial to monaxial diactins; 10, differentiation of dermal and choanosomal spicules; 11, reduction of body spiculation to one-layer of dermal stauractins; 12, oxyhexaster; 13, amphidisc; 14, rigid skeleton of hexactins fused in regular cubic array; 15, hemidiscs derived by reduction from amphidiscs; 16, rigid skeleton of fused lychnisc hexactins. Group extinctions are indicated by asterisks.

Molecular sequence studies have so far been unable to unambiguously determine the early branching pattern of sponge classes, and thus whether the phylum Porifera is monophyletic or paraphyletic (Boury-Esnault and Sole-Cava, 2004; Nichols, 2005). Of molecular analyses published between 1996 and 2005 (duplicate reports grouped as one analysis), six supported or did not refute monophyly while seven supported or did not refute paraphyly of Porifera (Mehl *et al.*, 1998; Boury-Esnault and Sole-Cava, 2004; Nichols, 2005; Peterson and Butterfield, 2005). For more recent publications, 2003–2005, these numbers are, respectively, two and three. Clearly, a consensus has not yet been reached regarding monophyly of Porifera from molecular work. A slightly different pattern is beginning to emerge regarding early branching within the phylum, only two of many possible alternatives of which have attracted support: (1) Hexactinellida and Demospongiae as sister groups of a clade excluding Calcarea (H+D/C), reported as support for a clade of siliceous sponges, or (2) Hexactinellida as a distinct lineage without sister grouping with either Demospongiae or Calcarea (H/D+C), interpreted as support for division of the Porifera into subphyla Symplasma (syncytial Hexactinellida) and Cellularia (Demospongiae and Calcarea), the proposal of Reiswig and Mackie (1983) based on patterns of tissue organisation. Of those same molecular analyses surveyed for monophyly of Porifera, for 1996–2005, five supported or did not refute Symplasma/Cellularia while seven supported or did not refute a siliceous grouping (Silicea of Bowerbank, 1864, being a preferable group name). For more recent publications, 2003–2005, these numbers are respectively zero and three. While recent results favour a clade of siliceous sponges, the level of statistical support for that position is generally inadequate to rule out the independent status of Hexactinellida, as favoured by palaeontological and histological data.

Estimated dates of major branch points in early metazoan evolution from amino acid sequences do not yet specifically address divergence time of hexactinellids from the other sponge classes, but they bracket it. Divergence of Eumetazoa and demosponges (*Geodia*) occurred 800 Ma according to analysis of S-type lectins (Hirabayashi and Kasai, 1993), and 650–665 Ma according to analysis of class II tyrosine kinases (Müller *et al.*, 1995). Using amino acid sequences from seven nuclear-encoded housekeeping genes, Peterson and Butterfield (2005) estimated the divergence of Metazoa (including Porifera) from Fungi at between 664 and 867 Ma by minimum evolution and maximum likelihood methods, respectively. They also calculated divergence of Eumetazoa from demosponge Porifera at between 634 and 826 Ma by the same methods. As their analysis favoured paraphyly of Porifera and sister grouping of Calcarea with Eumetazoa, both Demospongiae and Hexactinellida (no members included in the analysis) are presumed to have branched from the metazoan stem between these dates, either individually or together as a single clade. Since the earliest fossil

sponge spicules have been dated to about 600 Ma (Mehl *et al.*, 1998), the 'missing' fossil record of early metazoan evolution may be relatively short, 34–64 Ma, or long, 226–267 Ma.

9.4. Phylogeny within Hexactinellida

Molecular studies of hexactinellid tissues, unfortunately, are still too few to enable formation of phylogenetic hypotheses within the group. Systematists working with morphological evidence of Recent hexactinellids have made very few speculations on their phylogeny. Schmidt (1880) warned that dictyonal skeletons have likely been developed independently several times, hence the grouping of all dictyonal sponges in one taxon, Dictyonina, was unrealistic. This view was supported by Ijima's division (1927) of the dictyone hexactinellids into orders Hexactinosa and Lychniscosa on the basis of his contention that they had evolved independently from a protohexasterophoran ancestor. Mehl (1992) extended this separation, suggesting that dictyone Lychniscosa and lyssacine Euplectellidae, two groups sharing graphiocomes microscleres, were sister groups derived from a common ancestor. She grouped these together in the taxon Graphiocomida and pointed out that, if this grouping survived testing, the Recent order Lyssacina could no longer be considered monophyletic. Tabachnick and Menshinina (1999) developed a phylogeny within Amphidiscophora on the basis of spiculation and body form, concluding that the common ancestor, a cup-shaped form rooted in soft sediments, gave rise to two radiating lineages, a hyalonematid line and a pheronematid–monorhaphidid line. The long separation of the two main hexactinellid groupings, Amphidiscophora and Hexasterophora, continues to be supported by all workers and forms the cornerstone for speculation on phylogeny within the class.

More extensive hypotheses of hexactinellid phylogeny have been developed by palaeontologists attempting to integrate morphological information from both fossils and Recent specimens. Here we will not review these in detail, but concentrate on main aspects of interest to neontologists: characteristics of the basal group of hexactinellids and origin of the major recent groups.

In the classical scheme developed by Finks (1970, 1983, 2003a,b), the Middle Cambrian Protospongiidae, the first whole-body fossils of hexactinellids, are considered the basal stock from which all later groups derived. These were thin-walled, vasiform sponges with a large distal osculum and basal root tuft of simple diactins (Figure 59). Their body wall consisted of a single layer of stauractins or pentactins (never hexactins) of several discrete sizes arranged in parallel to form a characteristic pattern of quadrules of

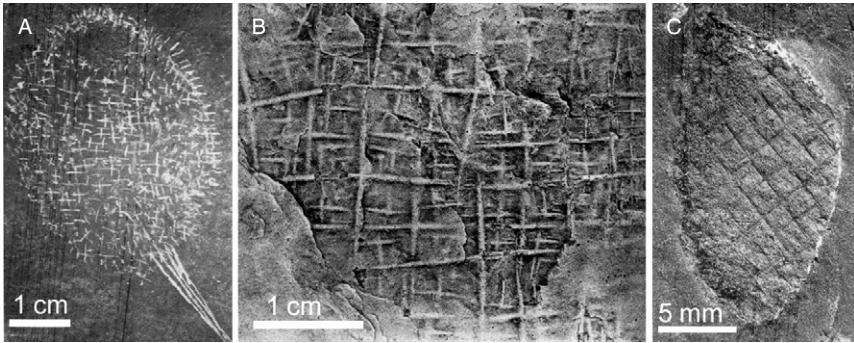


Figure 59 Representatives of the controversial Early Palaeozoic fossil family Protospongiidae. (A) *Protospongia tetranema* in which the spicules have been visually enhanced by white paint applied by the original describer, Sir W. Dawson (from Mehl, 1996). (B) Surface pattern of the single layer of stauractin spicules forming the characteristic quadrule pattern in *Protospongia hicksi*, from an enhanced photograph of a latex peel (from Rigby, 1986). (C) *Diagoniella robisoni*, a member of the second genus of Protospongiidae, in which the primary set of stauractins is oriented 45° from the body axis (from Mehl, 1996).

several size orders (Figure 59B). This structure is retained as the dermal skeleton to which several types of parenchymal skeletons were added internally in derived groups, Hintzespongioidea, Dictyospongioidea and Diere-spongioidea. In the contrasting scheme developed by Mehl-Janussen and coworkers (Mehl, 1991, 1992; Mehl *et al.*, 1998; Mehl-Janussen, 1999), based on the phylogenetic systematic conclusions reached by Reitner and Mehl (1996), and the occurrence of isolated hexactin spicules in Late Proterozoic rocks (noted above), the basal stock of hexactinellids cannot presently be characterised, but contained hexactine spicules, not stauractins, as original skeletal elements (Figure 58). Several Lower Cambrian fossils originally considered demosponges, for example *Quadrolaminiella*, are reinterpreted to be likely members of an early radiation of hexactinellids with dictyospongiid skeletons—thin body walls composed of diactin and sometimes hexactin dermalia in a regular rectangular pattern of longitudinal and transverse spicules. In this scheme, the Protospongiidae, rather than being basal to the entire class, is considered an offshoot that went extinct in mid-Palaeozoic and led to no existing members.

Origin of Amphidiscophora is partially obviated in Finks' scheme by assignment of most early Palaeozoic groups to this subclass, but a path leading to the diagnostic amphidisc microscleres was suggested. The paracavules (spicules with one hemispheric umbel on a tapering rod) which occur in the Mississippian dictyosponge *Griphiodictya* are suggested to have evolved to hemidisks (tapering rod with unequal umbels) in the Late

Carboniferous *Microhemidiscia* and to true amphidiscs (rod with two equal-size umbels) in the similar-aged *Uralonema*. The taxon Hemidiscosa (with hemidiscs) is considered a valid, if extinct, order of Amphidiscophora. Mehl (1991) pointed out that the then known stratigraphic sequence of occurrence of these spicules, hemidiscs (isolated) from Upper Cambrian, amphidiscs (isolated) from Upper Silurian and paraclavules (in *Uralonema*) from Mississippian, did not support Finks' derivation. Reitner and Mehl (1995) concluded that these three spicule types probably developed independently and the early Upper Cambrian hemidiscs (considered to be tylodiscs by Mehl, 1992) were probably not homologous with later Carboniferous forms. Mehl-Janussen (1999) considered the only acceptable evidence of Amphidiscophora to be true amphidiscs which occur first as isolated spicules in Upper Silurian. In her scheme, Amphidiscophora have a common ancestry with Brachiospongiidae, a group characterised by thick walls, radial lobate, cup- or vase-like shape, dermal layer as a fine net of stauractins in a regular quadrangular orientation, with hypodermalia as large hexactins with long proximal rays protruding far into the body wall and parenchymal spicules as hexactins of different size in irregular orientation. In contrast, Finks placed the Brachiospongiidae as ancestral to modern Hexasterophora. Contrary to Finks' suggestion, Mehl-Janussen regarded the Late Carboniferous hemidiscs as most likely derived from amphidiscs by reduction of one umbel, a process that probably occurred many times in the past and can even be documented in Recent forms. She considered Hemidiscaria (or Hemidiscosa) to be unsupported as a monophyletic taxon.

Origin of Hexasterophora in Finks' scheme (2003b) is intertwined with origin of Amphidiscophora. He considered it likely that the two main hexactinellid lineages were not differentiated in the Early Palaeozoic lineages, and interpreted the Mississippian dictyosponge, *Griphodictya epiphanes*, with oxyhexasters and paraclavules, as possessing the distinguishing characters of both major subclasses. By the Permian, the Brachiospongioidea, had taken on new body organisation, including thicker body wall and large hypodermal pentactins, that can be related to those of lyssacine hexasterophorans. He interpreted the Permian genus *Pileolites* to be a true hexactinosan and indicated that the aulocalycoid framework was primitive and developed into more regular dictyonal forms later. Mehl-Janussen (1999) accepted the earlier occurrence of oxyhexasters as isolated spicules from Lower Ordovician of Sweden (Mostler, 1986) as evidence of the existence of Hexasterophora by that time. She accepted oxyhexasters in the dictyosponge *Griphodictya epiphanes* as indication that the species, and the Dictyospongiidae, were members of Hexasterophora, but, as indicated above, she rejected the interpretation that paraclavules in that species are homologous with amphidiscs. She considered the stem Hexasterophora to encompass a presently uncharacterisable group of genera referred to informally as "Rossellimorpha"

(‘Rossellimorpha’ B in [Figure 57](#)), which gave rise to the Dictyospongiidae in the Ordovician, the dictyonine Hexactinosa in the Devonian, and the dictyonine Lychniscosa in the Middle Jurassic. The present Lyssacinosa arose as a gradual transition from the main stem group ([Figure 58](#)).

The overall pattern of diversification and extinction of hexactinellids is summarised by [Krautter \(2002\)](#). The class flourished and radiated rapidly during the Cambrian, giving rise to many new taxa and new skeletal plans, most of which diversified through the early Palaeozoic. In the later Palaeozoic, many families went extinct but the record between the Carboniferous and Triassic is very scarce. Most apparently died out by the Permian–Triassic boundary but at least four major lineages must have survived that barrier ([Figure 58](#)). The Hexactinosa underwent a major radiation and diversification during the Mesozoic, extending their distribution worldwide during the Late Triassic. They, together with the newly arisen and rapidly diversifying Lychniscosa, and lithistid demosponges, formed a discontinuous siliceous sponge reef belt spreading over more than 7000 km on the northern shelf of the Tethys Sea, the largest biological structure ever formed in the history of the Earth. Diversity of dictyonal hexactinellids continued to increase in the Cretaceous, but has gradually declined since the Late Cretaceous, leading to the present situation where hexactinellid faunas are generally dominated by lyssacine forms ([Brückner and Janussen, 2005](#)).

10. CONCLUSIONS

Hexactinellids are a very distinctive group with a long fossil record and have attracted continuous attention from taxonomists and palaeontologists since their first discovery, but it is only in the last 30 years that they have come into their own as living animals. This came about with the belated realisation that certain species could be collected alive and in good condition by SCUBA from shallow waters around Vancouver Island, and later from a subterranean cave in the Mediterranean. These findings immediately led to a variety of studies which have given us an increasingly clear picture of how glass sponges live, grow, feed, reproduce, and respond to environmental stimuli.

At the same time, advances in techniques for observing and monitoring the activities of benthic organisms *in situ* have contributed greatly to the overall picture, showing the importance of hexactinellids in deeper benthic ecosystems.

While all this has been going on, molecular biology has begun to make a growing impact in several areas. Molecular evidence, taken in conjunction with

palaeontological discoveries, makes it very likely that hexactinellids, with the possible exception of Placozoa (Dellaporta *et al.*, 2006), are the basal extant animal group. As such they are of unique interest from almost every evolutionary point of view, as much for those interested in the early evolution of conduction systems as for those tracing the history of molecules that play key roles in human physiology.

Molecular approaches will undoubtedly be applied increasingly to aspects of glass sponge physiology, biochemistry and development in the future, but we hope and expect that study of the living animals will not be neglected and that methods for maintaining them in captivity will be improved to the point that one or more species will become available for long-term studies in the laboratory. The difficulty of maintaining captive hexactinellids in good condition is perhaps the greatest barrier currently facing workers in this field and merits much closer attention than it has yet received.

ACKNOWLEDGEMENTS

This work was supported by grants from the Natural Sciences and Engineering Research Council of Canada. We thank those who contributed original illustrations. G.O.M. thanks Dorte Janussen, Gitai Yahel and Kurt Poeschel for critically reading certain sections. The photographs and drawing by Jan Köster were posted by him to the *Porifera* internet discussion list (<http://www.jiscmail.ac.uk/lists/porifera.html>) where they are still archived (April 1999). Heidi Schomann of the Institut für Meereskunde, Universität Kiel, kindly sent a photocopy of the unpublished thesis from which they were taken. S.P.L. thanks Kim Conway for comments on the ecology section. Original material from *Oopsacas* derives from work done by S.P.L. in collaboration with Nicole Boury-Esnault.

REFERENCES

- Aiello, E. (1974). Control of ciliary activity in Metazoa. In "Cilia and Flagella" (M. A. Sleight, ed.), pp. 353–376. Academic Press, London.
- Aizenberg, J., Sundar, V. C., Yablon, A. D., Weaver, J. C. and Chen, G. (2004). Biological glass fibers: Correlation between optical and structural properties. *Proceedings of the National Academy of Sciences of the United States of America* **101**, 3358–3363.
- Aizenberg, J., Weaver, J. C., Thanwala, M. S., Sundar, V. C., Morse, D. E. and Fratzl, P. (2005). Skeleton of *Euplectella* sp.: Structural hierarchy from the nanoscale to the macroscale. *Science* **309**, 275–278.

- Austin, W. C. (1983). Underwater birdwatching. *Canadian Technical Report of Hydrography and Ocean Sciences* **38**, 83–89.
- Austin, W. C. (1999). The relationship of silicate levels to the shallow water distribution of hexactinellids in British Columbia. *Memoirs of the Queensland Museum* **44**, 44.
- Austin, W. C. (2003). Sponge Gardens: A hidden treasure in British Columbia. <http://mareco.org/khoyatan/spongegardens>
- Barthel, D. (1992). Do hexactinellids structure Antarctic sponge associations? *Ophelia* **36**, 111–118.
- Barthel, D. (1995). Tissue composition of sponges from the Weddell Sea Antarctica: Not much meat on the bones. *Marine Ecology Progress Series* **123**, 149–153.
- Barthel, D. and Gutt, J. (1992). Sponge associations in the eastern Weddell Sea. *Antarctic Science* **4**, 137–150.
- Barthel, D. and Tendal, O. S. (1994). Antarctic Hexactinellida. In “Synopses of the Antarctic Benthos”, Vol. 6, p. 154. Koeltz Scientific Books, Koenigstein.
- Bavestrello, G., Burlando, B. and Sarà, M. (1988). The architecture of the canal systems of *Petrosia ficiformis* and *Chondrosia reniformis* studied by corrosion casts (Porifera, Demospongiae). *Zoomorphology* **108**, 161–166.
- Bavestrello, G., Benatti, U., Calcinai, B., Cattaneo-Vietti, R., Cerrano, C., Favre, A., Giovine, M., Lanza, S., Pronzato, R. and Sarà, M. (1998). Body polarity and mineral selectivity in the demosponge *Chondrosia reniformis*. *Biological Bulletin Marine Biological Laboratory, Woods Hole* **195**, 120–125.
- Bavestrello, G., Arillo, A. and Calcinai, B. (2003). The aquiferous system of *Scolymastra joubini* (Porifera, Hexactinellida) studied by corrosion casts. *Zoomorphology* **122**, 119–123.
- Bearer, E. L., DeGiorgis, J. A., Bodner, R. A., Kao, A. W. and Reese, T. S. (1993). Evidence for myosin motors on organelles in squid axoplasm. *Proceedings of the National Academy of Sciences of the United States of America* **90**, 11252–11256.
- Beaulieu, S. E. (2001a). Colonization of habitat islands in the deep sea: Recruitment to glass sponge stalks. *Deep-sea Research I* **48**, 1121–1137.
- Beaulieu, S. E. (2001b). Life on glass houses: Sponge stalk communities in the deep sea. *Marine Biology* **138**, 803–817.
- Bett, B. J. and Rice, A. L. (1992). The influence of hexactinellid sponge *Pheronema carpenteri* spicules on the patchy distribution of macrobenthos in the porcupine seabight (Bathyl NE Atlantic). *Ophelia* **36**, 217–226.
- Bidder, G. P. (1923). The relation of the form of a sponge to its currents. *Quarterly Journal of Microscopical Science* **67**, 293–323.
- Boury-Esnault, N. and de Vos, L. (1988). *Caulophacus cyanae*, n. sp., une éponge hexactinellide des sources hydrothermales. Biogéographie du genre *Caulophacus* Schulze, 1887. *Oceanologica Acta* **8**, 51–60.
- Boury-Esnault, N. and Rutzler, K. (1997). Thesaurus of sponge morphology. *Smithsonian Contributions to Zoology* **596**, 1–55.
- Boury-Esnault, N. and Sole-Cava, A. M. (2004). Recent contributions of genetics to the study of sponge systematics and biology. *Bollettino dei Musei e degli Istituti Biologici dell'Università di Genova* **68**, 3–18.
- Boury-Esnault, N. and Vacelet, J. (1994). Preliminary studies on the organization and development of a hexactinellid sponge from a Mediterranean cave, *Oopsacas minuta*. In “Sponges in Time and Space. Proceedings of the Fourth International Porifera Congress” (R. W. M. van Soest, T. M. G. van Kempen and J. Braekman, eds), pp. 407–416. AA Balkema, Rotterdam.

- Boury-Esnault, N., Efremova, S., Bézac, C. and Vacelet, J. (1999). Reproduction of a hexactinellid sponge: First description of gastrulation by cellular delamination in the Porifera. *Invertebrate Reproduction and Development* **35**, 187–201.
- Bowerbank, J. S. (1858). On the anatomy and physiology of the Spongiadae. Part I: On the spicules. *Philosophical Transactions of the Royal Society of London* **148**, 279–332.
- Bowerbank, J. S. (1864). “A Monograph of the British Spongiadae”, Vol. 1. Ray Society, London.
- Boyd, I. (1981). The spicule jungle of *Rhabdocalyptus dawsoni*: A unique microhabitat. B.Sc. Thesis, University of Victoria, Victoria, BC, Canada.
- Brasier, M. D., Green, O. and Shields, G. (1997). Ediacaran sponge spicule clusters from southwestern Mongolia and the origins of the Cambrian fauna. *Geology* **25**, 303–306.
- Brückner, A. and Janussen, D. (2005). *Rossella bromleyi* n. sp.: The first entirely preserved fossil sponge species of the genus *Rossella* (Hexactinellida) from the Upper Cretaceous of Bornholm, Denmark. *Journal of Paleontology* **79**, 21–28.
- Bütschli, O. (1901). Einige Beobachtungen über Kiesel- und kalknadeln von Spongien. *Zeitschrift für wissenschaftliche Zoologie* **69**, 235–286.
- Carter, H. J. (1885). Report on a collection of marine sponges from Japan made by Dr. J. Anderson. *Annals and Magazine of Natural History* **15**, 387–406.
- Cattaneo-Vietti, R., Bavestrello, G., Cerrano, C., Sarà, M., Benatti, U., Giovine, M. and Gaino, E. (1996). Optical fibres in an Antarctic sponge. *Nature* **383**, 397–398.
- Cerrano, C., Arillo, A., Bavestrello, G., Calcinai, B., Cattaneo-Vietti, R., Penna, A., Sarà, M. and Totti, C. (2000). Diatom invasion in the antarctic hexactinellid sponge *Scolymastra joubini*. *Polar Biology* **23**, 441–444.
- Cha, J. N., Shimizu, K., Zhou, Y., Christiansen, S. C., Chmelka, B. F., Stucky, G. D. and Morse, D. E. (1999). Silicatein filaments and subunits from a marine sponge direct the polymerization of silica and silicones *in vitro*. *Proceedings of the National Academy of Sciences of the United States of America* **96**, 361–365.
- Claus, C. F. W. (1868). Ueber *Euplectella aspergillum* (R. Owen). In “Ein Beitrag zur Naturgeschichte der Kieselschwämme”, N.G. Elwert’sche Universitäts-Buchhandlung, Marburg.
- Claus, C. F. W. (1872). “Grundzüge der Zoologie”, 2nd edn. N.G. Elwert, Marburg und Leipzig.
- Conway, K., Krautter, M., Vaughn Barrie, J., Whitney, F., Thomson, R. E., Reisinger, H. M., Lehnert, H., Mungov, G. and Bertram, M. (2005a). Sponge reefs in the Queen Charlotte Basin, Canada: Controls on distribution, growth and development. In “Cold-water Corals and Ecosystems” (A. Freiwald and J. M. Roberts, eds), pp. 605–621. Springer-Verlag, Berlin.
- Conway, K., Vaughn Barrie, J. and Krautter, M. (2005b). Geomorphology of unique reefs on the western Canadian shelf: Sponge reefs mapped by multibeam bathymetry. *Geo-Marine Letters* **25**, 205–213.
- Conway, K. W., Barrie, J. V., Austin, W. C. and Luternauer, J. L. (1991). Holocene sponge bioherms on the western Canadian continental shelf. *Continental Shelf Research* **11**, 771–790.
- Conway, K. W., Krautter, M., Barrie, J. V. and Neuweiler, M. (2001). Hexactinellid sponge reefs on the Canadian continental shelf: A unique “living fossil”. *Geoscience Canada* **28**, 71–78.
- Conway, K. W., Vaughn Barrie, J. and Krautter, M. (2004). Modern siliceous sponge reefs in a turbid, siliciclastic setting: Fraser River delta, British Columbia, Canada. *Neues Jahrbuch für Geologie und Paläontologie Monatshefte* **6**, 335–350.

- Cook, S. E. (2005). Ecology of the Hexactinellid sponge reefs on the Western Canadian continental shelf. M.Sc. Thesis, University of Victoria, Victoria.
- Croce, G., Frache, A., Milanesio, M., Viterbo, D., Bavestrello, G., Benatti, U., Giovine, M. and Amenitsch, H. (2003). Fiber diffraction study of spicules from marine sponges. *Microscopy Research and Technique* **62**, 378–381.
- Dahlgren, U. and Kepner, W. A. (1930). “Principles of Animal Histology”, Macmillan, New York.
- Dayton, P. K. (1979). Observations of growth, dispersal and population dynamics of some sponges in McMurdo Sound, Antarctica. *Colloques internationaux du C.N.R.S.* **291**, 271–282.
- Dayton, P. K. (1989). Interdecadal variation in an Antarctic sponge and its predators from oceanographic climate shifts. *Science* **245**, 1484–1486.
- Dayton, P. K., Robilliard, G. A., Paine, R. T. and Dayton, L. B. (1974). Biological accommodation in the benthic community at McMurdo Sound, Antarctica. *Ecological Monographs* **44**, 105–128.
- Dellaporta, S. L., Xu, A., Sagasser, S., Jakob, W., Moreno, M. A., Buss, L. W. and Schierwater, B. (2006). Mitochondrial genome of *Trichoplax adhaerens* supports Placozoa as the basal lower metazoan phylum. *Proceedings of the National Academy of Sciences of the United States of America* **103**, 8751–8756.
- Dendy, A. (1926). On the origin, growth and arrangement of sponge spicules: A study in symbiosis. *Quarterly Journal of Microscopical Science* **70**, 1–74.
- Drum, R. W. (1968). Electron microscopy of siliceous spicules from the freshwater sponge *Heteromyenia*. *Journal of Ultrastructure Research* **22**, 12–21.
- Ehrlich, H., Hanke, T., Simon, P., Goebel, C., Heinemann, S., Born, R. and Worch, H. (2005). Demineralization of natural silica based biomaterials: New strategy for the isolation of organic frameworks. *Biomaterialien* **6**, 297–302.
- Fernandez-Busquets, X. and Burger, M. M. (1999). Cell adhesion and histocompatibility in sponges. *Microscopy Research and Technique* **44**, 204–218.
- Finks, R. M. (1970). The evolution and ecologic history of sponges during Palaeozoic times. In “The Biology of the Porifera” (W. G. Fry, ed.), pp. 3–22. Academic Press, London.
- Finks, R. M. (1983). Fossil Hexactinellida. In “Sponges and Spongiomorphs, Notes for a Short Course. Studies in Geology (7)” (J. K. Rigby and C. W. Stearn, eds), pp. 101–105. Department of Geological Sciences, University of Tennessee, Knoxville, Tennessee.
- Finks, R. M. (2003a). Evolution and ecological history of sponges during Paleozoic times. In “Treatise on Invertebrate Paleontology, Part E, Porifera, Revised, Vol. 2: Introduction to the Porifera” (R. L. Kaesler, ed.), pp. 261–274. The Geological Society of America, Boulder, Colorado.
- Finks, R. M. (2003b). Paleozoic Hexactinellida: Morphology and phylogeny. In “Treatise on Invertebrate Paleontology, Part E, Porifera, Revised, Vol. 2: Introduction to the Porifera” (R. L. Kaesler, ed.), pp. 135–154. The Geological Society of America, Boulder, Colorado.
- Fraser, C. M. (1932). A comparison of the marine fauna of the Nanaimo region with that of the San Juan Archipelago. *Transactions of the Royal Society of Canada* **26**, 49–70.
- Garrone, R. (1969). Collagène, spongine et squelette mineral chez l'éponge *Haliclona rosea* (O.S.) Démonponge, Haploscléride. *Journal de Microscopie* **8**, 581–598.
- Garrone, R., Simpson, T. L. and Pottu-Boumendil, J. (1981). Ultrastructure and deposition of silica in sponges. In “Silicon and Siliceous Structures in Biological

- Systems" (T. L. Simpson and B. E. Volcani, eds), pp. 495–525. Springer-Verlag, New York.
- Gehling, J. G. and Rigby, J. K. (1996). Long expected sponges from the neoproterozoic Ediacara fauna of South Australia. *Journal of Paleontology* **70**, 185–195.
- Ghield, J. (1991). The sponges that spanned Europe. *New Scientist* **2**, 58–62.
- Goodall, H. (1985). Membrane channels: Bridging the junctional gap. *Nature* **317**, 286–287.
- Green, C. R. and Bergquist, P. R. (1982). Phylogenetic relationships within the invertebrata in relation to the structure of septate junctions and the development of occluding junctional types. *Journal of Cell Science* **53**, 279–305.
- Guilbault, J.-P., Krautter, M., Conway, K. W. and Barrie, J. V. (2006). Modern foraminifera attached to Hexactinellid sponge meshwork on the West Canadian Shelf: Comparison with Jurassic Counterparts from Europe. *Palaeontologia Electronica* **9**(1)3A:48p, 6.3MB http://palaeo-electronica.org/paleo/2006_1/sponge/issue1_06.htm
- Gundacker, D., Leys, S. P., Schröder, H. C., Müller, I. M. and Müller, W. E. G. (2001). Isolation and cloning of a C-type lectin from the hexactinellid sponge *Aphrocallistes vastus*: A putative aggregation factor. *Glycobiology* **11**, 21–29.
- Harrison, F. W. and de Vos, L. (1991). Porifera. In "Microscopic Anatomy of Invertebrates" (F. W. Harrison and J. A. Westfall, eds), pp. 29–89. Wiley-Liss, New York.
- Hartman, W. D. (1983). Modern Hexactinellida. In "Sponges and Spongiomorphs, Notes for a Short Course" (T. W. Broadhead, ed.). Department of Geological Sciences, University of Tennessee, Knoxville, Tennessee.
- Hirabayashi, J. and Kasai, K. (1993). The family of metazoan metal-independent beta-galactoside-binding lectins: Structure, function and molecular evolution. *Glycobiology* **3**, 297–304.
- Hooper, J. A. and Van Soest, R. W. M. (2002). Systema Porifera. In "A Guide to the Classification of Sponges". Kluwer Academic/Plenum Publishers, New York.
- Hooper, J. N. A. and Wiedenmayer, F. (1994). Porifera. In "Zoological Catalogue of Australia" (A. Wells, ed.), pp. 1–632. CSIRO, Australia, Melbourne.
- Ijima, I. (1901). Studies on the Hexactinellida. Contribution I (Euplectellidae). *Journal of the College of Science of the Imperial University of Tokyo* **15**, 1–299.
- Ijima, I. (1904). Studies on the Hexactinellida. Contribution IV. (Rossellidae). *Journal of the College of Science of the Imperial University of Tokyo* **28**, 13–307.
- Ijima, I. (1927). The Hexactinellida of the Siboga Expedition. *Siboga Expedition Reports* **6**, 1–383, 26 plates.
- Imsiecke, G. (1993). Ingestion, digestion, and egestion in *Spongilla lacustris* (Porifera, Spongillidae) after pulse feeding with *Chlamydomonas reinhardtii*. *Zoomorphology* **113**, 233–244.
- Imsiecke, G., Steffen, R., Custodio, M., Borojevic, R. and Müller, W. E. G. (1995). Formation of spicules by sclerocytes from the freshwater sponge *Ephydatia muelleri* in short-term cultures *in vitro*. *In vitro Cellular and Developmental Biology-Animal* **31**, 528–535.
- Jamieson, G. S. and Chew, L. (2002). Hexactinellid sponge reefs: Areas of interest as marine protected areas in the north and central coast areas. *Canadian Science Advisory Secretariat. Department of Fisheries and Oceans*, 1–78.
- Kachar, B. and Reese, T. S. (1988). The mechanism of cytoplasmic streaming in characean algal cells: Sliding of endoplasmic reticulum along actin filaments. *Journal of Cell Biology* **106**, 1545–1552.

- Kent, W. S. (1870). On two new siliceous sponges taken in the late dredging expedition of the yacht 'Norna' off the coasts of Spain and Portugal. *Annals and Magazine of Natural History* **6**, 217–224.
- Kirkpatrick, R. (1910). On Hexactinellida sponge spicules and their names. *Annals and Magazine of Natural History* **5**, 208–213, 347–350.
- Koltun, V. M. (1967). Vitreous sponges of the northern and far-eastern seas of the USSR. *Opredeliteli po Faune S.S.S.R.* **94**, 1–124.
- Koonce, M. P., Euteneuer, U., McDonald, K. L., Menzel, D. and Schliwa, M. (1986). Cytoskeletal architecture and motility in a giant freshwater amoeba, *Reticulomyxa*. *Cell Motility and the Cytoskeleton* **6**, 521–533.
- Köster, J. (1997). Untersuchungen zur Ultrastuktur antarktischer Hexactinelliden (Porifera) Diploma Thesis, Institut für Meereskunde, Christian-Albrechts-Universität, Kiel, Germany.
- Krasko, A., Lorenz, B., Batel, R., Schröder, H. C., Müller, I. M. and Müller, W. E. G. (2000). Expression of silicatein and collagen genes in the marine sponge *Suberites domuncula* is controlled by silicate and myotrophin. *European Journal of Biochemistry* **267**, 4878–4887.
- Krautter, M. (2002). Fossil Hexactinellida: An Overview. In "Systema Porifera: A Guide to the Classification of Sponges" (J. N. A. Hooper and R. W. M. Van Soest, eds), pp. 1211–1223. Kluwer Academic/Plenum Publishers, New York.
- Krautter, M., Conway, K. W., Barrie, J. V. and Neuweiller, M. (2001). Discovery of a "Living Dinosaur": Globally unique modern hexactinellid sponge reefs off British Columbia, Canada. *Facies* **44**, 265–282.
- Kube-Grandenath, E. and Schliwa, M. (1995). Gamma tubulin of *Reticulomyxa filosa*: Amino acid sequence and expression in bacteria. *European Journal of Cell Biology Suppl.*, 199a.
- Lawn, I. D., Mackie, G. O. and Silver, G. (1981). Conduction system in a sponge. *Science* **211**, 1169–1171.
- Leinfelder, R. R., Krautter, M., Laternser, R., Nose, M., Schmid, D. U., Schweigert, G., Werner, W., Keupp, H., Brugger, H., Herrmann, R., Rehfeld-Kiefer, U. Schröder, J. H. *et al.* (1994). The origin of Jurassic reefs: Current research developments and results. *Facies* **31**, 1–56.
- Leys, S. P. (1995). Cytoskeletal architecture and organelle transport in giant syncytia formed by fusion of hexactinellid sponge tissues. *Biological Bulletin Marine Biological Laboratory, Woods Hole* **188**, 241–254.
- Leys, S. P. (1996). Cytoskeletal architecture, organelle transport, and impulse conduction in hexactinellid sponge syncytia Doctoral Dissertation, University of Victoria, Victoria.
- Leys, S. P. (1997). Sponge cell culture: A comparative evaluation of adhesion to a native tissue extract and other culture substrates. *Tissue and Cell* **29**, 77–87.
- Leys, S. P. (1998). Fusion and cytoplasmic streaming are characteristics of at least two hexactinellids: Examination of cultured tissue from *Aphrocallistes vastus*. In "Sponge Sciences—Multidisciplinary Perspectives" (Y. Watanabe and N. Fusetani, eds), pp. 215–226. Springer-Verlag, Tokyo.
- Leys, S. P. (1999). The choanosome of hexactinellid sponges. *Invertebrate Biology* **118**, 221–235.
- Leys, S. P. (2003a). Comparative study of spiculogenesis in demosponge and hexactinellid Larvae. *Microscopy Research and Technique* **62**, 300–311.
- Leys, S. P. (2003b). The significance of syncytial tissues for the position of the Hexactinellida in the Metazoa. *Integrative and Comparative Biology* **43**, 19–27.

- Leys, S. P. and Lauzon, N. R. J. (1998). Hexactinellid sponge ecology: Growth rates and seasonality in deep water sponges. *Journal of Experimental Marine Biology and Ecology* **230**, 111–129.
- Leys, S. P. and Mackie, G. O. (1994). Cytoplasmic streaming in the hexactinellid sponge *Rhabdocalyptus dawsoni* (Lambe 1873). In “Sponges in Time and Space” (R. W. M. van Soest, T. M. G. van Kempen and J. Braekman, eds), pp. 417–423. AA Balkema, Rotterdam.
- Leys, S. P. and Mackie, G. O. (1997). Electrical recording from a glass sponge. *Nature* **387**, 29–30.
- Leys, S. P. and Meech, R. W. (2006). Physiology of coordination in sponges. *Canadian Journal of Zoology* **84**, 288–306.
- Leys, S. P. and Reiswig, H. M. (1998). Nutrient transport pathways in the neotropical sponge *Aplysina*. *Biological Bulletin Marine Biological Laboratory, Woods Hole* **195**, 30–42.
- Leys, S. P. and Tompkins, G. J. (2004). Glass sponges arrest pumping in response to increased sediment loads. *Integrative and Comparative Biology* **44**, 719.
- Leys, S. P., Mackie, G. O. and Meech, R. W. (1999). Impulse conduction in a sponge. *Journal of Experimental Biology* **202**, 1139–1150.
- Leys, S. P., Wilson, K., Holeton, C., Reiswig, H. M., Austin, W. C. and Tunnicliffe, V. (2004). Patterns of glass sponge (Porifera, Hexactinellida) distribution in coastal waters of British Columbia, Canada. *Marine Ecology Progress Series* **283**, 133–149.
- Leys, S. P., Cheung, E. and Boury-Esnault, N. (2006). Embryogenesis in the glass sponge *Oopsacas minuta*: Formation of syncytia by fusion of blastomeres. *Integrative and Comparative Biology* **46**(2), 104–117.
- MacGinitie, G. E. (1939). The method of feeding of tunicates. *Biological Bulletin Marine Biological Laboratory, Woods Hole* **77**, 443–447.
- Mackie, G. O. (1979). Is there a conduction system in sponges? *Colloques Internationaux du Centre National de la Recherche Scientifique* **291**, 145–151.
- Mackie, G. O. (1981). Plugged syncytial interconnections in hexactinellid sponges. *Journal of Cell Biology* **91**, 103a.
- Mackie, G. O. and Singla, C. L. (1983). Studies on hexactinellid sponges. I. Histology of *Rhabdocalyptus dawsoni* (Lambe, 1873). *Philosophical Transactions of the Royal Society of London Series B* **301**, 365–400.
- Mackie, G. O., Lawn, I. D. and Pavans de Ceccatty, M. (1983). Studies on hexactinellid sponges. II. Excitability, conduction and coordination of responses in *Rhabdocalyptus dawsoni* (Lambe 1873). *Philosophical Transactions of the Royal Society of London Series B* **301**, 401–418.
- Maldonado, M., Carmona, M. C., Uriz, M. J. and Cruzado, A. (1999). Decline in Mesozoic reef-building sponges explained by silicon limitation. *Nature* **401**, 785–788.
- Marshall, W. (1875). Untersuchungen über Hexactinelliden. *Zeitschrift für wissenschaftliche Zoologie* **25**, 142–243.
- McClay, D. R. (1972). Cell aggregation: Properties of cell surface factors from five species of sponge. *Journal of Experimental Zoology* **186**, 89–102.
- Mehl, D. (1991). Are protospongiidae the stem group of modern hexactinellids? In “Fossil and Recent Sponges” (J. Reitner and H. Keupp, eds), pp. 43–53. Springer-Verlag, Berlin.
- Mehl, D. (1992). Die Entwicklung der Hexactinellida seit dem Mesozoikum. Paläobiologie, Phylogenie und Evolutionsökologie. *Berliner geowissenschaftliche Abhandlungen* **E2**, 1–164.

- Mehl, D. (1996). Phylogenie und Evolutionsökologie der Hexactinellida (Porifera) im Paläozoikum. *Geologische-Paläontologische Mitteilungen Innsbruck* **4**, 1–55.
- Mehl, D. and Fürsich, F. T. (1997). Middle Jurassic Porifera from Kachchh, western India. *Paläontologische Zeitschrift* **71**, 19–33.
- Mehl, D. and Reiswig, H. M. (1991). The presence of flagellar vanes in choanomeres of Porifera and their possible phylogenetic implications. *Zeitschrift für zoologische und systematische Evolutionsforschung* **29**, 312–319.
- Mehl, D., Reitner, J. and Reiswig, H. M. (1994). Soft tissue organization of the deep-water hexactinellid *Schaudinmia arctica* Schulze, 1900 from the arctic seamount Vesterisbanken (Central Greenland Sea). *Berliner geowissenschaftliche Abhandlungen* **E13**, 301–313.
- Mehl, D., Müller, I. and Müller, W. E. G. (1998). Molecular biological and paleontological evidence that Eumetazoa, including Porifera (sponges), are of monophyletic origin. In “Sponge Sciences: Multidisciplinary Perspectives” (Y. Watanabe and N. Fusetani, eds), pp. 133–156. Springer-Verlag, Tokyo.
- Mehl-Janussen, D. (1999). Die frühe Evolution der Porifera: Phylogenie und Evolutionsökologie der Poriferen im Paläozoikum mit Schwerpunkt der desmentragenden Demospongiae (“Lithistide”). *Münchener Geowissenschaftliche Abhandlungen, Reihe A* **37**, 1–72.
- Mehl-Janussen, D. (2000). Schwämme in der fossilen Überlieferung. *Zentralblatt für Geologie und Paläontologie, Teil I* **1/2**, 15–26.
- Mezitt, A. A. and Lucas, W. J. (1996). Plasmodesmal cell-to-cell transport of proteins and nucleic acids. *Plant Molecular Biology* **32**, 251–273.
- Miller, K. E. and Joshi, H. C. (1996). Tubulin transport in neurons. *Journal of Cell Biology* **133**, 1355–1366.
- Minchin, E. A. (1909). Sponge-Spicules. A summary of present knowledge. *Ergebnisse und Fortschritte der Zoologie* **2**, 171–274.
- Morris, R. H., Abbott, D. P. and Haderlie, E. C. (1980). “Intertidal Invertebrates of California”. Stanford University Press, Stanford, CA.
- Mostler, H. (1986). Beitrag zur stratigraphischen Verbreitung und phylogenetischen Stellung der Amphidiscophora und Hexasterophora (Hexactinellida, Porifera). *Mitteilungen der Österreichische Geologische Gesellschaft* **78**, 319–359.
- Müller, W. E. G., Conrad, J., Zahn, R. K., Steffen, R., Uhlenbruck, G. and Müller, I. (1984). Cell adhesion molecule in the hexactinellid *Aphrocallistes vastus*: Species-unspecific aggregation factor. *Differentiation* **26**, 30–35.
- Müller, W. E. G., Müller, I., Rinkevich, B. and Gamulin, V. (1995). Molecular evolution: Evidence for the monophyletic origin of multicellular animals. *Naturwissenschaften* **82**, 36–38.
- Müller, W. E. G., Koziol, C., Müller, I. M. and Wiens, M. (1999). Towards an understanding of the molecular basis of immune responses in sponges: The marine demosponge *Geodia cydonium* as a Model. *Microscopy Research and Technique* **44**, 219–236.
- Müller, W. E. G., Krasko, A., Le Pennec, G., Steffen, R., Wiens, M., Ammar, M. S. A., Müller, I. M. and Schröder, H. (2003). Molecular mechanism of spicule formation in the demosponge *Suberites domuncula*: Silicatein–collagen–myotrophin. *Progress in Molecular and Subcellular Biology* **33**, 195–221.
- Müller, W. E. G., Wendt, K., Geppert, C., Wiens, M., Reiber, A. and Schröder, H. C. (2006). Novel photoreception system in sponges? Unique transmission properties of the stalk spicules from the hexactinellid *Hyalonema sieboldi*. *Biosensors and Bioelectronics* **21**, 1149–1155.

- Neuweiler, M. (2000). Untersuchungen an Kieselnadeln rezenter hexactinellider Schwämme. Diplomarbeit. Universität Stuttgart, Stuttgart.
- Nichols, S. A. (2005). An evaluation of support for order-level monophyly and interrelationships within the class Demospongiae using partial data from the large subunit rDNA and cytochrome oxidase subunit. I. *Molecular Phylogenetics and Evolution* **34**, 81–96.
- Nicol, J. A. C. (1967). “The Biology of Marine Animals”. Pitman, London.
- Okada, Y. (1928). On the development of a hexactinellid sponge, *Farrea sollasii*. *Journal of the Faculty of Science of the Imperial University of Tokyo* **4**, 1–29.
- Owen, R. (1843). Description of a new genus and species of sponge (*Euplectella aspergillum*, Ow.). *Transactions of the Royal Society of London* **3**, 203–206.
- Pavans de Ceccatty, M. (1982). *In vitro* aggregation of syncytia and cells of a hexactinellida sponge. *Developmental and Comparative Immunology* **6**, 15–22.
- Pavans de Ceccatty, M. (1989). Les éponges, à l’aube des communications cellulaires. *Pour la Science* **142**, 64–72.
- Pavans de Ceccatty, M. and Mackie, G. (1982). Genèse et évolution des interconnexions syncytiales et cellulaires chez une éponge Hexactinellide en cours de réaggrégation après dissociation *in vitro*. *Comptes Rendus de l’Académie des Sciences Paris* **294**, 939–944.
- Pavans de Ceccatty, M., Gargouil, M. and Coraboef, E. (1960). Les réactions motrices de l’éponge siliceuse *Tethya lyncurium* à quelques stimulations expérimentales. *Vie et Milieu* **11**, 594–600.
- Perez, T. (1996). La rétention de particules par une éponge hexactinellide, *Oopsacas minuta* (Leucopsacidae): le rôle du réticulum. *Comptes Rendus de l’Académie des Sciences Paris, Sciences de la Vie* **319**, 385–391.
- Peterson, K. J. and Butterfield, N. J. (2005). Origin of the Eumetazoa: Testing ecological predictions of molecular clocks against the Proterozoic fossil record. *Proceedings of the National Academy of Sciences of the United States of America* **102**, 9547–9552.
- Pisera, A. (1997). Upper Jurassic siliceous sponges from the Swabian Alb: Taxonomy and paleoecology. *Paleontologia Polonica* **57**, 3–216.
- Pisera, A. and Lévi, C. (2002). ‘Lithistid’ Demospongiae. In “Systema Porifera: A Guide to the Classification of Sponges” (J. A. Hooper and R. W. M. Van Soest, eds), pp. 299–301. Kluwer Academic/Plenum Publishers, New York.
- Pomel, A. (1872). Paléontologie ou Description des animaux fossiles de la province d’Oran, Zoophytes. 5^e Fascicule, Spongiaires. A.D. Perrier, Oran.
- Puce, S., Calcinai, B., Bavestrello, G., Cerrano, C., Gravili, C. and Boero, F. (2005). Hydrozoa (Cnidaria) symbiotic with Porifera: A review. *Marine Ecology* **26**, 73–81.
- Pueschel, C. M. (1989). An expanded survey of the ultrastructure of red algal pit plugs. *Journal of Phycology* **25**, 625–636.
- Reed, C., Greenberg, M. J. and Pierce, S. K. (1976). The effects of the cytochalasins on sponge cell reaggregation: New insights through the scanning electron microscope. In “Aspects of Sponge Biology” (F. W. Harrison and R. R. Cowden, eds), pp. 153–169. Academic Press, Inc., New York.
- Reid, R. E. H. (1958). A monograph of the Upper Cretaceous Hexactinellida of Great Britain and Northern Ireland. Part I. *Palaeontographical Society Monograph* **111**, 1–46.
- Reid, R. E. H. (2003). Hexactinellida: General morphology and classification. In “Treatise on Invertebrate Paleontology, Part E, Porifera, Revised, Vol. 2: Introduction to the Porifera” (R. L. Kaesler, ed.), pp. 127–134. The Geological Society of America, Boulder, Colorado.

- Reiswig, H. M. (1971a). The axial symmetry of sponge spicules and its phylogenetic significance. *Cahiers de Biologie Marine* **12**, 505–514.
- Reiswig, H. M. (1971b). *In situ* pumping activities of tropical demospongiae. *Marine Biology* **9**, 38–50.
- Reiswig, H. M. (1979a). Histology of Hexactinellida (Porifera). *Colloques internationaux du Centre national du Recheches scientifiques* **291**, 173–180.
- Reiswig, H. M. (1979b). A new sponge with rapid contraction systems. Annual Meeting of the Canadian Society of Zoology. May, 1979. Laval University, Quebec. p. 83a.
- Reiswig, H. M. (1990). *In situ* feeding in two shallow water hexactinellid sponges. In “New Perspectives in Sponge Biology” (K. Rutzler, ed.), pp. 504–510. Smithsonian Institution Press, Washington, DC.
- Reiswig, H. M. (1991). New perspectives on the hexactinellid genus *Dactylocalyx* Stuchbury. In “Fossil and Recent Sponges” (J. Reitner and H. Keupp, eds), pp. 7–20. Springer-Verlag, Berlin.
- Reiswig, H. M. (1992). First Hexactinellida (Porifera) (glass sponges) from the Great Australian Bight. *Records of the South Australian Museum* **26**, 25–36.
- Reiswig, H. M. (2002a). Family Diapleuridae Ijima, 1927. In “Systema Porifera: A Guide to the Classification of Sponges” (J. N. A. Hooper and R. W. M. Van Soest, eds), pp. 1383–1385. Kluwer Academic/Plenum Publishers, New York.
- Reiswig, H. M. (2002b). Order Aulocalycoida Tabachnick and Reiswig, 2000. In “Systema Porifera: A Guide to the Classification of Sponges” (J. N. A. Hooper and R. W. M. Van Soest, eds), p. 1361. Kluwer Academic/Plenum Publishers, New York.
- Reiswig, H. M. (2006). Classification and phylogeny of Hexactinellida (Porifera). *Canadian Journal of Zoology* **84**(2), 195–204.
- Reiswig, H. M. (2004). Hexactinellida after 132 years of study—what’s new? *Bollettino dei Musei e degli Istituti Biologici dell’Università di Genova* **68**, 71–84.
- Reiswig, H. M. and Mackie, G. O. (1983). Studies on hexactinellid sponges III. The taxonomic status of Hexactinellida within the Porifera. *Philosophical Transactions of the Royal Society of London Series B* **301**, 419–428.
- Reiswig, H. M. and Mehl, D. (1991). Tissue organization of *Farrea occa* (Porifera, Hexactinellida). *Zoomorphology* **110**, 301–311.
- Reiswig, H. M. and Mehl, D. (1994). Reevaluation of *Chonelasma* (Euretidae) and *Leptophragmella* (Craticulariidae) (Hexactinellida). In “Sponges in Time and Space” (R. W. M. van Soest, T. M. G. van Kempen and J.-C. Braekman, eds), pp. 151–165. AA Balkema, Rotterdam.
- Reiswig, H. M. and Tsurumi, M. (1996). A new genus and species of Aulocalycidae, *Leioplegma polyphyllon* (Porifera: Hexactinellida) from the Blake Ridge off South Carolina. *Bulletin of Marine Science* **58**, 764–774.
- Reitner, J. and Mehl, D. (1995). Early paleozoic diversification of sponges: New data and evidences. *Geologische-Paläontologische Mitteilungen Innsbruck* **20**, 335–347.
- Reitner, J. and Mehl, D. (1996). Monophyly of the Porifera. *Verhandlungen des naturwissenschaftlichen Vereins in Hamburg* **36**, 5–32.
- Rigby, J. K. (1986). Sponges of the Burgess Shale, Middle Cambrian, British Columbia, Canada. *Paleontographica Canadiana* **2**, 1–105.
- Rigby, J. K. (2004). Classification. In “Treatise on Invertebrate Paleontology, Part E, Porifera, Revised. Vol. 3. Porifera (Demospongiae, Hexactinellida, Heteractinida, Calcareia)” (R. L. Kaesler, ed.), pp. 1–8. The Geological Society of America, Boulder, Colorado.
- Robinow, C. and Kellenberger, E. (1994). The bacterial nucleoid revisited. *Microbiological Reviews* **58**, 211–232.

- Salomon, D. and Barthel, D. (1990). External choanosome morphology of the hexactinellid sponge *Aulorosella vanhoeffeni* Schulze and Kirkpatrick 1910. *Senckenbergiana maritima* **21**, 87–99.
- Sancetta, C. (1989). Spatial and temporal trends of diatom flux in B.C. fjords. *Journal of Plankton Research* **11**, 503–520.
- Sandford, F. (2003). Physical and chemical analysis of the siliceous skeletons in six sponges of two groups (Demospongiae and Hexactinellida). *Microscopy Research and Technique* **62**, 336–355.
- Sarà, M., Bavestrello, G., Cattaneo-Vietti, R. and Cerrano, C. (1998). Endosymbiosis in sponges: Relevance for epigenesis and evolution. *Symbiosis* **25**, 57–70.
- Sarikaya, M., Fong, H., Sunderland, N., Flinn, B. D., Mayer, G., Mescher, A. and Gaino, E. (2001). Biomimetic model of a sponge-spicular optical fiber—mechanical properties and structure. *Journal of Materials Research* **16**, 1420–1428.
- Schmid, V. and Bally, A. (1988). Species specificity in cell-substrate interactions in medusae. *Developmental Biology* **129**, 573–581.
- Schmid, V., Bally, A., Beck, K., Haller, M., Schlage, W. K. and Weber, C. (1991). The extracellular matrix (mesoglea) of hydrozoan jellyfish and its ability to support cell adhesion and spreading. *Hydrobiologia* **216/217**, 3–10.
- Schmidt, O. (1870). “Grundzüge einer Spongien-fauna des Atlantischen Gebietes”. Engelmann, Leipzig.
- Schmidt, O. (1880). “Die Spongien des Meerbusen von Mexico (und des Carai-bischen Meeres)”. Zweites (Schluss-) Heft. Gustav Fisher, Jena.
- Schröder, H. C., Krasko, A., Gundacker, D., Leys, S. P., Müller, I. M. and Müller, W. E. (2003a). Molecular and functional analysis of the (6–4) photolyase from the hexactinellid *Aphrocallistes vastus*. *Biochimica et Biophysica Acta* **1651**, 41–49.
- Schröder, H. C., Krasko, A., Le Pennec, G., Adell, T., Wiens, M., Hassanein, H., Müller, I. and Müller, W. E. G. (2003b). Silicase, an enzyme which degrades biogenous amorphous silica: Contribution to the metabolism of silica deposition in the demospunge *Suberites domuncula*. *Progress in Molecular and Subcellular Biology* **33**, 249–268.
- Schuchert, P. and Reiswig, H. M. (2006). *Brinckmannia hexactinellidophila*, n. g., n. spec., a hydroid living in tissues of glass sponges of the reefs, fjords and seamounts of Pacific Canada and Alaska. *Canadian Journal of Zoology* **84**, 564–572.
- Schultze, M. J. S. (1860). “Die Hyalonemen. Ein Beitrag zur Naturgeschichte der Spongien”. Adolph Marcus, Bonn.
- Schulze, F. E. (1880). On the structure and arrangement of the soft parts in *Euplectella aspergillum*. *Royal Society of Edinburgh Transactions* **29**, 661–673.
- Schulze, F. E. (1886). Über den Bau und das System der Hexactinelliden. *Abhandlungen der Königlichen Akademie der Wissenschaften zu Berlin (Physikalisch-Mathematisch Classe)* **1886**, 1–97.
- Schulze, F. E. (1887). Report on the Hexactinellida collected by H.M.S. “Challenger” during the years 1873–1876. *Zoology* **21**, 1–513, 104 pls.
- Schulze, F. E. (1899). Zur Histologie der Hexactinelliden. *Sitzungsberichte der Deutsches Akademie von Wissenschaft* **14**, 198–209.
- Schulze, F. E. (1900). Berichte der Commission für oceanographische Forschungen. Zoologische Ergebnisse. XVI. Hexactinelliden des Rothen Meeres. *Denkschriften der Kaiserlichen Akademie der Wissenschaften. Mathematisch-Naturwissenschaftliche Classe* **69**, 311–324.
- Schulze, F. E. (1904). Hexactinellida. *Wissenschaftliche ergebnisse der Deutschen Tiefsee-Expedition auf dem Dampfer “Valdivia” 1898–1899* **4**, 1–266, 52 pls.

- Schwab, D. W. and Shore, R. E. (1971). Mechanism of internal stratification of siliceous sponge spicules. *Nature (London)* **232**, 501–502.
- Sebens, K. P. (1987). The ecology of indeterminate growth in animals. *Annual Review of Ecology and Systematics* **18**, 371–407.
- Shimizu, H., Cha, J., Stucky, G. D. and Morse, D. E. (1998). Silicatein alpha: Cathepsin L-like protein in sponge biosilica. *Proceedings of the National Academy of Sciences of the United States of America* **95**, 6234–6238.
- Simpson, T. L. (1984). “The Cell Biology of Sponges”. Springer-Verlag, New York.
- Simpson, T. L., Garrone, R. and Mazzorana, M. (1983). Interaction of germanium with biosilicification in the freshwater sponge *Ephydatia mülleri*: Evidence of localized membrane domains in the silicalemma. *Journal of Ultrastructure Research* **85**, 159–174.
- Simpson, T. L., Langenbruch, P. F. and Scalera-Liaci, L. (1985). Silica spicules and axial filaments of the marine sponge *Stelletta grubii* (Porifera, Demospongiae). *Zoomorphology* **105**, 375–382.
- Sollas, W. J. (1879). Observations on *Dactylocalyx pumiceus* (Stutchbury), with a description of a new variety, *Dactylocalyx Stutchburyi*. *Journal of the Royal Microscopical Society* **2**, 122–133.
- Steiner, M., Mehl, D., Reitner, J. and Erdtmann, B.-D. (1993). Oldest entirely preserved sponges and other fossils from the Lowermost Cambrian and new facies reconstruction of the Yangtze platform (China). *Berliner geowissenschaftliche Abhandlungen* **E9**, 293–329.
- Sundar, V. C., Yablon, A. D., Grazul, J. L., Ilan, M. and Aizenberg, J. (2003). Fibre-optical features of a glass sponge. *Nature* **424**, 899–900.
- Tabachnick, K. R. (1991). Adaptation of the hexactinellid sponges to deep-sea life. In “Fossil and Recent Sponges” (J. Reitner and H. Keupp, eds), pp. 378–386. Springer-Verlag, Berlin, Heidelberg.
- Tabachnick, K. R. and Janussen, D. (2004). Description of a new species and subspecies of *Fieldingia*, erection of a new family fieldingidae and a new order Fieldingida (Porifera; Hexactinellida; Hexasterophora). *Bollettino dei Musei e degli Istituti Biologici dell'Università di Genova* **68**, 623–637.
- Tabachnick, K. R. and Lévi, C. (1997). Amphidiscophoran Hexasterophora. *Berliner geowissenschaftliche Abhandlungen* **20**, 147–157.
- Tabachnick, K. R. and Menshenina, L. L. (1999). An approach to the phylogenetic reconstruction of Amphidiscophora (Porifera: Hexactinellida). *Memoirs of the Queensland Museum* **44**, 607–615.
- Tabachnick, K. R. and Reiswig, H. M. (2002). Dictionary of Hexactinellida. In “Systema Porifera: A Guide to the Classification of Sponges” (J. N. A. Hooper and R. W. M. Van Soest, eds), pp. 1224–1229. Kluwer Academic/Plenum Publishers, New York.
- Takahashi, K., Baba, S. A. and Murakami, A. (1973). The ‘excitable’ cilia of the tunicate. *Ciona intestinalis*. *Journal of the Faculty of Sciences, University of Tokyo (Section IV)* **13**, 123–137.
- Thomson, C. W. (1868). On the “vitreous” sponges. *Annals and Magazine of Natural History* **1**, 114–132.
- Thomson, C. W. (1869). On *Holtenia*, a genus of vitreous sponges. *Philosophical Transactions of the Royal Society of London* **159**, 701–720.
- Travis, K. D. F., Franciois, C. J., Bonar, L. C. and Glimcher, M. J. (1967). Comparative studies of the organic matrices of invertebrate mineralized tissues. *Journal of Ultrastructure Research* **18**, 519–550.

- Uriz, M. J., Turon, X., Becerro, M. A. and Agell, G. (2003). Siliceous spicules and skeleton frameworks in sponges: Origin, diversity, ultrastructural patterns, and biological functions. *Microscopy Research and Technique* **62**, 279–299.
- Vacelet, J. (1996). Deep-sea sponges in a Mediterranean cave. In “Deep-sea and Extreme Shallow-water Habitats: Affinities and Adaptations” (F. Uiblein, J. Ott and M. Stachowitsch, eds), Biosystematics and Ecology Series 11, pp. 299–312.
- Vacelet, J., Boury-Esnault, N. and Harmelin, J. (1994). Hexactinellid Cave, a unique deep-sea habitat in the scuba zone. *Deep-sea Research* **41**, 965–973.
- Van de Vyver, G. and Buscema, M. (1981). Capacités morphogènes des cellules d'éponges dissociées. *Annales de la Société Royale Zoologique de Belgique* **111**, 9–19.
- Van Tright, H. (1919). Contribution to the physiology of the fresh-water sponges (Spongillidae). *Tijdschrift voor Diergeneeskunde* **17**, 1–220.
- Vosmaer, G. and Pekelharing, C. (1898). Über die Nahrungsaufnahme bei Schwämmen. *Archives für Anatomie und Physiologie*, 168–186.
- Wachtmann, D. and Stockem, W. (1992a). Microtubule- and microfilament-based dynamic activities of the endoplasmic reticulum and the cell surface in epithelial cells of *Spongilla lacustris* (Porifera, Spongillidae). *Zoomorphology* **112**, 117–124.
- Wachtmann, D. and Stockem, W. (1992b). Significance of the cytoskeleton for cytoplasmic organization and cell organelle dynamics in epithelial cells of fresh-water sponges. *Protoplasma* **169**, 107–119.
- Wachtmann, D., Stockem, W. and Weissenfels, N. (1990). Cytoskeletal organization and cell organelle transport in basal epithelial cells of the freshwater sponge *Spongilla lacustris*. *Cell and Tissue Research* **261**, 145–154.
- Wakelam, M. J. O. (1988). Myoblast fusion—A mechanistic analysis. In “Current Topics in Membranes and Transport” (F. Bronner and N. Duzgunes, eds), pp. 88–107. Academic Press, London.
- Weaver, J. C. and Morse, D. E. (2003). Molecular biology of demosponge axial filaments and their roles in biosilicification. *Microscopy Research and Technique* **62**, 356–367.
- Weissenfels, N. and Landschoff, H. W. (1977). Bau und Funktion des Süßwasserschwammes *Ephydatia fluviatilis* L. (Porifera). IV. Die Entwicklung der monaxialen SiO₂-Nadeln in Sandwich-Kulturen. *Zoologische Jahrbücher Abteilung für Anatomie* **98**, 355–371.
- Weissenfels, N., Wachtmann, D. and Stockem, W. (1990). The role of microtubules for the movement of mitochondria in pinacocytes of fresh-water sponges (Spongillidae, Porifera). *European Journal of Cell Biology* **52**, 310–314.
- Weltner, W. (1882). Beiträge zur Kenntniss des Spongien Inaugural-Dissertation, Universität Freiburg, Freiburg im Breisgau, Germany.
- Werner, B. (1959). Das Prinzip des endlosen Schleimfilters beim Nahrungserwerb wirbelloser Meerestiere. *Internationale Revue des gesamten Hydrobiologie* **44**, 181–216.
- Whitney, F., Conway, K., Thomson, R., Barrie, J. V., Krautter, M. and Mungov, G. (2005). Oceanographic habitat of sponge reefs on the Western Canadian Continental Shelf. *Continental Shelf Research* **25**, 211–226.
- Wiens, M. and Müller, W. E. G. (2006). Cell death in Porifera: Molecular players in the game of apoptotic cell death in living fossils. *Canadian Journal of Zoology* **84**, 307–321.
- Wildon, D. C., Thain, J. F., Minchin, P. E. H., Gubb, I. R., Reilly, A. J., Skipper, Y. D., Doherty, H. M., O'Donnell, P. J. and Bowles, D. J. (1992). Electrical

- signalling and systemic proteinase inhibitor induction in the wounded plant. *Nature* **360**, 62–65.
- Willenz, P. and Van de Vyver, G. (1982). Endocytosis of latex beads by the exopinacoderm in the fresh water sponge *Ephydatia fluviatilis*: An *in vitro* and *in situ* study in SEM and TEM. *Journal of Ultrastructure Research* **79**, 294–306.
- Willenz, P. and Van de Vyver, G. (1984). Ultrastructural localization of lysosomal digestion in the fresh water sponge *Ephydatia fluviatilis*. *Journal of Ultrastructure Research* **87**, 13–22.
- Wilson, H. V. (1907). On some phenomena of coalescence and regeneration in sponges. *Journal of Experimental Zoology* **5**, 245–258.
- Woodland, W. (1908). Some observations on the scleroblastic development of hexactinellid and other silicious sponge spicules. *Quarterly Journal of Microscopical Science* **52**, 139–157.
- Wyeth, R. C. (1999). Video and electron microscopy of particle feeding in sandwich cultures of the hexactinellid sponge *Rhabdocalyptus dawsoni*. *Invertebrate Biology* **118**, 236–242.
- Wyeth, R. C., Leys, S. P. and Mackie, G. O. (1996). Use of sandwich cultures for the study of feeding in the hexactinellid sponge *Rhabdocalyptus dawsoni* (Lambe, 1892). *Acta Zoologica* **77**, 227–232.
- Yahel, G., Eerkes-Medrano, D. I. and Leys, S. P. (2007b). Size independent selective filtration of ultraplankton by hexactinellid glass sponges. *Aquatic Microbial Ecology* (in press).
- Yahel, G., Whitney, F., Reisinger, H. M., Eerkes-Medrano, D. I. and Leys, S. P. (2007a). *In situ* feeding and metabolism of glass sponges (Hexactinellida, Porifera) studied in a deep temperate fjord with a remotely operated submersible. *Limnology and Oceanography* **52** (in press).
- Yu, W., Centonze, V. E., Ahmad, F. J. and Baas, P. W. (1993). Microtubule nucleation and release from the neuronal centrosome. *Journal of Cell Biology* **122**, 349–359.